SYNTHESIS, CHARACTERIZATION AND ANTI-BACTERIAL STUDIES OF HYDRAZIDE SCHIFF BASES OF ACETYLACETONATE METAL COMPLEXES

BY

Charity Wokwu Dikio

Student Number: 209044845

DISSERTATION SUBMITTED IN FULFILMENT OF THE REQUIREMENT FOR THE AWARD OF THE DEGREE OF MAGISTER TECHNOLOGIAE IN CHEMISTRY

VAAL UNIVERSITY OF TECHNOLOGY

DEPARTMENT OF CHEMISTRY

SUPERVISOR: **Dr. F.M. MTUNZI**

Co-SUPERVISOR: **Prof. A. M SIPAMLA**

JUNE 2014

DECLARATION

I, Charity Wokwu Dikio, declare that this dissertation is my own work. It is being submitted in fulfilment for the award of the degree, Master of Technology in Chemistry, Vaal University of Technology, Vanderbijlpark. It has not been submitted before for any degree or examination at this or any other University.

---------- On this ----------day of ----------2014

(Candidate)

---------- On this ----------day of ----------2014

(Supervisor)

---------- On this ----------day of ----------2014

(Co-Supervisor)

DEDICATION

This project is dedicated to my Children Ezekiel Ukarionisofien Ikechi, Natasha Umeonisofien Chioma, Grace Onisokumen Ukechi and all those who have encouraged me or contributed in any way to the success of this project.

ACKNOWLEDGEMENTS

I wish to gratefully thank the following people for their contributions towards the success of this project.

1. Dr. FM Mtunzi, my supervisor, mentor and friend. Your enthusiasm, encouragement, support, advices and guidance throughout this project is highly appreciated. Your patience is unprecedented.
2. Prof EB Naidoo, HOD (Chemistry). For the opportunity to carry out this research at Vut and providing an enabling environment. Your zeal, financial support and commitment towards the completion of this work is highly appreciated.
3. Prof ED Dikio, my husband and mentor. Your love, support, patience, encouragement, sacrifices and expertise were unsurpassable.
4. Dr. Collins Ateba for his assistance with the antibacterial screening.
5. Patrick Ngoy for his assistance with Instrumental Analysis.
6. The Staff at the Department of Chemistry, Vaal University of Technology, Vanderbijlpark for their friendliness.
7. The Almighty God, for good health, vision and provision.

PRESENTATIONS AND WORKSHOPS ATTENDED

PRESENTATIONS

1. Oral Presentation**: CW Dikio**, FM Mtunzi, M Kabamba, EE Ebenso, and ED Dikio, South African Chemical Institute (SACI) Young Chemist's Symposium, University of Johannesburg, Johannesburg, South Africa. 13th September **2013**. Hydrazide Schiff bases of Oxovanadium (1V) Complexes: Synthesis and Spectroscopic studies.

2. Oral Presentation: **CW Dikio**, FM Mtumzi, ED Dikio, South African Chemical Institute (SACI), 41ST SACI NATIONAL CONVENTION, Chemistry for Africa: New Perspectives in the 21st Century, River Park Conference Center, East London, South Africa. 1st - 6thDecember, **2013**. Hydrazide Schiff base of Oxovanadium (1V) Complexes: Synthesis, Spectroscopic and Antibacterial Studies.

WORKSHOPS

1. Indo-South Africa Symposium on Nanotechnology and Innovations, Unisa, Pretoria, South Africa. 12-15th March, **2012.**

ABSTRACT

Infectious diseases, a group of illnesses caused by specific pathogens or its toxins is a leading cause of death globally. Treatment with antibiotics is a key intervention in the control and management of many infectious disease. However, the increasing incidence of antibiotics failure, due to the emergence of drug resistant pathogens, is rendering the use of antibiotics chemotherapy ineffective. A possible solution is to synthesize new compounds with broad spectrum characteristics and superior drug performances as alternative to conventional antibiotics. Schiff Bases are biologically active ligands. They form metal complexes with superior biological activities. This research aims to synthesize some Schiff Base metal complexes and investigate their biological effects on *Staphylococcus aureus and Enterococcus faecalis.*

Metal acetylacetonates of Vanadium, Copper, Cobalt, Zinc, Magnesium, Manganese, Cadmium, Nickel and Iron were synthesized and characterized by Fourier transform infrared spectroscopy. Four Schiff bases, LI, L2, L3 and L4 were also synthesized by the condensation of 4-(diethylamino)-2-hydroxybenzaldehyde with 4-nitrobenzohydrazide and 4-methoxybenzohydrazide to form L1 and L2. 4-(dimethylamino) benzaldehyde was reacted with 4-nitrobenzohydrazide and 4-methoxybenzohydrazide to form L3 and L4 respectively.

The Schiff base ligands were then reacted with synthesized Vanadium, manganese, cobalt and magnesium acetylacetonates to form Schiff base complexes (SBC 1A to 4D).

Schiff bases ligands and complexes were characterized by FT-IR, ^{1}H-NMR, ^{13}C-NMR, TGA and DTA. Fourier Transform infrared spectroscopy (FTIR) of the acetylacetonates showed the formation of metal acetylacetonates as characterized by the absence of the carbonyl stretching ν(C=O) vibration in metal acetylacetonate spectra as compared to pure acetylacetone. Metal acetylacetonates also showed the presence of metal oxygen vibration frequency, ν(M-O-C), in the spectra obtained. Thermogravimetric analysis (TGA) and Derivative or Differential Thermogravimetric analysis (DTA) of the Schiff base ligands showed the presence of a single decomposition product in L1, L2, L3 and L4 indicating the formation of a single reaction product while those of Schiff base complexes showed the formation of several decomposition products.

Proton and carbon thirteen Nuclear Magnetic Resonance (^{1}H- and ^{13}C-NMR) spectroscopy of the Schiff base ligands indicated the presence of hydrogen and carbon-13 in different environments.

The chemical shifts of the hydrogens and carbon-13 provided evidence that Schiff base ligands were formed. The strongest evidence is the presence of the azomethine hydrogen and carbon in the spectra of the Schiff base ligands. The presence of aromatic hydrogens and carbon at chemical shift environments found in literature also confirmed the formation of Schiff base ligand. The NMR spectra of Schiff base complexes showed the presence of azomethine (HC=N) and aromatic hydrogens at expected chemical shifts.

The synthesized Schiff bases and their corresponding metal complexes were screened for their in-vitro antibacterial activities against two Gram-positive (*Staphylococcus aureues and Enterococcus feacalis*) bacterial strains by the Agar-well diffusion methods.The ligands and complexes were tested against confirmed *S. aureus* and *E. faecalis* strains and only 4 exhibited antimicrobial activities. The ligands and complexes were effective against the *S. aureus*and *E. faecalis* isolates.

TABLE OF CONTENTS

	Page
Declaration	ii
Dedication	iii
Acknowledgements	iv
Presentations and Workshops	v
Abstract	vi
Table of contents	viii
List of Abbreviations	xi
List of Figures	xii
List of Tables	xv
CHAPTER 1: INTRODUCTION	
1.1 BACKGROUND	1
1.2 SCHIFF BASE	2
1.3 RATIONAL AND MOTIVATION	5
1.4 PROBLEM STATEMENT	6
1.5 AIMS	6
1.6 OBJECTIVES OF THE RESEARCH	6
REFERENCES	8
CHAPTER 2: LITERATURE REVIEW	
2.1. INTRODUCTION	12
2.2. SCHIFF BASES	12
2.2.1. DESCRIPTION	12
2.2.2 SYNTHESIS OF SCHIFF BASES	13
2.2.3. APPLICATIONS OF SCHIFF BASES	15
2.2.3.1 ANTIBACTERIAL	15
2.2.3 2 CORROSION CONTROL	16

2.2.3.3 COLORANTS 18

2.2.3.4 CATALYSTS 18

2.3 METALS UNDER INVESTIGATION 19

2.3.1 VANADIUM 19

2.3.2 COBALT 20

2.3.3 MANGANESE 20

2.3.4 MAGNESIUM 21

2.4 THE ACETYL ACETONATE LIGAND **21**

2.5 MICRO-ORGANISMS **21**

REFERENCES **23**

CHAPTER 3: METHODS AND METHODOLOGY

3.1 INTRODUCTION 26

3.2 EXPERIMENTAL 26

3.2.1 CHEMICALS AND MATERIALS 26

3.3 SYNTHETIC PROCEDURE **27**

3.3.1. SYNTHESIS OF METAL ACETYL ACETONATES 27

3.3.2. SYNTHESIS OF SCHIFF BASE LIGANDS 33

3.3.3. SYNTHESIS OF SCHIFF BASE COMPLEXES 37

3.4 CHARACTERIZATION TECHNIQUES **55**

3.4.1 FOURIER TRANSFORM INFRARED SPECTROSCOPY (FT-IR) 55

3.4.2 ULTRAVIOLET –VISIBLE SPECTROSCOPY (UV-Vis) 56

3.4.3 PROTON NUCLEAR MAGNETIC RESONANCE SPECTROSCOPY (^{1}H NMR) 57

3.4.4 THERMOGRAVIMETRIC ANALYSIS (TGA) 60

3.5 BIOLOGICAL TESTING **61**

REFERENCES **62**

CHAPTER 4: RESULTS AND DICUSSION

4.1 METAL ACETYLACETONATES **65**

4.1.1 SYNTHESIS 65

4.1.2 FTIR 66

4.2 SCHIFF BASE LIGANDS **73**

4.2.1 FTIR 73

4.2.2 TGA/DTA 78

4.2.3 NMR 82

4.3 SCHIFF BASE COMPLEXES **88**

4.3.1. SYNTHESIS

4.3.2 FTIR 88

4.3.3 NMR 98

4.3.4 TGA/DTA 118

4.4 BIOLOGICAL EVALUATION **130**

4.5 REFERENCES 145

CHAPTER 5: CONCLUSION

5.1 CONCLUSIONS 146

LIST OF ABBREVIATIONS

FT-IR	Fourier Transform Infrared
TGA	Thermo-gravimetric Analysis
DTA	Differential Thermo-gravimetric Analysis
C13-NMR	Carbon 13 Nuclear Magnetic Resonance
H-NMR	Proton Nuclear Magnetic Resonance
UV-vis	Ultraviolet Visible
E. Coli	*Escherichia Coli*
S. aureus	*Staphylococcus aereus*
E. faecalis	*Enterococcus faecalis*
S. typhi	*Salmonella typhi*
MeOH	Methanol
Acac	Acetylacetone
M(acac)n	Metal acetalacetonates
LI	N-{(E)-[4-(diethylamino)-2-hydroxyphenyl]methylidene}-4-nitrobenzohydrazide
L2	N-{(E)-[4-(diethylamino)-2-hydroxyphenyl]methylidene}-4-methoxybenzohydrazide
L3	N-{(E)-[4-(dimethylamino)phenylmethylidene}-4-nitrobenzohydrazide
L4	N-{(E)-[4-(dimethylamino)phenyl]methylidene}-4-nitrobenzohydrazide
SBC	Schiff base complex

LIST OF FIGURES

4.1	FT-IR spectrum of pure acetylacetone	66
4.2	FT-IR spectrum of Cobalt(II) acetylacetonate	67
4.3	FT-IR spectrum of Copper (II) acetylacetonate	68
4.4	FT-IR spectrum of vanadium acetylacetonate	69
4.5	FT-IR spectrum of zinc(II)acetylacetona	70
4.6	FT-IR spectrum of ligand L1	72
4.7	FT-IR spectrum of ligand L2	73
4.8	FT-IR spectrum of ligand L3	74
4.9	FT-IR spectrum of ligand L4	75
4.10	Thermo-gravimetric and derivative thermo-gravimetric analysis of ligand L1	77
4.11	Thermo-gravimetric and derivative thermo-gravimetric analysis of ligand L2	78
4.12	Thermo-gravimetric and derivative thermo gravimetric analysis of ligand L3	79
4.13	Thermo-gravimetric and derivative thermo-gravimetric analysis of ligand L4	80
4.14	Proton and Carbon-13 NMR of ligand L1	83
4.15	Proton and Carbon-13 NMR of ligand L2	84
4.16	Proton and Carbon-13 NMR of ligand L3	85
4.17	Proton and Carbon-13 NMR of ligand L4	86
4.18	FT-IR spectrum of Schiff base complex 1A	88
4.19	FT-IR spectrum of Schiff base complex 1B	88
4.20	FT-IR spectrum of Schiff base complex 1C	89
4.21	FT-IR spectrum of Schiff base complex 1D	89

4.22 FT-IR spectrum of Schiff base complex 2A 90

4.23 FT-IR spectrum of Schiff base complex.2B 90

4.24 FT-IR spectrum of Schiff base complex.2C 91

4.25 FT-IR spectrum of Schiff base complex.2D 91

4.26 FT-IR spectrum of Schiff base complex 3A 92

4.27 FT-IR spectrum of Schiff base complex 3B 92

4.28 FT-IR spectrum of Schiff base complex 3C 93

4.29 FT-IR spectrum of Schiff base complex3D 993

4.30 FT-IR spectrum of Schiff base complex 4A 94

4.31 FT-IR spectrum of Schiff base complex 4B 94

4.32 FT-IR spectrum of Schiff base complex 4C 95

4.33 FT-IR spectrum of Schiff base complex.4D 95

4.34 Proton and Carbon-13 NMR of Schiff base complex 1A 99

4.35 Proton and carbon-13 NMR of Schiff base complex 1B 100

4.36 Proton and Carbon-13 NMR of Schiff base complex 1c 101

4.37 Proton and Carbon-13 NMR of Schiff base complex 1D 102

4.38 Proton and Carbon-13 NMR of Schiff base complex 2A 103

4.39 Proton and Carbon-13.NMR of Schiff base complex 2B 104

4.40 Proton and Carbon-13 NMR of Schiff base complex 2C 105

4.41 Proton and Carbon-13 NMR of Schiff base complex 2D 106

4.44 Proton and carbon-13 NMR of Schiff base complex 3C 109

4.45 Proton and carbon-13 NMR of Schiff base complex 3D 110

4.46 Proton and carbon-13 NMR of Schiff base complex 4A 111

4.47 Proton and carbon-13 NMR of Schiff base complex 4B 112

4.48 proton and carbon-13 NMR of Schiff base complex 4C 113

4.49 Proton and carbon-13 NMR of Schiff base complex 4D 114

4.50 Thermogravimetric and Derivative Thermogravimetric analysis of Schiff base complex 1A 119

4.51 Thermogravimetric and DerivativeThermogravimetric analysis of Schiff base complex 1B 120

4.52 Thermogravimetric and Derivative Thermogravimetric analysis of Schiff base complex 1C 121

4.53 Thermogravimetric and Derivative Thermogravimetric analysis of Schiff base complex 1D 122

4.54 Thermogravimetric and Derivative Thermogravimetric analysis of Schiff base complex 2A 123

4.55 Thermogravimetric and Derivative Thermogravimetric analysis of Schiff base complex 3A 124

4.56 Thermogravimetric and Derivative Thermogravimetric analysis of Schiff base complex 3C 125

4.57 Thermogravimetric and Derivative Thermogravimetric analysis of Schiff base complex 3D 126

4.58 Thermogravimetric and derivative thermogravimetric analysis of Schiff base complex.4A 127

4.59 Thermogravimetric and derivative thermogravimetric analysis of Schiff base complex 4B 128

LIST OF TABLES

4.3	FT-IR absorption bands of ligands L1-L4	76
4.4	Chemical shifts of proton NMR of ligands L1-L4	82
4.5	Chemical shifts of Carbon-13 NMR of the ligands L1-L4	82
4.6	Formation Schiff Base metal Complexes	87
4.7	FT-IR absorption bands of Schiff base complexes	96
4.8	Chemical Shifts of Proton NMR of Schiff base complexes 1A to 4D	115
4.9	Chemical Shifts of Carbon-13 complexes 1A to 4D	116

CHAPTER 1

INTRODUCTION

1.1.Background

Bacterial infections result in about 17 million deaths globally per year, mostly in children and the elderly [1]. There are several antibiotics chemotherapeutic drugs available for the treatment of diseases caused by bacteria, however, the growing incidence of antibiotics resistance, due to antibiotics misuse, is posing a significant threat to the control and management of infectious diseases. This problem is exacerbated by the genetic ability of bacteria to acquire and transmit resistance against the drugs used as therapeutic agents making the available antibiotics obsolete [2]. Despite advances made in antibiotics chemotherapy, the morbidity and mortality associated with bacterial infections remain significant. The complexities of these diseases necessitates the design and development of a new/novel class of compounds that will exhibit superior potency, selectivity and inferior cytotoxicity compared to existing antibacterial compounds.

A popular drug design strategy involves the inclusion of transition metal ions, often incorporated into compounds of known therapeutic value. One notable example is that of ferroquine, a metal based drug, in which ferrocene was incorporated into the lateral side-chain of chloroquine to enhance its drug activities [4]. Ferroquineis reported to be highly effective against chloroquine-resistant strains of the malarial parasite.

Motivated by the recorded successes of ferroquine and following the same targeted approach to introduce multi-functionalities: this project aims to incorporate metal ions into the molecular scallop of some Schiff base derivatives with the expectations that their potency may be significantly enhanced as well.

Schiff bases, a class of organic ligands noted for their multiple medicinal benefits such as innate antibacterial properties, good architectural diversity and excellent coordination capacity are very attractive materials for the design of chemotherapeutic agents with potential application for the

control of bacterial infections [3, 5-7]. Moreover, Schiff bases have numerous applications in drug design, development and enhancement of drug performances [8].

Motivated by the recorded successes of ferroquine, and following the same targeted approach to introduce multi-functionalities: this project aims to synthesize incorporating metal ions into some Schiff base derivatives may to targets with significant biological importance as an alternative replacement to conventional antibiotics which have become ineffective.

1.2. Schiff bases

Schiff bases are a family of organic compounds characterized by the presence of a carbon-nitrogen double bonds (C=N) [5]. They are also known as anils, imines or azomethines. Schiff bases are found, naturally, in some plant species. They are synthesized by the condensation of primary amines with carbonyl compounds [3]

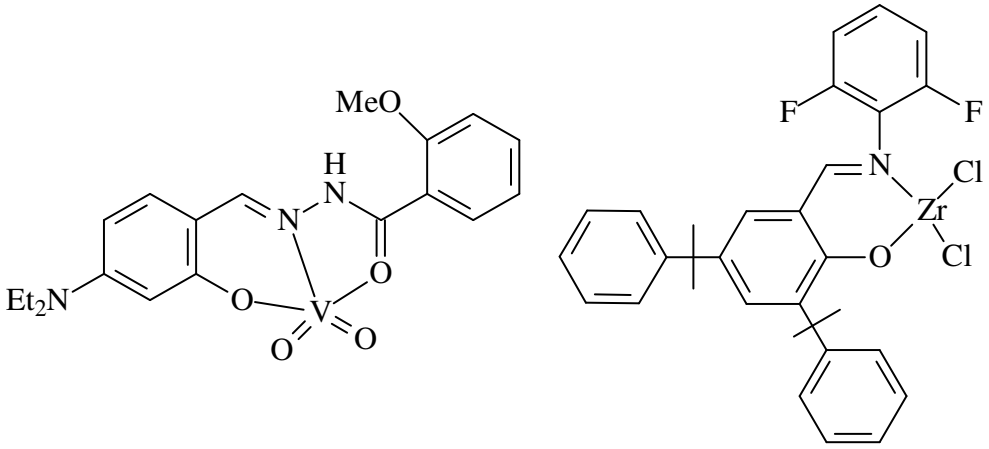

Figure 1.1: Example of Schiff base complexes of vanadium and zinc metals [3]

Schiff bases and their complexes are very attractive materials for several applications due to their desirable features such as structural similarities with natural biological substances, relatively simple preparation procedures, synthetic flexibility that enables design of suitable structural properties, selectivity and sensitivity towards the central metal atom rich architectural variety and amazing coordination capacity [5, 8, 9-14].

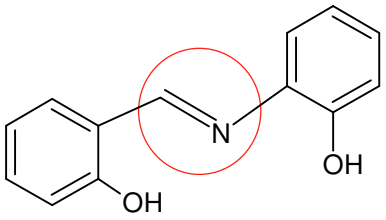

Figure 1.2: Structure of a Schiff base showing an azomethine linkage [3].

A number of Schiff bases have shown interesting pharmacological activities such as antibacterial, antifungal, antitumor, anticancer, anti-inflammatory, antiviral, anti-proliferative and diuretic activities [3, 7, 8, 15-19].The azomethine linkage (C=N), a prominent feature of Schiff bases has been reported to be responsible for their biological activities

Schiff bases are known to display significant structural diversity. Some biologically important Schiff base derivatives include the imidazoles, pyrimidines, Hydrazides and hydrazones [20-23]. The diversity in the structure of Schiff bases is very useful in designing material of desired properties to suit specific goals. The Sulfonamide derivatives exhibit a broad spectrum of pharmacological activities due to the presence of the sulfonamide (SO_2NH) moiety. Pyrimidine derivatives have been extensively studied due to their occurrence in living systems, and their varied pharmacological activities such as antitumor, antiviral, anti-inflammatory, antipyretic, antimicrobial and antifungal properties. The imidazole derivatives have received growing attention for properties, such as herbicidal, fungicidal, analgesic, anti-inflammatory and antithrombotic activities. Hydrazide derivatives have been reported to possess a broad spectrum of antibacterial activities [4, 6, 10, 11]. They also act as good potential for oral drugs used for the treatment of genetic disorders like thalassemia.

All these properties have recommended Schiff bases fora wide range of applications in various fields of science such as in agriculture, pharmaceutical industries, chemical industries and clinical biology [21-24]. They are used as raw material in organic synthesis, pigments, dyes, catalysts, polymer stabilizers, packaging material and corrosion inhibitors [3, 7, 20, 22]. Schiff bases also play significant roles in fundamental biological functions such as photosynthesis and transport of oxygen in mammalian and other respiratory systems [23].

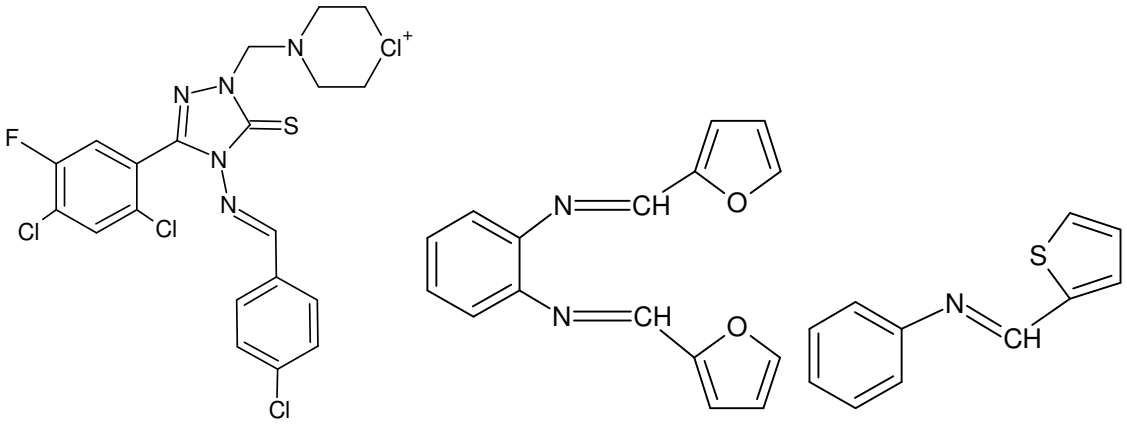

Figure 1.3: Some structures of bioactive Schiff bases

Recently, interests in the coordination chemistry of Schiff bases has escalated due to their medicinal applications. A number of Schiff base complexes have shown remarkable pharmacological activities [23, 25-28]. They are extensively used by the pharmaceutical industries for drug design, development and enhancement of drug activities [29-32]. Research has shown that incorporating a small amount of transition metal into Schiff base enhances their biological activities and decreases the cytotoxic effect of both the Schiff base ligands and the transition metal ions [32-33]. Schiff base complexes are also used for medical testing directed towards the discovering of effective and safe therapeutic agents for the treatment of various diseases including cancers [32].

Considering that, recently, some convectional antibiotics are no longer effective in the management of bacterial infections [1], and taking into account the biological importance of Schiff base complexes: this study aims to synthesize some Hydrazide Schiff bases and their metal complexes and evaluate their effects on selected pathogens with the expectation that this study may lead to novel targets that could effectively control resistant pathogens.

A search through literature reveals that data on the antibacterial activities of certain hydrazide Schiff bases and their metal complexes are available [26];however, data on the antibacterial activities of Schiff bases derived from 4-nitrobenzohydrazide and 4-methozybenzohydrazide and their corresponding metal complexes namely Co(III), Mn(IV), Mg(II) and VO(IV) do not exist.

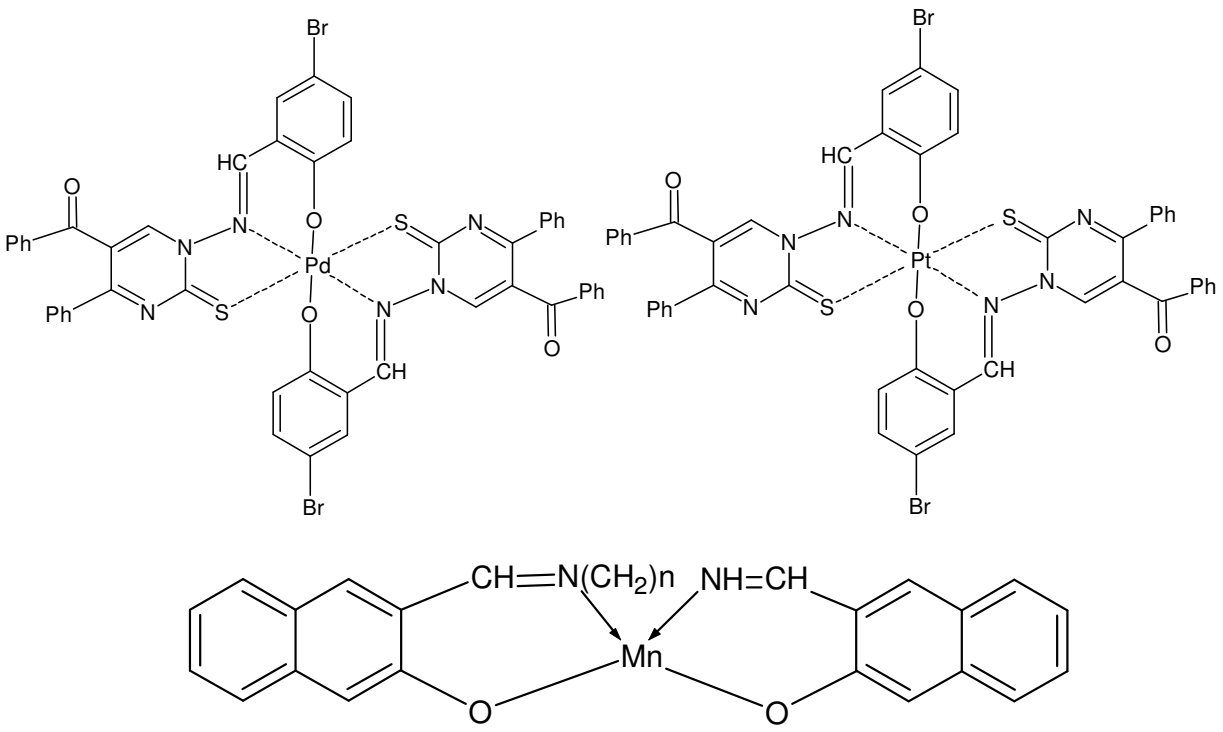

Figure 1.4: Structures of some biologically active Schiff base complexes [24].

1.3. Rational and Motivation

It has been demonstrated that some drugs show increased activities when administered as metal complexes than as organic compounds [32]. The incorporation of transition metal ions into Schiff base structures enhances their biological activity and reduces the cytotoxic effects of the Schiff bases and the metal ions on the hosts. Although transition metals are toxic, it has been reported that in trace amounts, they are essential for the normal functioning of living organisms [33]. It is, therefore, not surprising that metal complexes are of great interest as potential therapeutic agents.

Recently, the emergence of antibiotics resistant pathogens due to antibiotics misuse is posing a significant threat to the management of diseases associated with bacterial infections [1]. Despite advances in antibiotics chemotherapy, mortality and morbidity associated with infectious diseases remain significant [1]. In order to prevent a potential crises it is necessary to develop, a new class of antibacterial agents with superior potency, selectivity and inferior cytotoxicity as a replacement to current antibiotics which have become obsolete.

Schiff bases, a class of therapeutic agents with desirable properties such as innate antibacterial activities, preparative accessibility and amazing coordination capacity promises to be a material

of choice for the synthesis of a chemotherapeutic agent with potential applications for the control of bacterial infections. [3, 5]. This studies may result in achieving novel targets with significant antibacterial activities as an alternative to traditional antibiotics which has become ineffective in the control of bacterial infections.

1.4. Problem Statement

Antibiotics chemotherapy provides an effective and efficient means of controlling and containing many infectious diseases even serious ones like Tuberculosis. However, the emergence of antibiotics resistant strains of bacteria due to antibiotic misuse is posing a significant threat to the management of diseases associated with bacterial infections. This problem is further exacerbated by the emergence of pathogens with intrinsic ability to resist antibiotics. Despite advances made in antibiotic chemotherapy, mortality and morbidity associated with bacterial infections remain significant. In order to prevent a potential crises, it is necessary to develop a more effective antibacterial agents with superior selectivity, potency and inferior cytotoxicity compared to conventional antibiotics. To the best of our knowledge, Vanadium, Cobalt, Manganese, and Mg have not been used with 4-nitrobenzohydrazide and 4-methozybenzohydrazidefor the synthesis of hydrazide Schiff base complexes.

1.5. Aims

The aims of this study is to synthesize and characterize some hydrazide Schiff bases and their metal complexes and evaluate their biological effects on selected pathogens.

1.6. Objectives of the Research

In order to achieve the aims of this research the following objectives are proposed.

- To synthesize some hydrazide Schiff base ligands using 4-nitrobenzohydrazide and 4-methozybenzohydrazides;
- To synthesize various metal acetylacetonates;
- To synthesize metal complexes of the Schiff base ligands;

- To characterize the synthesized Schiff base ligands and their metal complexes using FT-IR, H-NMR, C-13-NMR TGA and DTA.
- To evaluate the effects of the free Schiff bases and their metal complexes on selected pathogenic microbes.

REFERENCES

[1] IQBAL, J., SIDDIQUI, R., KAZMI, SU., KHAN, NA. **(2013)**. A Simple Assay to Screen Antimicrobial Compounds Potentiating the Activity of Current Antibiotics. BioMed Res. Int.

[2] BAMAS, SS., JAYASURYA, KS., SANKARANARAYANAN, S., BAMA,P**. (2012**). Antibacterial Activity of Different Phytochemical Extracts from the Leaves of *T.Procumbens.* Linn.: Identification and Mode of Action of the Terpenoid Compound as Antibacterial*. Int. J. of Pharm. Sci*. Vol. 4

[3] Da SILVA, CM., da SILVA DL., MODOLO, LV., ALVES, RB., de RESENDE, MA., MARTINS, CVB., de FATIMA, A**. 2011**. Schiff bases: A Short review of their antimicrobial activities. *J Adv Res*.

[4] MURUGANANDAM, L. KUMAR, K.K., BALASUBRAMANIAN, K. **2013**. Synthesis, characterization, antibacterial, antifungal and anticancer studies of a new antimetabolite: N-[(Diphenylamino)methyl]acetamide and some of its inner transition metal chelates. *Chem. Sci. Trans.* 2(2), 379 – 384.

[5] SHIVHARE, S., MISHRA, R., GHARIA, A., GAUTAM, MD. **2012.** Synthesis, Characterization and Antimicrobial Studies of Cu(II), Co(II) and Ni(II) Complexes with Schiff Base derived from N-amino rhodanine and salicylaldehyde. *Int. J. Pharm. Pharmcl. Sci.*4(1)

[6] SALLOMI, I.J. & SHAHEEN, A.J. **1994**. Complexes of hydrazide Schiff bases. *Trans Metal Chem*. 19, 275-276

[7] PRAKASH, A & ADHIKARI, D. **2011**. Application of Schiff bases and their metal complexes- A Review. *Int. J. ChemTech Res*. (3). 1891-1896.

[8] BAL, M., CEYHAN, G., AVAR, B., KOSE, M. **2014**. Synthesis and X-ray powder diffraction, electrochemical, and genotoxic properties of a new azo-Schiff base and its metal complexes. *Turk. J. Chem*. (38) 222-241.

[9] IBRAHIM, MN & SHARIF, SAI. **2011**. Synthesis, Characterization and Use of Schiff bases as Fluorimetric Analytical Reagents (Part 11*). E-J Chem*. 8(1), 180-184

[10] SAHEBALZAMANI, S., GHAMMAMY, S., MEHRANI K., SALIMI, F**. 2010**. Synthesis, Characterization and thermal analysis of Hg(II) complexes with hydrazide ligands. *DerChemicaSinica*. 1(1): 67-72.

[11] BRUCKNER, C., RETTIG, SJ.,DOLPHIN DAVID. **2000**. 2-PyrrolyLthiones as MonoanionicBidentate N,S-Chelators: Synthesis and Molecular Structure of 2-Pyrrolthionnato Complexes of Nickel (II), Cobalt (III), Mercury(II). *Inorg. Chem*. 39: 6100-6106.

[12] POURALIMARDAN, O., CHAMAYOU, A., JANIAK, C., HOSSEINI-MONFARED, H. **2007**. Hydrazone Schiff base-manganese (11) Complexes: Synthesis, Crystal Structure and catalytic reactivity. *InorganicaChimicaActa*. 360: 1599-1608.

[13] BOGHAEI, DM., GHARAGOZLOU, M**. 2007**. Spectral Characterization of novel ternary zinc(II) Complexes containing 1,10-phenanthroline and Schiff bases derived from amino acids and salicylaldehyde-5-sulfonates. *SpectrochimicaActa*. 67: 944-949.

[14] BENABID, S., DOUADI, T., DEBAB, H., De BACKER, M., SAUVAGE, F**. 2012**. Synthesis, Spectroscopic, and Electrochemical Characterization of a Schiff base: 4,4 – bis[(4-diethylaminosalicylaldehyde)diphenyl methane]diimine and its Complexes with Copper(II), Cobalt(II), and Cadmium(II*). Met.-Org., and Nano-Met. Chem*. 42: 1-8.

[15] KUMAR, K. S., GANGULY, S., VEERASAMY, R., De CLERCQ, E**.2010.**Synthesis, antiviral activities and cytotoxicity evaluation of Schiff bases of some 2-phenyl quinqzoline-4(3)H-ONES. *Eur. J. Med. Chem*. 45: 5474-5479.

[16] JARRAHPOUR, A., KHALILI, D., De CLERCQ, E., SALMI, C., BRUNEL, JM. **2007** .Synthesis, Antibacterial, Antifungal and Antiviral activity evaluation of some new bis-Schiff bases of is a tin and their derivatives. *Molecules*. 12(8): 1720-1730

[17] VICINI, P., GERONNIKAKI, A., INCERTI, M., BUSONERA, B., PONI, G., CABRAS, CA.,La COLLA, P**. 2003**. Synthesis and Biological Evaluation of benzo[d]isothiazole, benzothiazole and thiazole Schiff bases. *Bioorg. Med.Chem*. 11: 4785-4789.

[18] CHEM, LX., TANG, JJ., LUO, H., JIN, XL., DAI, F., YANG, J., QIAN, YP., LI, XZ., ZHOU, B. **2010**. Antioxidant and Antiproliferative Activities of hydroxyl-substituted Schiff bases. *Bioorg. Med. Chem. Lett*. 20: 2417-2420.

[19] SRIDHAR, SK., SARAVAN, M., RAMESH, A**. 2001**. Synthesis and antibacterial screening of hydrazones, Schiff and Mannich bases of is a tin derivatives. *Eur. J. Med. Chem*. 36: 615-625.

[20] ASHRAF, MA., MAHMOO, K., WAJID, A. Synthesis, Characterization and Biological Activity of Schiff bases. *Int. Conf. on Chem and Chem Pro.* Vol. 10.

[21] UPADHAYAY, N. **2013**. Synthesis, Characterization and Biological Studies of Some Thiocyanato-bridgeed Bimetallic Complexes Containing Co(II), Cd (11), Hg(11) and N,N-Bis(benzylidene)-1,2-phenylene-diamine Schiff base. *ChemSci Trans*. 2 (2), 455-460.

[22] BARTYZEL, A**. 2013**. Synthesis, Crystal Structure and Characterization of Manganese (111) complex containing a tetradentate Schiff base. *J. Coord. Chem*. (66). 4292-4303.

[23] AKBARI, A &ALINIA, Z. **201**3. Synthesis, Characterization and DFT calculation of a Pd(11) Schiff base complex. *Turk J Chem*. (37) 867-878.

[24] MOHAMED, GG., OMAR, MM., HINDY, AM. **2006.** Metal complexes of Schiff bases: Preparation, characterization and biological activity. *Turk. J. Chem*. (30), 361 – 382.

[25] PAWANOJ, AA&MEHTA, BH**. 2009**. Synthesis, characterization and X-ray diffraction studies of Co(II), Ni(II) and Pd(II) complexes of Schiff base derived from 3-Hydroxy benzaldehyde and 3-hydroxy-2-naphthoic hydrazide. *A. J. Chem*. 21(9), 6869 – 6876.

[26] SINGH, J., SINGH, P. **2012**. Synthesis, spectroscopic characterization, and invitro antimicrobial studies of pyridine-2-carboxylic acid N-(4-chloro-benzyl)-hydrazide and its Co(II), Ni(II) and Cu(II) complexes. *Bioinorg. Chem. Appl.* DOI: 10.1155/104549.

[27] UR-REHMAN, S., FAIZ, A., NAWAZ, R. **2013**. Synthesis, characterization, thermal and antibacterial study of a novel sulfonamide derivative, N-[(*E*)-pyridin-3-ylmethylidene]benzenesulfonamide and its Co(II) and Zn(II) complexes. *J. Chil. Chem. Soc*. 58(1), 1624 – 1627.

[28] GULCAN, M., SONMEZ, M., BERBER, I. **2012**. Synthesis, characterization and antimicrobial activity of a new pyrimidine Schiff base and its Cu(II), Ni(II), Co(II), Pt(II) and Pd(II) complexes. *Turk J. Chem,* (36), 189 – 200.

[29] DAMAVANDI, S. 2011. Schiff base transition metal complex catalyzed one pot synthesis of 2-aryl-1*H*-phenanthro[9,10-d]imidazoles. *Synth. React. Inorg. Met-org. Chem.* (41) 1274 – 1277.

[30] CANPLAT, E., SAHAL, H., KAYA, M. & GUR, S., **2014,** Synthesis, characterization, antibacterial and antifungal activities studies of copper(II), cobalt(II) and zinc(II) complexes of the Schiff base ligand derived from 4,4-diaminodiphenylether. *J. Chem. Soc. Pak.* 36(1), 106 – 112.

[31] MALIK, S., GHOSH, S., JAIN, B., SINGH, A., BHATTACHARYA, N. **2013**. Synthesis, characterization and biological evaluation of some 3d-metal complexes of Schiff base derived from xipamide drug. *J. Chem*. DOI: 10.1155/549805.

[32] PRASHANTI, Y., KIRANMAI, K., IRA., SATHIS, KK., CHITYANA, VK., SHIVARAG**. 2012**. Spectroscopic Characterization and Biological Activity of Mixed Ligand Complexes of Ni(11) with 1,10-Phenanthroline and Heterocyclic Schiff bases. *BioinorgChem and Appl.*

[33] MALHOTRA, E., KAUSHIK, NK.,MALHORA, HS. **2006.** Synthesis and studies of ionic chelates of halfnocene with guanine. *Indian J. Chem***.**45A, 370-376.

CHAPTER 2

LITERATURE REVIEW

2.1. Introduction

With the growing rate of mortality and modality associated with bacterial infections, there has been an increasing emphasis on the development of novel antibacterial compounds with superior potency, selectivity and inferior cytotoxicity as an alternative replacement to conventional antibiotics which have become ineffective in the management of bacterial infections. Schiff bases, a class of therapeutic agents, with proven antibacterial activities have been shown to possess interesting moieties for the design of effective antibacterial agents.

This chapter is divided into three sections. Section 2.2 gives a detailed description of Schiff bases. reviews the pharmacological activities of Schiff bases.

2.2 Schiff bases

2.2.1 Description

Schiff bases are a class of organic compounds characterized by the presence of a carbon nitrogen double bond (C=N) in which the nitrogen atom is connected to an aryl or alkyl group, not hydrogen [1]. Structurally, a Schiff base is a nitrogen analogue of an aldehyde or ketone in which the carbonyl group has been replaced by an azomethine or imine linkage [2]. The common structural feature of these class of compounds is the azomethine functional group (C=N). Schiff bases are represented by the general formula RHC=N-RI, where R and R1 are alkyl, aryl, cycloalkyl or heterocyclic groups which may be substituted with various substituents [3-4]. These compounds are also referred to as anils, imines or azomethines.

Schiff bases are found in living systems where they play important roles in many metabolic processes. They are also present in certain plant species and can be synthesized in the laboratory [2]

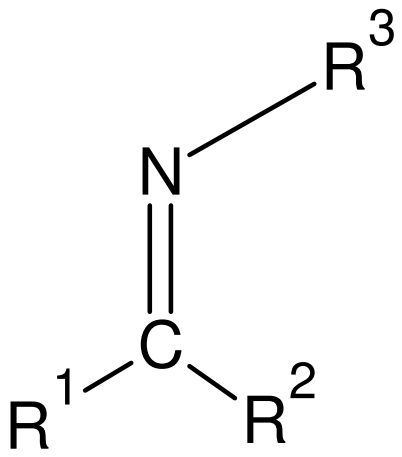

R^1, R^2 and or R^3 are alkyl or aryl

Figure 2.1: General structure of a Schiff base showing an azomethine bond.

2.2.3 Synthesis of Schiff bases

There are several methods developed for the synthesis of Schiff bases, perhaps the most common is the classical method reported by Schiff in 1864 [2, 5-9]. Since then, several other methods have been developed. The classical method involve the refluxing of a carbonyl compound such as aldehydes or ketones with amines in organic solvents under azeotropic conditions [2, 5]. Catalysts were used to accelerate the reaction process. Molecular sieves were used to remove the water formed in the system. The efficiency of this method was dependent on the use of highly electrophilic carbonyl compounds and strongly nucleophilic amines [7].

Later development saw the use of dehydrating agents such as tetramethyl orthosilicate or trimethyl orthoformate to remove the water formed in the system

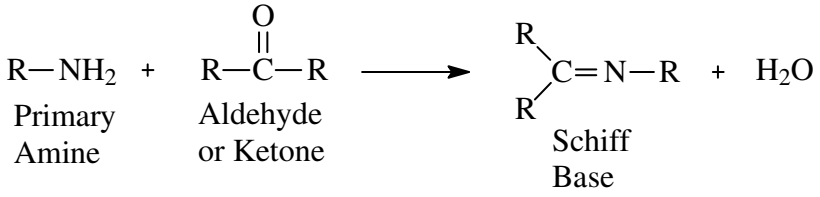

Scheme 2.1: General reaction equation for the preparation of a Schiff base.

The mechanism of Schiff base formation is really a sequence of two steps. The first step is the nucleophilic addition of the amine to the carbonyl compound to form an unstable compound called carbinolamine. The second step involves the elimination of water molecule from the carbinolamine to form Schiff base and water. This is the rate determining step. Both reactions are reversible and require the use of catalysts or the application of heat. However, separating the water from the Schiff base helps drive the reaction to completion. Otherwise aqueous hydrolysis of the carbinolamine to form the amines is possible under certain conditions.

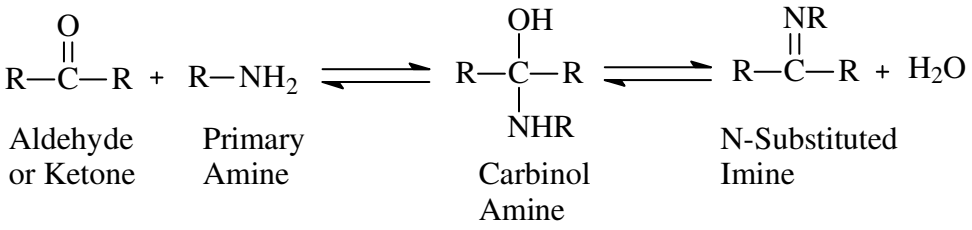

Scheme 2.2: General reaction mechanism for the formation of a Schiff base.

Since the classical method reported by Schiff, a number of innovations and new technique have been reported such as solvent- free/clay/microwave irradiation, solid state synthesis, K-10/microwave, water suspension medium, infrared irradiation/no solvent, silica/ultrasound irradiation solvent-free/CaO/microwave [2]. Among these innovations, microwave irradiation has been extensively used because of its operational simplicity, enhanced reaction rates and greater selectivity. It is also less environmentally problematic because it abolishes the excessive use of organic solvents.

Recent years have witnessed a major drive to increase the efficiency of organic transformations while lowering the amount of waste materials. Many organic solvents are volatile and hazardous to both the environment and human health. The replacement of volatile organic solvents in organic reaction processes is an important green chemistry goal. The use of water as a biodegradable, noninflammable and readily available resource is attractive. Furthermore, the solvent-free or solid state reaction are green methods in the organic synthesis which have numerous advantages including: reduced pollution, lower costs and simplicity in process and handling [5].

2.2.4 Applications of Schiff bases

Schiff bases are one of the largest and most commonly used organic compounds today [2,8]. They are extensively studied, and their chemistry have become a subject of great interests due to their unique characteristics and diversified applications. Schiff bases and their derivatives are very attractive materials for several applications due to the unique properties of the azomethine linkage [2]. Which include inherent pharmacological activities and excellent co-ordination capacity. They also possess a number of other desirable features, including . They are used in various fields of science especially in the area of biological analysis, agriculture, analytical chemistry, food industries, organic synthesis and pharmaceutical [8].

2.2.4.1 Antimicrobial activities

Schiff bases containing the sulfonamide moiety are effective in inhibiting the growth of some bacterial pathogens [9]. Antimicrobial evaluation of compounds derived from 4-amino benzene sulfonamide showed promising inhibitory activities against Gram positive bacteria *(Bacillus subtilis*, *Staphylococcus aureus*), Gram negative bacteria *(Escherichia Coli, Salmonella Typhi*); and fungal strains (*Candida albicans* and *Aspergillus niger*). However, the results indicate that the activities were lower than the reference drugs (ciprofloxacin and ketoconazole). These inhibitory activities were attributed to the presence of the azomethine and sulfonamide functional groups.

Schiff bases derived from guanine and hafnocene as well as their Cd(II) and Hg(III) complexes have been reported to exhibit inhibitory activities against the following organisms- (bacteria) *Escherichia. coli and Pseudomonas aerugenosa* and (fungi) *Aspergillus niger* and *Aspergillus awamori* [10]. However, the results indicates that the complexes had increased activities as compared to the free ligands.

Schiff base containing the thiocyanato moiety and their Co(II), Cd(II) and Hg(II) metal complexes showed significant toxic effect against the fungi *A flavus*. and *F solani*. However the results indicates that all the metal complexes were more active than their corresponding Schiff bases, probably due to the more lipophilic character of the complexes [II].

Isatin derived Schiff bases were reported to possess a broad spectrum of biological activities such as antiviral, anti-HIV, antiprotozoal, anthelmintic and anticonvulsant activities [4]. The synthesis

and antimicrobial activities of a series of Isatin Schiff bases against twenty-eight bacterial strains of clinical interest has recently been reported [6]. Results indicate that the biological activities one of such compounds was more potent against *E. coli, Vibrio cholera Entherococcus faecalis* and *Proteus shigelloides* than sulfathoxazole (reference drug). The MIC values for the compound against the bacteria ranged between 0.3-4.9 ug/mL while the MIC values for the sulfamethazole (reference drug) against the same bacterial strains were in the range of 312- 5000 ug/Ml. thus the isatin derivative was notable between 1020- 4160 fold more potent than the sulphamethoxazole.

Schiff bases derived from aryl aldehydes and aromatic heteroamines were reported to exhibit significant activities against *S. aureus, E. coli, B.subtilis, A. niger and Chara corda*. However, those ligands containing chloro group in the aldehydic group were found to be more potent against all the tested bacterial strains. This increase in potency is due to the toxicity of the chloro group to the micro-organisms [4].

Xipamide Salicylaldimine and its Hg(II), Zn(II) and VO(IV) complexes have been reported to possess good antifungal activities against A. niger and Aspergillus flavus. The metal complexes were found to display superior activities as compared to the ligands. However, these activities were lower than the standard drug except the VO(IV) complexes which exhibited higher biological activities than the standard drug griseofulvin [12].

2.2.4.2 Corrosion control

Corrosion is the oxidative deterioration of a metal, such as the conversion of iron to rust, a hydrated iron(III)oxide ($Fe_2O_3.H_2O$) [13]. Corrosion commonly occurs at metal surfaces in the presence of both oxygen and moisture.

$2Fe_{(s)} \rightarrow 2Fe^{2+}_{(aq)} + 4e^-$ (Oxidation of iron at points of stress in the crystal lattice)

$O_{2(g)} + H_2O_{(l)} + 4e^- \rightarrow 4OH^-_{(aq)}$ (Reduction of water at carbon impurities site)

$2Fe_{(s)} + O_{2(g)} + H_2O_{(l)} \rightarrow Fe(OH)_2$ (Overall equation)

$Fe(OH)_{2(s)} \rightarrow Fe(OH)_3$

$Fe(OH)_{3(s)} \rightarrow Fe_2O_3.nH_2O_{(s)}$ (rust)

Scheme 2.3: Rusting Reaction Mechanism

Corrosion problems have received considerable attention due to their huge economic and safety consequences. The use of inhibitors is one of the most practicable methods for corrosion control. Inhibitors prevent, or at least minimize, corrosion by shielding the base metal from oxygen and moisture. There are several commercially available corrosion inhibitors such as aldehydes or amines, however, the development of better and more efficient corrosion inhibitors is an active area of research.

Several Schiff base derivatives have been reported as effective corrosion inhibitors for a variety of metals and alloys in acidic media [14-16]. These activities are probably due to the presence of the azomethine linkage (C=N). The principal interaction between the inhibitor and the metal surface is chemisorption [12]. The azomethine linkage are capable of forming bonds with the metal surface by electron transfer. Nucleophilic centers, such as oxygen and nitrogen atoms, of the Schiff bases have free electron pairs which are readily available for sharing. They create multiple absorption sites for the Schiff base thus enabling stable monolayer formation on the metal surface [12].

Figure 2.2: Corrosion of iron

2.2.2.3 Colorants

Schiff bases such as Azo group constitute an important class of organic colorants. They have received considerable attention due to their impressive and desirable properties. They are used extensively as dyestuffs for wool, leather, food packaging material, textile and synthetic fabrics because of their extraordinary coloring properties [3,17]. They are also used as chromogenic reagents for the determination of Nickel in food samples [17].

2.2.2.4 Catalysts

A catalyst is a substance which alters the rate of a chemical reaction without being chemically changed at the end of the reaction [18]. Usually, a catalyst speeds up the rate of a reaction by providing an alternative pathway with a lower activation energy. Catalysts play significant roles in chemical industries. They are used to favor the formation of specific products, lower temperatures, save time, energy and cost.

Schiff base derivatives have been used as catalysts in the hydrogenation of hydrocarbons [19,20]

2.2 Metals under investigation

2.3.1 Vanadium

Vanadium compounds play essential roles in catalysis, biological modelling and design of molecular magnets [22]. Several therapeutic properties have been recorded for vanadium compounds. Vanadium compounds stimulate glucose synthesis, glycogen synthesis in the liver, glucose uptake, and glucose oxidation in skeletal muscles and adipocytes. Vanadium compounds also increase Calcium influx, inhibits Ca-Mg ATPase in plasmatic membranes and enhances K uptake in plants. Other pharmacological properties of vanadium compounds include insulin enhancing effects, hormonal, cardiovascular, anti-carcinogenic, antitumor, anti-amoebic, anti-protozoan and antibacterial activities [1-3]. Enzymes containing vanadium such as vanadium nitrogenases and vanadate-dependent halo-peroxidasehave recently been found in in living organisms [23-27]. These discoveries have further escalated interests in the coordination chemistry of vanadium.

2.3.2 COBALT

Cobalt is essential to all animals. It is a key constituent of cobalamine, also known as vitamin B12,

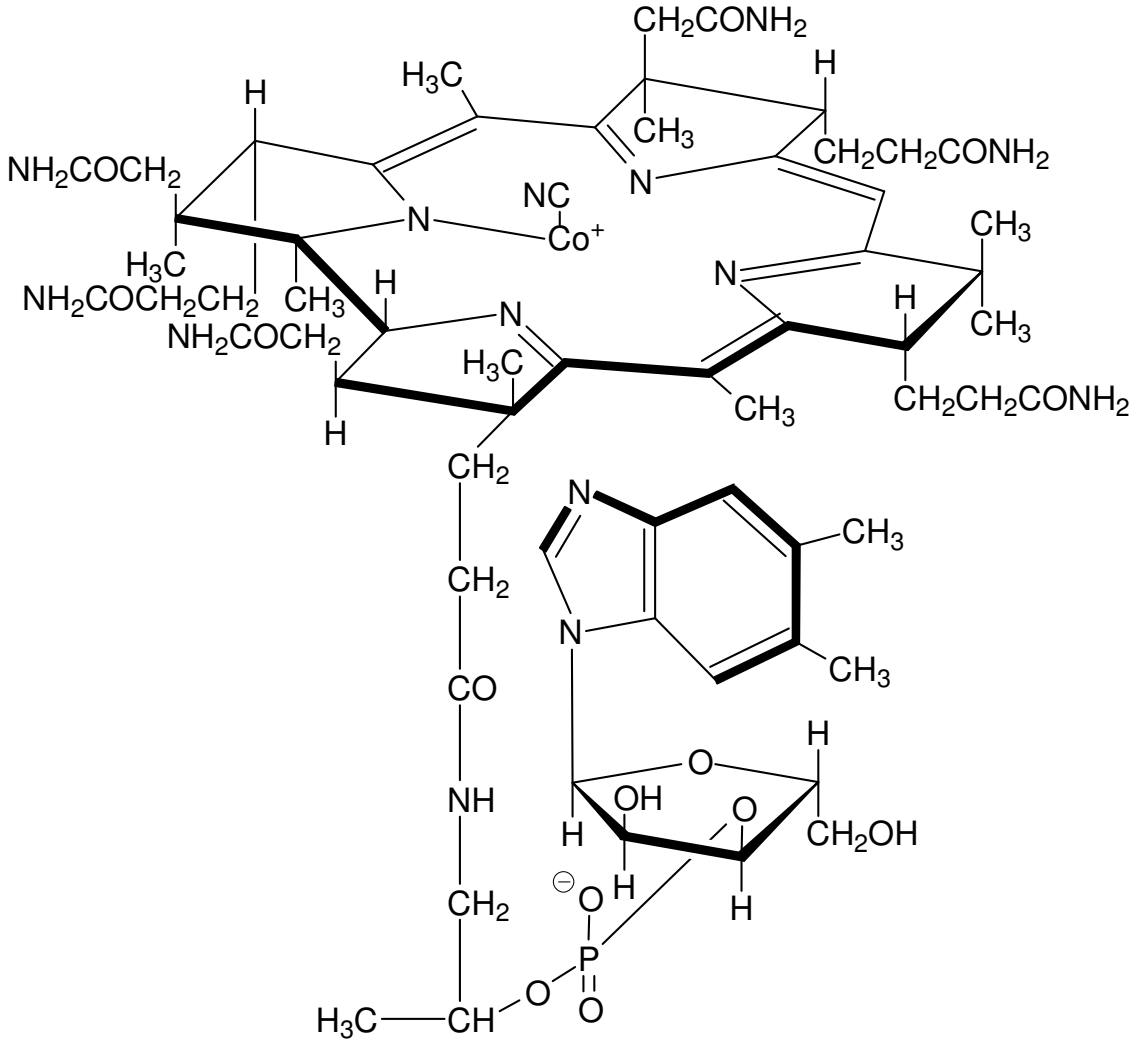

Figure 2.2: Structure of vitamin B12 showing the presence of cobalt.

2.3.3 Manganese

Manganese is an essential trace nutrient in all forms of life. They possess a broad spectrum of pharmacological activities. They function as cofactors for a large variety of enzymes with many functions. They play essential roles in detoxification of superoxide free radicals in organisms, and

in photosynthesis. They are used in the treatment of fish diseases. They are essential ingredients in fertilizers.

2.3.4 Magnesium

In human biology, magnesium is the eleventh most abundant element by mass. Magnesium ions are essential to all living cells, where they play major in manipulating important biological polyphosphate compounds like ATP, DNA and RNA. In vegetation, magnesium is the metallic ion at the center chlorophyll and it is a common additives to fertilizers.

Magnesium possess a broad spectrum of pharmacological properties and have varied applications in medicine. They are used as antiseptics, laxatives, antacids and in the treatment of eclampsia [6].

2.4. Acetyl acetonate ligands

Metal acetylacetonates are coordination complexes derived from the acetylacetonate anion and metal ions, usually transition metals. The ligand acetylacetonate is often abbreviated acac. Typically both oxygen atoms bind to the metal to form a six-membered chelate ring. The simplest complexes have the formula $M(acac)_3$ and $M(acac)_2$. Mixed-ligand complexes, e.g. $VO(acac)_2$, are also numerous. Variations of acetylacetonate have also been developed with myriad substituents in place of methyl [1]. Many such complexes are soluble in organic solvents, in contrast to the related metal halides. Because of these properties, acac complexes are sometimes used as catalyst precursors and reagents. Applications include their use as NMR "shift reagents" and as catalysts for organic synthesis, and precursors to industrial hydroformylation catalysts. $C_5H_7O_2^-$ in some cases also binds to metals through the central carbon atom; this bonding mode is more common for the third-row transition metals such as platinum(II) and iridium(III).

2.5 Micro-organisms

Infectious diseases are a group of illnesses caused by pathogens. The infective pathogens include bacteria, fungi, viruses, protozoa and parasites. Infectious diseases are a leading cause of death globally. Treatment with antibiotics is effective in the control and management of many infectious diseases. However, the emergence of pathogens that are resistant to antibiotic chemotherapy is a major draw-back. A possible solution is to develop new therapies that will fight more aggressively against resistant pathogens.

References

[1] SHIVHARE, S., MISHRA, R., GHARIA, A., & GAUTAM, MD. (**2012**). Synthesis, Characterization and Antimicrobial Studies of Cu (11), Co (11) and Ni (11) Complexes with Schiff bases derived from N-amino rhodanine and salicylaldehyde. *Int. J. Pharm. PHARM. Sci*., 4(1): 394-397).

[2] da SILVER, CM., da SILVER, DL., MODOLO, LV., ALVES, RB., de RESENDE, MA., MARTINS, CVB., de FATIMA, A. (**2011**):, Schiff bases: A short review of their antimicrobial activities. *J. Adv. Res.* (2): 1-8.

[3] BAL, M., CEYHAN, G., AVAR, B., KOSE, M. **2014**. Synthesis and X-ray powder diffraction, electrochemical, and genotoxic properties of a new azo-Schiff base and its metal complexes. *Turk. J. Chem*. (38): 222-241.

[4] ASHRAF, MA., MAHMOO, K., WAJID, A. 2011. Synthesis, Characterization and Biological Activity of Schiff bases. *Int. Conf. on Chem and Chem Pro.* Vol. 10.

[5] ZAREI, M & JARRAHPOUR, A**. 2011**. Green and efficient Synthesis of azo Schiff base. Iranian. *J.Sci & Tech*. A3: 235-242.

[6] QIN, W., LONG, S., PANUNZIO, M., BIONDI, S**. 2013**. Schiff bases: A Short Survey on an Evergreen Chemistry Tool. *Molecules*. (18): 12264-12289

[7] CHAKRABORTI, AK., BHAGAT,S., RUDRAWAR, S. **2004**. Magnesium perchlorate as an efficient catalyst for the synthesis of imines and phenylhydrazones. *Tetrahedron Lett*. 45(41): 7641-7644.

[8] SIDDIQUE, M., BIN SAEED, A., DOGAR, NA., AHMAD, S. **2013**. Biological Potential of Hydrazide Based Schiff bases. *J. Sci. & Inn. Res*. 2(3): 651-657

[9] KUMAR, S., NIRANJAN, MS., CHALUVARAJU, KC., JAMAKHANI, CM &KADADEVAR, D. **(2010)**. Synthesis and antimicrobial study of some Schiff bases of sulfonamides. *J. Curr. Pharm. Res*. 1: 39-42.

[10] MALHOTRA, E., KAUSHIK, NK., MALHORA., HS, **2006.** Synthesis and studies of ionic chelates of halfnocene with guanine. *Indian J. Chem*. 45: 370-376.

[11] UPADHAYAY, N. **2003**. Synthesis, Characterization and Biological Studies of some thiocyano-bridged Bimetalic Complexes Containing Co (11), Cd (11), Hg(11) and N, N'-Bis(benzylidene)-1,2-phenylene-diamine Schiff base. *Chem Sci Trans*. (2): 55-460.

[12] MALIK, S., GHOSH, S., JAIN, B., SINGH, A., BHATTACHARYA, N. **2013**. Synthesis, characterization and biological evaluation of some 3d-metal complexes of Schiff base derived from xipamide drug. *J. Chem*. DOI: 10.1155/549805.

[13] MCMURRY, J., FAY, RC. **2004.** Chemistry, 4th ed. Pearson Education LTD, New Jersey, 790 – 792.

[14] PAUL, A., JOBY THOMAS, K., RAPHAEL, VP., SCHAJU, KS. **2012**. http://www.hindawi.com//journals//isrn.corrosion

[15] SAFAK, S., DURAN, B., YURT, A., TURKOGHE, G.**2012**. Schiff bases as Corrosion Inhibitor for Aluminum in HCL Solution. Corrosion Science 54: 251-259.

[16] BARTYZEL, A**. 2013**. Synthesis, Crystal Structure and Characterization of Manganese (111) complex containing a tetra dentate Schiff base. *J. Coord. Chem*. (66). 4292-4303.

[17] PRAKASH, A & ADHIKARI, D. **2011**. Application of Schiff bases and their metal complexes- A Review. *Int. J. ChemTech Res*. (3): 1891-1896.

[18] EARL, B & WILFORD, LDR. GCSE Chemistry. **2000**, John Murray (Publishers). 50 Albermarie Street. London WIX 4BD. 144-1896.

[19] BADER, NR, **2010**. Applications of Schiff bases Chelates in Quantitative Analysis: A Review. RASAYAN. *J. Chem*., 3(4): 660-670.

[20] KUMAR, S., DHAR, DN., SAXENA, PN. **2009**. Applications of Metal Complexes of Schiff Bases: A Review. *J. Sci. & Ind. Res.,* 68: 181-187.

[21] ASIF, I., ALI, S., SHAHZADI, S., MAHMOOD, S. Vanadium(III) Complexes of Oxygen Donor Ligands; Their Synthesis, Spectral Characterization and Antimicrobial Studies. **2007**. *J. Chinese Chem. Soc*. (54)9: 23-30.

[22] DEVI, RK., DEVI, SP., SINGH, RK. **2012**. Synthesis, Characterization and DNA Interaction Study of a New Oxo-vanadium (1V) Complex Containing Acetyl-acetone and Dicyandiamide as Ligands. *Spec. Letts*. (45)(: 93-103.

[23] CUI, Y., CAI, Y., CHEN, W**. 2011**. Synthesis and Crystal Structures of Schiff base Oxo-vanadium (V) Complexes [VO(BN)(OCH3)]2 and [VO2(BM)]. *Syn. and React. in Inorg Met-Org, and Nano-Met. Chem*. 41: 1244-1248.

[24] REHDER, D. **1999**. The coordination chemistry of Vanadium as related to its biological functions. *Coord. Chem. Rev*.(182): 297-322.

[25] GOLDWASER, I., GEFEL, D., GERSHONOV, E., FRIDKIN, M., SHECHTER, Y. **2000**. Insulin- like effects of Vanadium: Basic and Clinical Implications. *J. Inorg. Biochem*. 80: 21-25

[26] GRANS, DC. **2000**. Chemistry and insulin-like properties of vanadium (1V) and vanadium (V) compounds. *J. Inorg. Biochem*. (80): 123-131

[27] BALLISTRERI, FP., BARBUZZI, EGM., TOMASELLI, GA., TOSCANO, RM. **2000.** Insulin mimesis of vanadium derivatives, oxidation of cysteine by V(V) oxodiperoxo complexes. *J. Inorg. Biochem*. 80: 123-131.

CHAPTER 3

METHODS AND METHODOLOGY

3.1 Introduction

With the increasing number of antibiotics resistant pathogens [[1-2], there has been a growing emphasis on the development of novel antibacterial compounds with superior potency and inferior cytotoxicity as an alternative replacement to conventional antibiotics which have presently become ineffective.

Schiff bases, a class of organic ligands with multiple medicinal benefits and intriguing features such as inherent antibacterial activities, excellent coordination capacity and preparative accessibility, are very attractive material for the design and development of chemotherapeutic agents with potential application for the control of resistant pathogens [3-6]. From literature, incorporating a small amount of metal ions into the molecular scaffold of Schiff bases is an effective way to harness their medicinal benefits and enhance their potency [7-8].

This chapter consists of three sections. The first section describes the synthetic strategy employed in the synthesis of Schiff bases and their metal complexes. The second section outlines the analytical techniques used in characterizing the synthesized compounds. While the third section describes the in vitro antibacterial screening of the Schiff bases and their metal complexes against selected pathogens.

3.2 Experimental

3.2.1 Chemicals and material

All the chemicals used in this project were of analytical reagent (AR) grade and used as received from the suppliers without further purifications. The chemicals were obtained from different suppliers as indicated. The following chemicals:-Methanol, Dimethyl sulfoxide. Dimethyl formamide, Hydrogen peroxide, distilled Acetyl acetone, acetone, 4-methoxbenzhydrazide, 4-diethyl (amino)-2-hydroxybenzaldehyde, 4-dimethyl(amino)-2 hydroxybenzaldehyde, 4-

nitrobenzohydrazide, Cadium acetate dihydrate and Cobalt(II) acetatetetrahydratewere purchased locally from Sigma-Aldrich. Magnesium Chloride hexahydrate, Potassium permanganate, Vanadium pentoxide, Ferric Chloride hexahydrate, Nickel(II) Chloridehexahydrate, Zinc(II) acetate, Copper(II) acetate, Calcium Chloride, Potassium Hydroxideand Sodium Hydroxide were purchased from LABCHEM. Distilled water, where neededwas used throughout this project.

The micro-organisms (*Enterococcus faecalis and Staphylococcus aereus*) used in biological testing were obtained from the Department of Microbiology, University of the North-West.

3.3 Synthetic procedure

3.3.1 Synthesis of Metal Acetylacetonates

Acetyl acetonatesalts of VO(II), Co(III), Co(II), Mn(IV), Mg(II), Cu(II), Ni(II), Fe(III), Zn(II) and Cd(II) were prepared by reacting their metal hydroxideswith acetylacetone (12). The resulting crystals were separated by filtration using whateman No. 2 filter paper and dried in a vacuum desiccator for 48 hrs.

3.3.1.1 Synthesis of Vanadyl Acetylacetonate: $VO(acac)_2$

Vanadium pentoxide (5g, 3.56 mmol) was dissolved in 20 ml water in a 500 ml beaker. 30% hydrogen peroxide (37.37 ml, 329.88 mmol) was added drop wise in an ice cold condition and stirred till a clear dark solution was formed (12). Distilled acetylacetone (19.84 ml, 192.5 mmol) was added to the dark solution. Vigorous effervescent took place after 15 min. Stirring for a further 30min led to the formation of brown microcrystalline compound. The reaction mixture was heated at 70ºC for 15 min under stirring. The precipitate turned olive green with shiny crystalline appearance and the solution also turned green. The mixture was concentrated by heating on steam bath for 30min and then placed in an ice-water bath for 15 min. The Green crystals of vanadyl acetylacetonate formed was filtered using Whatman No. 2 filter paper, washed with acetone and placed in a desiccator for 48 hrs to dry over anhydrous $CaCl_2$. The equation for the reaction is given in Scheme 1.

$$C_5H_8O_2 + V_2O_5 \xrightarrow[H_2O_2]{} VO(C_5H_7O_2)_2$$

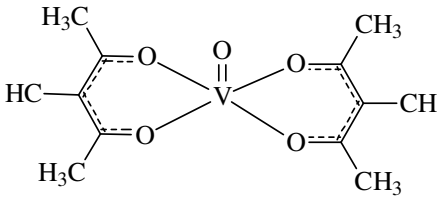

3.3.1.2 Synthesis of Magnesium Acetylacetonate dihydrate

Magnesium Chloride hexahydrate (10 g, 49.19 mmol) was dissolved in 200 ml water in a 500 ml beaker. KOH (20%) was added slowly with constant stirring to precipitate the metal as its hydroxide. The addition of the alkali was continued until the pH of the solution was raised to.8. The metal hydroxide formed was repeatedly washed with water to remove all traces of the alkali followed by decantation and finally filtered using Whatman No. 2 filter paper.

The $Mg(OH)_2$ formed was quantitatively transferred into a 250 ml beaker. Distilled acetylacetone (11.15 ml, 108.21 mmol) was added drop wise with stirring. An exothermic reaction took place leading to the formation of a white crystalline compound. The crystals were allowed to stand at room temperature for 30 min and then placed on an ice-water bath for 15 min. The white crystals of Magnesium acetylacetonate formed was filtered using Whatman No. 2 filter paper and dried in a desiccator over anhydrous $CaCl_2$ for 48 hrs. The equations for the reactions are given in Scheme 2.

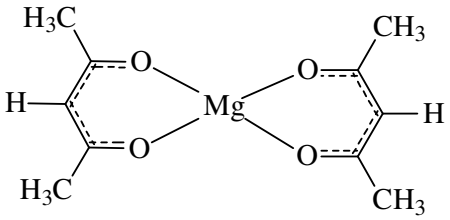

3.3.1.3 Synthesis of Cobalt(II) Acetylacetonate Dihydrate $Co(acac)_2$

Cobalt(II) acetate tetrahydrate (10 g, 40.1 mmol) was dissolved in 200 ml water in a 500 ml beaker [12]. KOH (20%) was slowly added with constant stirring. Initially a blue precipitate was formed. The precipitate was stirred for 10min and allowed to stand for 30min. The color of the precipitate changed from blue to green and finally to pink, to generate the Cobalt (II) hydroxide (pH- 8). The metal hydroxide formed was washed free of alkali by repeatedly washing with water followed by decantation and finally filtered through Whatman No. 2 filter paper.

The pink Cobalt(II) hydroxide was quantitatively transferred into a beaker (100 ml), acetylacetone (9.1 ml, 88.2 mmol) was added and mixed thoroughly with a glass rod. An exothermic reaction took place leading to the formation of pink shiny crystals of $Co(acac)_3.2H_2O$. The compound was allowed to stand at temperature for 30min, and in an ice-water bath for 15min. The crystals were recovered by filtration and dried in a dessicator over anhydrous CaO for 48 hrs. The equations for the reactions are given in Scheme 1.

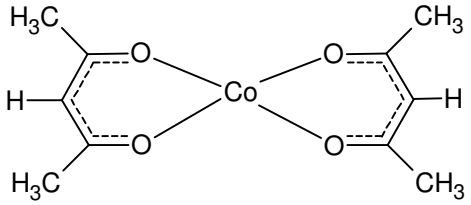

3.3.1.4 Synthesis of Cobalt (III) acetylacetonate $Co(acac)_3$.

Cobalt (11) acetate tetrahydrate (10g, 40.1mmol) was dissolved in 200 ml water in a 500 ml. KOH (20%) was added slowly with constant stirring. Initially a blue precipitate was formed. The precipitate was stirred for 10 min and allowed to stand for 30 min. The color of the precipitate changed from blue to green and finally to pink, to generate the Cobalt(II) hydroxide (pH- 8). The metal hydroxide formed was washed free of alkali by repeatedly washing with water followed by decantation and finally followed by filtration through Whatman No. 2 filter paper.

The pink Cobalt(II) hydroxide was quantitatively transferred into a 250 ml beaker. 11ml of acetylacetone was added, and mixed thoroughly with a glass rod. An exothermic reaction took place leading to the formation of pink shiny crystals of $Co(acac)_2.2H_2O$. 30% hydrogen peroxide (11.36 mL, 100.25 mmol) was added drop wise with constant stirring and the green mixture heated

on a steam bath for complete oxidation of oxidation of Co(II) to Co(III) and expulsion of hydrogen peroxide. The mixture was cooled at room temperature for 30min with occasional stirring. The beaker was placed in an ice-water bath for 15min. The green crystals of $Co(acac)_3.2H_2O$ formed was recovered by filteration using Whateman No. 2 filter paper and dried in a desiccator over anhydrous calcium oxide. The equations for the chemical reactions are given in Scheme 4.

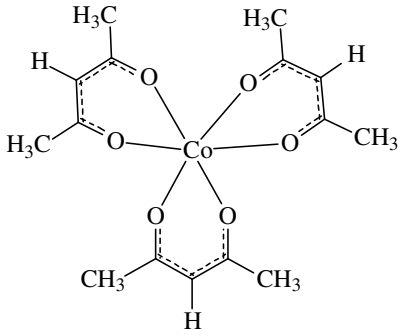

3.3.1.5 Synthesis of Manganese (1V) acetylacetonate $Mn(acac)_2$.

Powdered $KMnO_4$ (5.0 g, 31.7 mmol) was dissolved in 100 ml water in a 250 ml beaker by slight warming over a steam bath. The solution was filtered with a Whatman No. 2 filter paper and transferred to 250 ml beaker. 22 ml of acetylacetone (22.0 mL, 220 mmol) was added to the beaker. The whole mixture was stirred for 15min over steam bath and allowed to cool for 10min. The dark brown shinny crystals of $Mn(acac)_3$ formed was recovered by filtration through a Whatman No. 2 filter paper and dried in vacuo over fused $CaCl_2$. The equation for the reaction is given in Scheme 5.

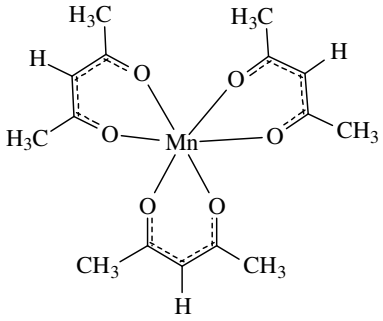

3.3.1.6 Synthesis of Iron(III) acetylacetonate ($Fe(acac)_3$).

Iron(III) Chloride was dissolved in 200 ml water in a 500 ml beaker. KOH (20%) was added slowly with constant stirring to precipitate the Iron(III) hydroxide as desired. The addition of alkali was

continued until the pH of the solution was raised to 8. The suspended precipitate was allowed to settle with the supernatant liquid becoming colorless. The flocculent was washed several times with water by decantation, and filtered through Whatman No. 2 filter paper and again washed twice with cold water. The Iron(III) hydroxide formed was quantitatively transferred into a 250 ml beaker. 11.1 ml of acetylacetone was added to the slurry and mixed thoroughly with a glass rod. The whole mixture was allowed to stand at room temperature for 30min with occasional stirring. An exothermic reaction took place leading to the formation of a deep red shiny crystals of $Fe(acac)_3$. The reaction container was then placed on an ice-water bath for 15 min. The compound formed was recovered by filtration through Whatman No. 2 filter paper and dried in a desiccator over anhydrous $CaCl_2$. The equations for the chemical reactions are given in Scheme 6.

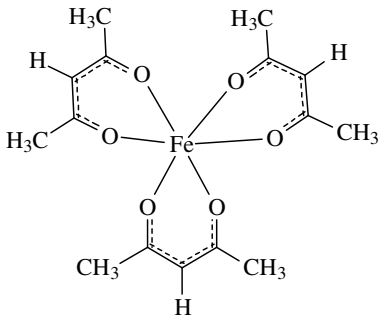

3.3.1.7 Synthesis of Nickel(II) acetylacetonate dihydrate

Nickel(II) chloride hexahydrate (15 g, 68.18 mmol) was dissolved in 200 ml water in a 500 ml beaker. 20% aqueous solution of KOH was added slowly with constant stirring to precipitate the metal as its hydrated oxide. The addition of alkali was continued till the pH of the solution was raised to 8. The precipitate was recovered by filtration through Whatman No. 2 filter paper, washed several times with water to remove traces of the alkali and quantitatively transferred into a 250 ml beaker 15.45 ml of acetyl acetone was added to the precipitate and mixed thoroughly with a glass rod. An exothermic reaction took place leading to the formation of blue shiny crystals of $Ni(acac)_2.2H_2O$. The semi-solid mass was continuously stirred for 10min, the sample was kept at room temperature for 30min and placed in an ice-water bath for 15 min. The compound was recovered by filtration and dried in a desiccator over anhydrous Calcium Chloride.

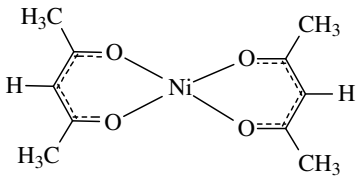

3.3.1.8 Synthesis of Copper(II) acetylacetone

Copper(II) acetate monohydrate (1 g, 50.09 mmol) was dissolved in (300 mL) water in a beaker (500 mL) by warming at 60ºC for 15 min [12]. The solution was cooled at room temperature for 30 min. 20% aqueous solution of KOH was added slowly with constant stirring to precipitate the metal as its hydrated oxide. The addition of the alkali was continued until the PH of the solution was raised to 8. The metal hydroxide formed was washed free of alkali by repeatedly washing with water followed by decantation. Acetylacetone (1 ml) was added drop wise with constant stirring. An exothermic reaction took place leading to the formation of blue shiny crystals of $Cu(acac)_2$. The beaker was allowed to stand at room temperature for 30 min and then placed on an ice-water bath for 15 min. The blue crystals of Copper(II) acetylacetonate formed was recovered by filtration using Whatman No. 2 filter paper and dried in a desiccator over anhydrous $CaCl_2$.

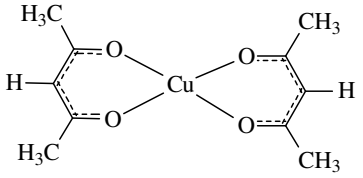

3.3.1.9 Synthesis of Zinc(II) acetylacetonate

Zinc(II) acetate dihydrate (1 g, 4.6 mmol) was dissolved in 100 ml water in a 250 ml beaker. 5% aqueous solution of NaOH was added slowly with constant stirring to precipitate the metal as $Zn(OH)_2$. The addition of the alkali was continued until the pH of the solution was raised to 8. The metal hydroxide formed was washed free of alkali by repeated washing with water by decantation. The sample was centrifuged and rinsed with water. 1 ml of acetylacetone was added to the centrifuge tube and stirred with a glass rod. An immediate reaction took place leading to the formation of white crystals of $Zn(acac)_2.xH_2O$. The crystals were quantitatively transferred to Whatman No. 2 filter paper and dried in a desiccator over anhydrous $CaCl_2$ for 48 hrs.

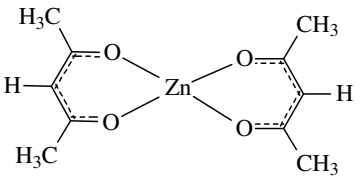

3.3.1.10 Synthesis of Cadmium acetylacetonate

Cadmium(II) acetate dihydrate (10 g, 49.19 mmol) was dissolved in 200 ml water in a 500 ml beaker. Aqueous solution of KOH (20%) was added slowly with constant stirring to precipitate Cadmiun(II) hydroxide. The addition of the alkali was continued until the pH of the solution was raised to 8. The metal hydroxide was washed free of alkali by repeated washing with water followed by decantation. The sample was centrifuged and rinsed with water. Distilled acetylacetone (10 ml) was added into the centrifuge tube and stirred with a glass rod. An exothermic reaction took place leading to the formation of white shiny crystals of Cadmium(II) acetylacetonate. The sample was filtered with Whatman No. 2 filter paper and dried in a desiccator over anhydrous $CaCl_2$ for 48 hrs. The equations for the reactions are given in Scheme 10.

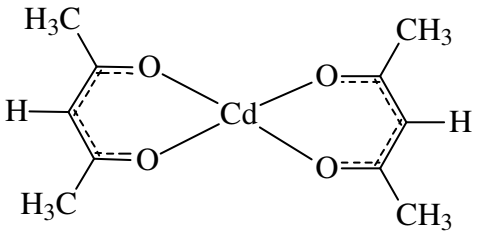

3.3.2 Synthesis of Schiff bases

The Schiff base ligands were prepared according to the method described in the literature [13]. A stoichiometric quantities of the respective aldehyde (10 mmol) and amine (10 mmol) were dissolved in 100 ml methanol [13] and refluxed at 70^{o}C for 2h. The resultant mixture was cooled to room temperature and then concentrated to a volume of 20 ml. The solid product formed was recovered by filtration, washed with methanol and dried in a desiccator over anhydrous calcium chloride. This procedure was adopted for the synthesis of all the four Schiff base ligands.

3.3.2.1 Synthesis of Schiff base ligand L1

A stoichiometric amounts of 4-(diethylamino)-2-hydroxybenzaldehyde (10 mmol) and 4-nitrobenzohydrazide (10 mmol) were dissolved in 100ml methanol in a 250ml round bottom flask. The mixture was stirred vigorously for 20 min, and refluxed at 70oc for 2 h in a round bottom flask equipped with a water condenser [14]. The resulting solution was cooled to room temperature and the volume reduced to 20 ml. The solid product formed was recovered by filtration using Whatman No. 2 filter paper, washed with methanol and dried over anhydrous calcium chloride in a vacuum desiccator.

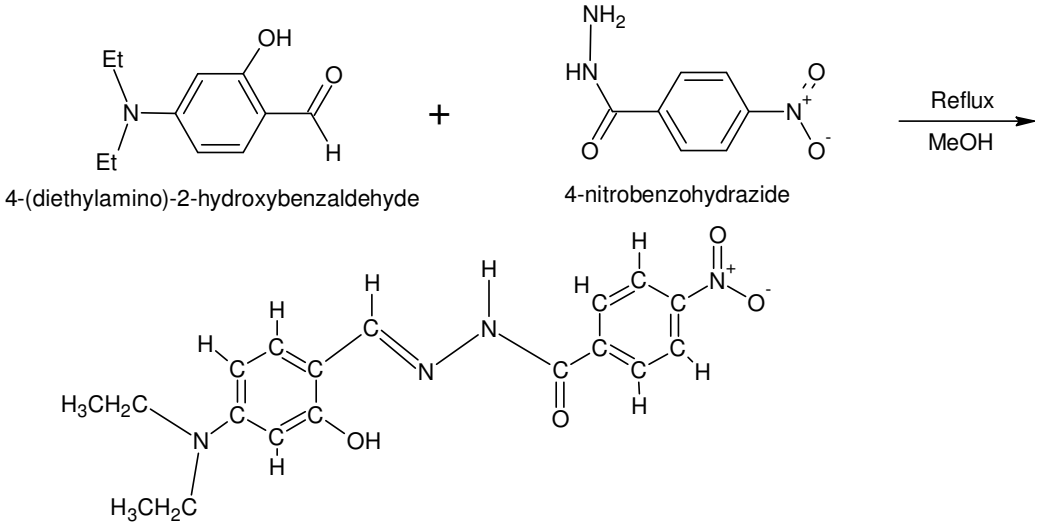

4-(diethylamino)-2-hydroxybenzaldehyde

4-nitrobenzohydrazide

N-{(*E*)-[4-(diethylamino)-2-hydroxyphenyl]methylidene}-4-nitrobenzohydrazide

3.3.2.2 Synthesis of Schiff base L2

The method used for the synthesis of Schiff base ligand L2 was similar to the one reported in the literature for the synthesis of ligand L1 [3]. A stoichiometric amounts of a (10 mmol) and b (10 mmol) were dissolved in 100ml methanol in a round bottom flask, accompanied by vigorous stirring for 20 min. The mixture was refluxed, in a round bottom flask fitted with a water condenser, at 70^{o}C for 2h. The resultant solution was cooled to room temperature and concentrated to a volume of 20 ml in a fume cupboard. The solid product formed was recovered by filtration through Whatman No. 2 filter paper, washed with methanol and dried over anhydrous calcium chloride in a vacuum desiccator.

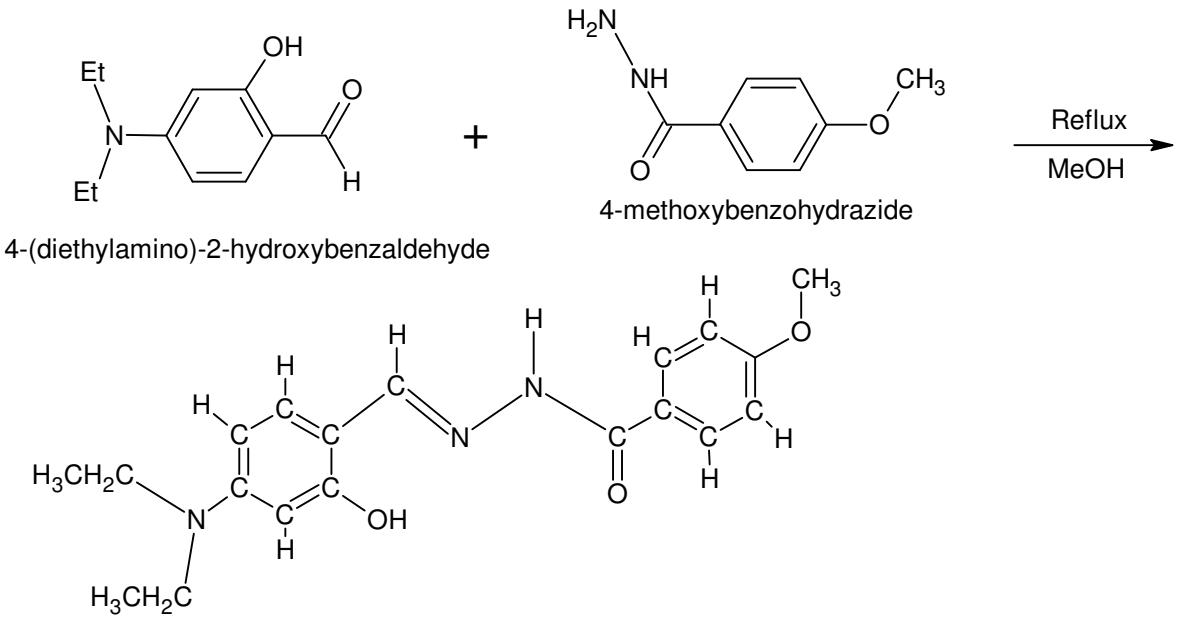

4-(diethylamino)-2-hydroxybenzaldehyde

4-methoxybenzohydrazide

N'-{(*E*)-[4-(diethylamino)-2-hydroxyphenyl]methylidene}-4-methoxybenzohydrazide

3.3.2.3 Synthesis of Schiff base L3

An identical method reported in the literature for the synthesis of L1 was adopted for the synthesis of L3 [14]. A stoichiometric quantities of a (10 mmol) and b (10mmol) were dissolved in 100ml methanol in a round bottom flask, accompanied by vigorous stirring for 20min.The mixture was refluxed, in a round bottom flask equipped with a condenser, at 70oc for 2h. The resultant solution was cooled to room temperature and concentrated to a volume of 20ml. The solid product formed was recovered by filtration, washed with methanol and dried over calcium chloride in a vacuum desiccator.

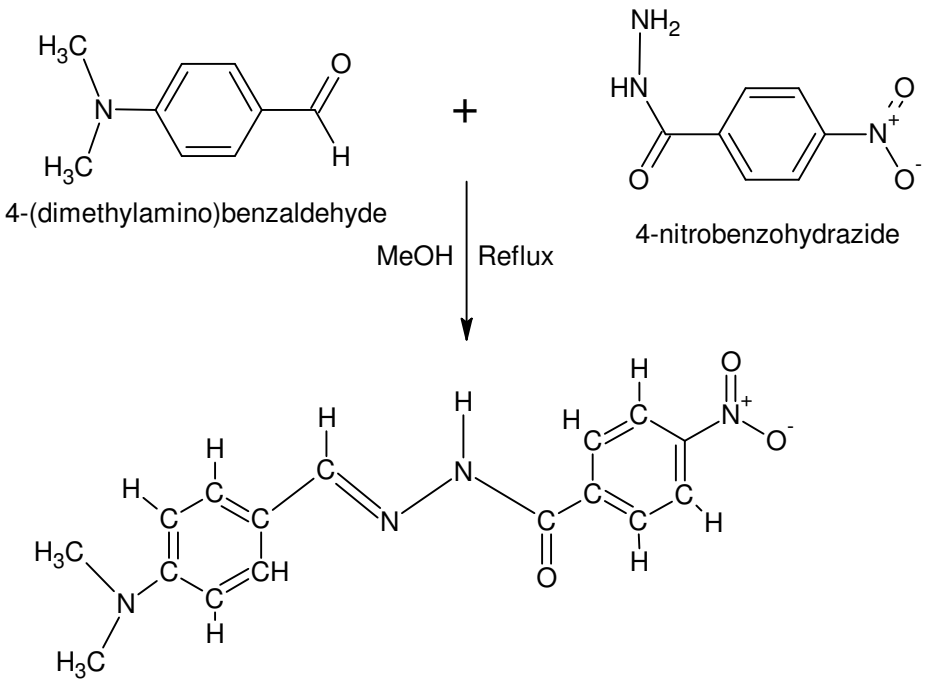

N'-{(*E*)-[4-(dimethylamino)phenyl]methylidene}-4-nitrobenzohydrazide

3.3.2.4 Synthesis of Schiff base L4

An identical method reported in the literature for the synthesis of L1 was adopted for the synthesis of L4 [14]. A stoichiometric quantities of a (10 mmol) and b (10mmol) were dissolved in 100ml methanol in a 250ml round bottom flask, accompanied by vigorous stirring for 20 min.The mixture was refluxed in a round bottom flask equipped with a water condenser, at 70oc for 2h. The resultant solution was cooled to room temperature and concentrated to a volume of 20ml. The solid product formed was recovered by filtration, washed with methanol and dried over calcium chloride in a vacuum desiccator.

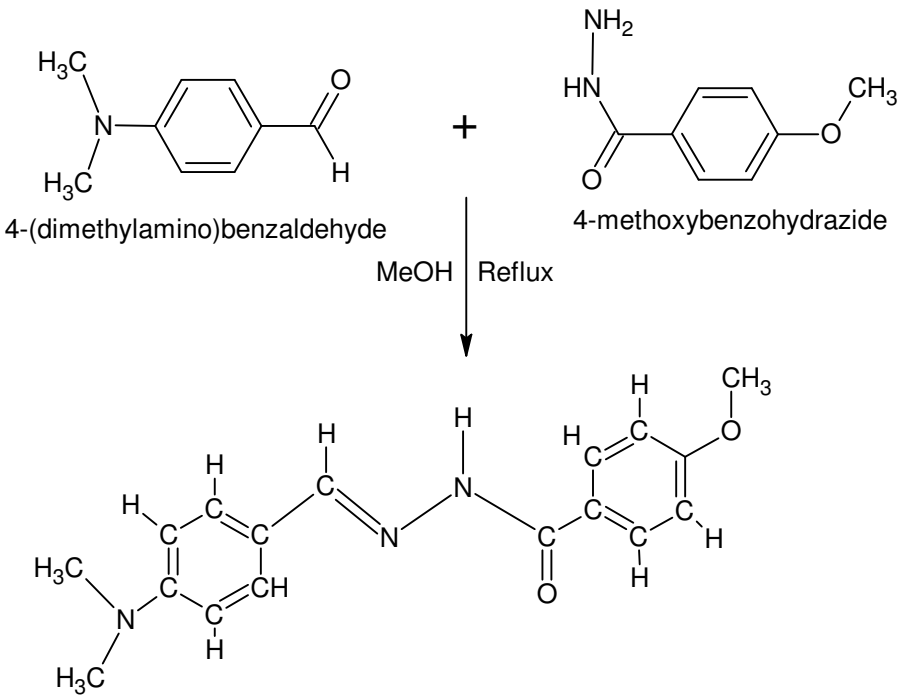

N'-{(*E*)-[4-(dimethylamino)phenyl]methylidene}-4-methoxybenzohydrazide

3.3.3 Synthesis of Schiff base complexes

Equimolar quantities of Schiff base ligand L1 and metal acetylacetonate salts- were dissolved in 30 ml methanol in a round bottom flask fitted with a water condenser. The mixture was stirred vigorously for 20 min. and refluxed over a steam bath at 70ºC for 1 hr. The resultant solution was left overnight in a fume cupboard at ambient temperature until all traces of the solvent had evaporated. The solid formed was washed with methanol and dried over anhydrous calcium chloride in a vacuum desiccator for 48 hrs.

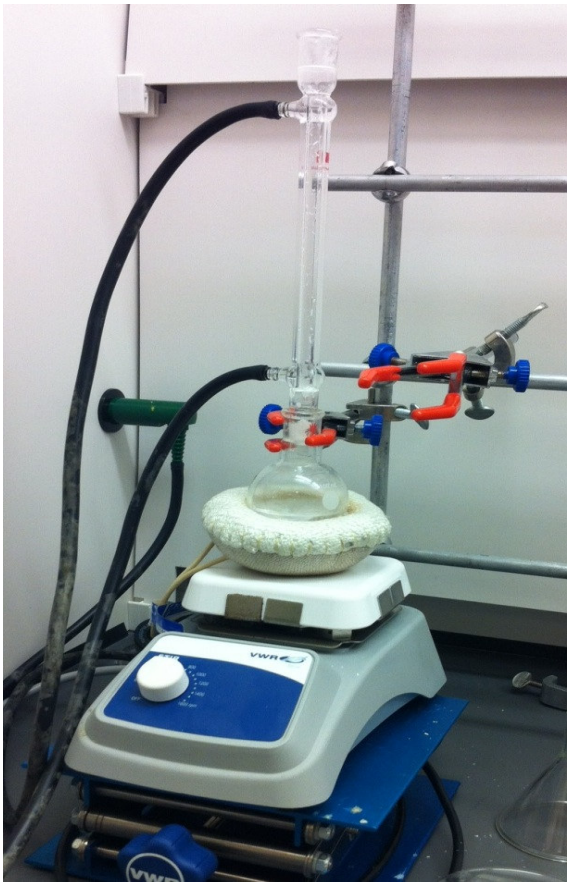

Figure 3.1: Photo of reflux condenser.

3.3.3.1 Synthesis of Schiff base complexes 1-4

A stirred solution of L1 and $VO(acac)_2$, $Mn(acac)_3$, $Co(acac)_3$ and $Mg(acac)_2$, (0.01 mol) respectively were mixed in a 250 ml round bottom flask fitted with a water condenser. The mixture was refluxed over a steam bath for 1h. The resultant solution was left overnight in a fume cupboard at ambient temperature until all traces of the solvent had evaporated. The solid obtained was washed with methanol and dried in a vacuum desiccator over anhydrous calcium hydroxide for 48 hrs.

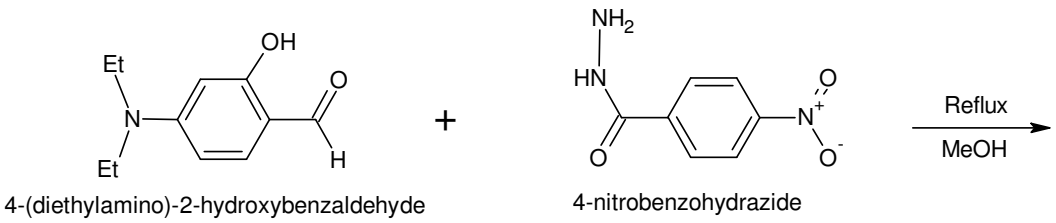

4-(diethylamino)-2-hydroxybenzaldehyde

4-nitrobenzohydrazide

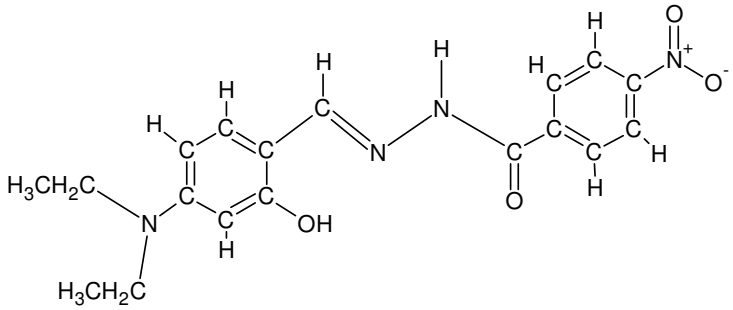

Ligand 1

N'-{(*E*)-[4-(diethylamino)-2-hydroxyphenyl]methylidene}-4-nitrobenzohydrazide

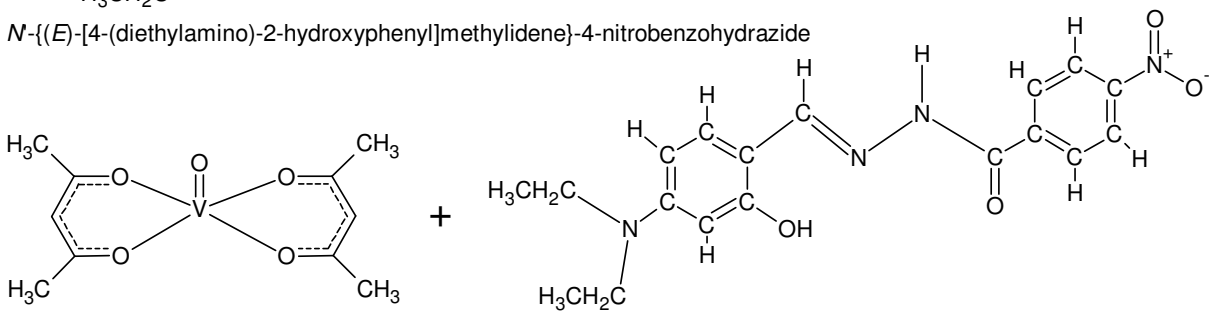

N'-{(*E*)-[4-(diethylamino)-2-hydroxyphenyl]methylidene}-4-nitrobenzohydrazide

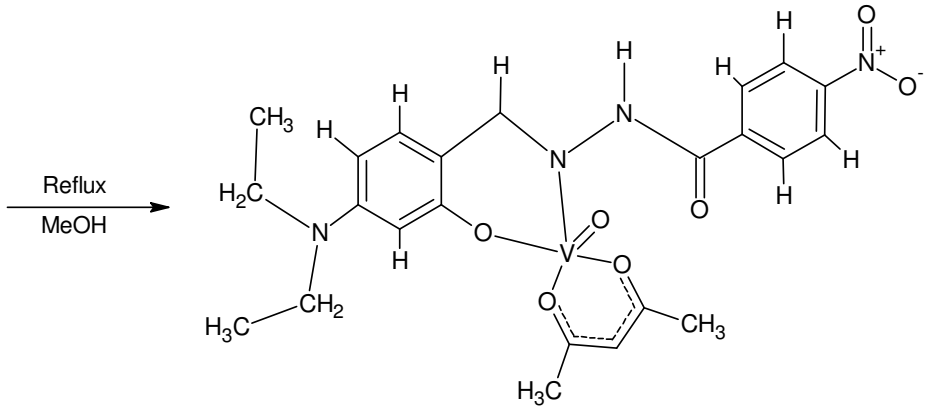

Schiff Base Complex 1A (SBC1A)

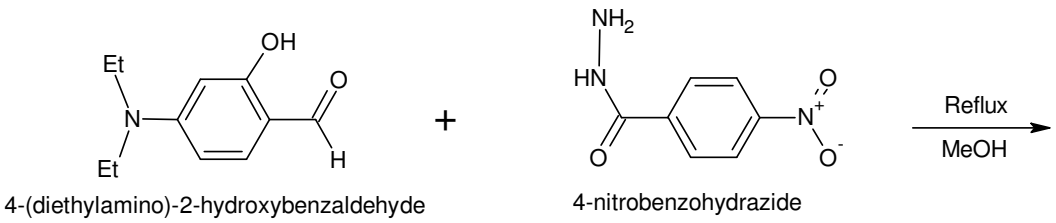

4-(diethylamino)-2-hydroxybenzaldehyde

4-nitrobenzohydrazide

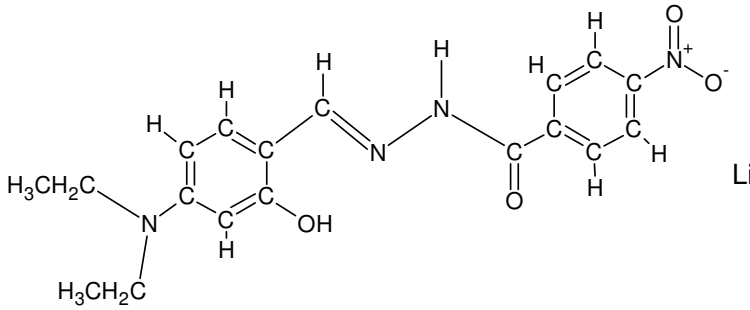

Ligand 1

N'-{(*E*)-[4-(diethylamino)-2-hydroxyphenyl]methylidene}-4-nitrobenzohydrazide

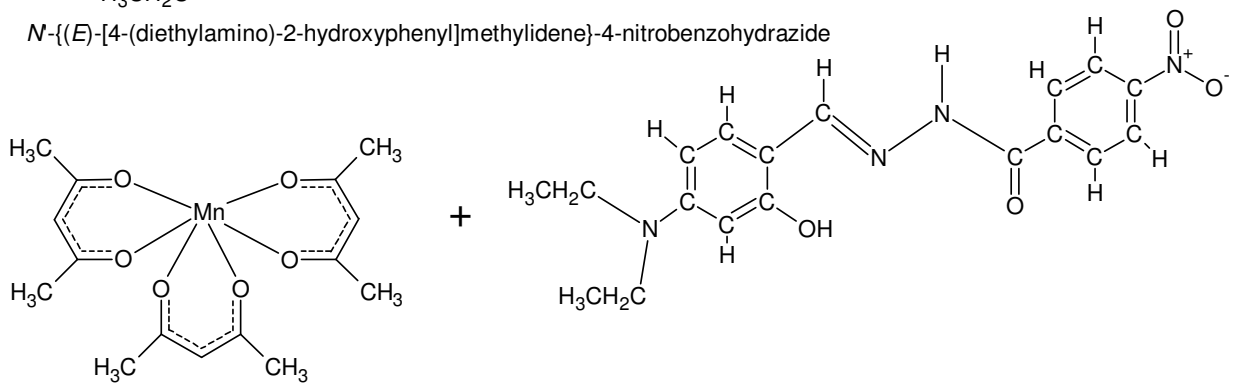

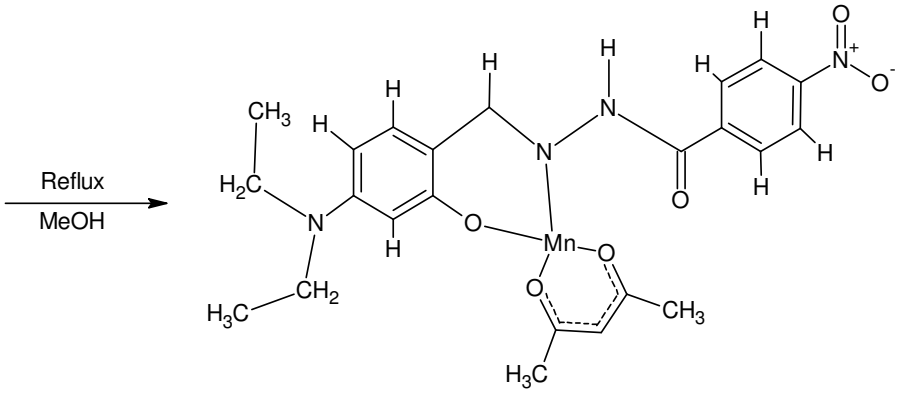

Schiff Base Complex 2A (SBC 2A)

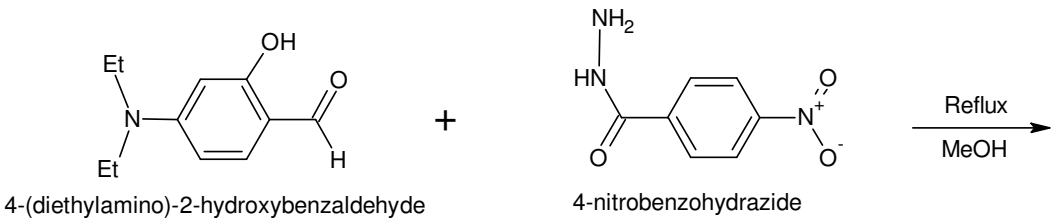

4-(diethylamino)-2-hydroxybenzaldehyde

4-nitrobenzohydrazide

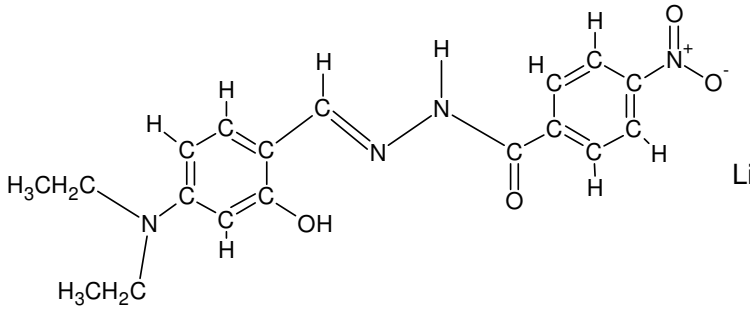

Ligand 1

N'-{(*E*)-[4-(diethylamino)-2-hydroxyphenyl]methylidene}-4-nitrobenzohydrazide

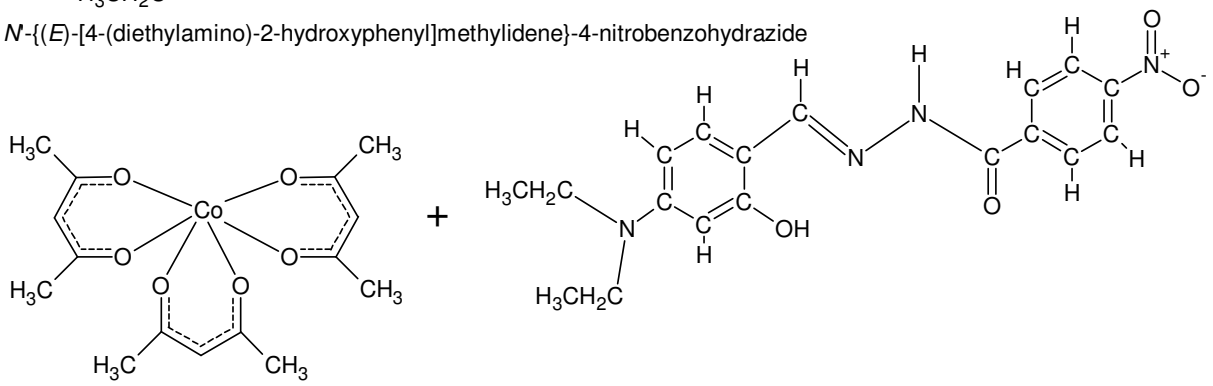

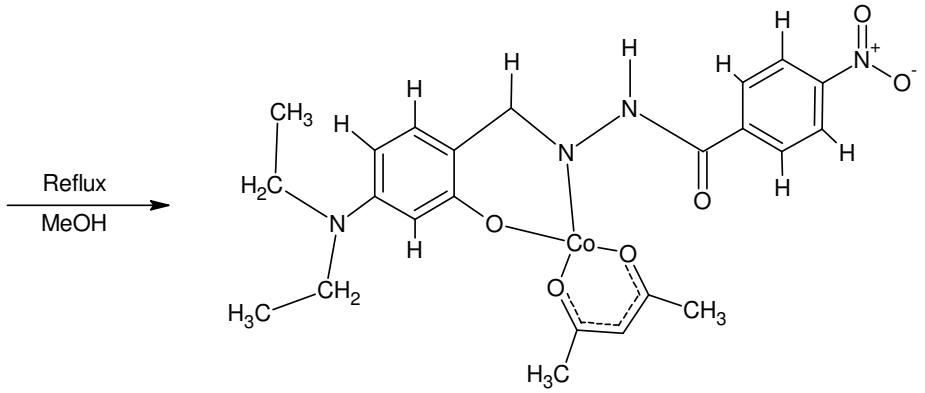

Schiff Base Complex 3A (SBC 3A)

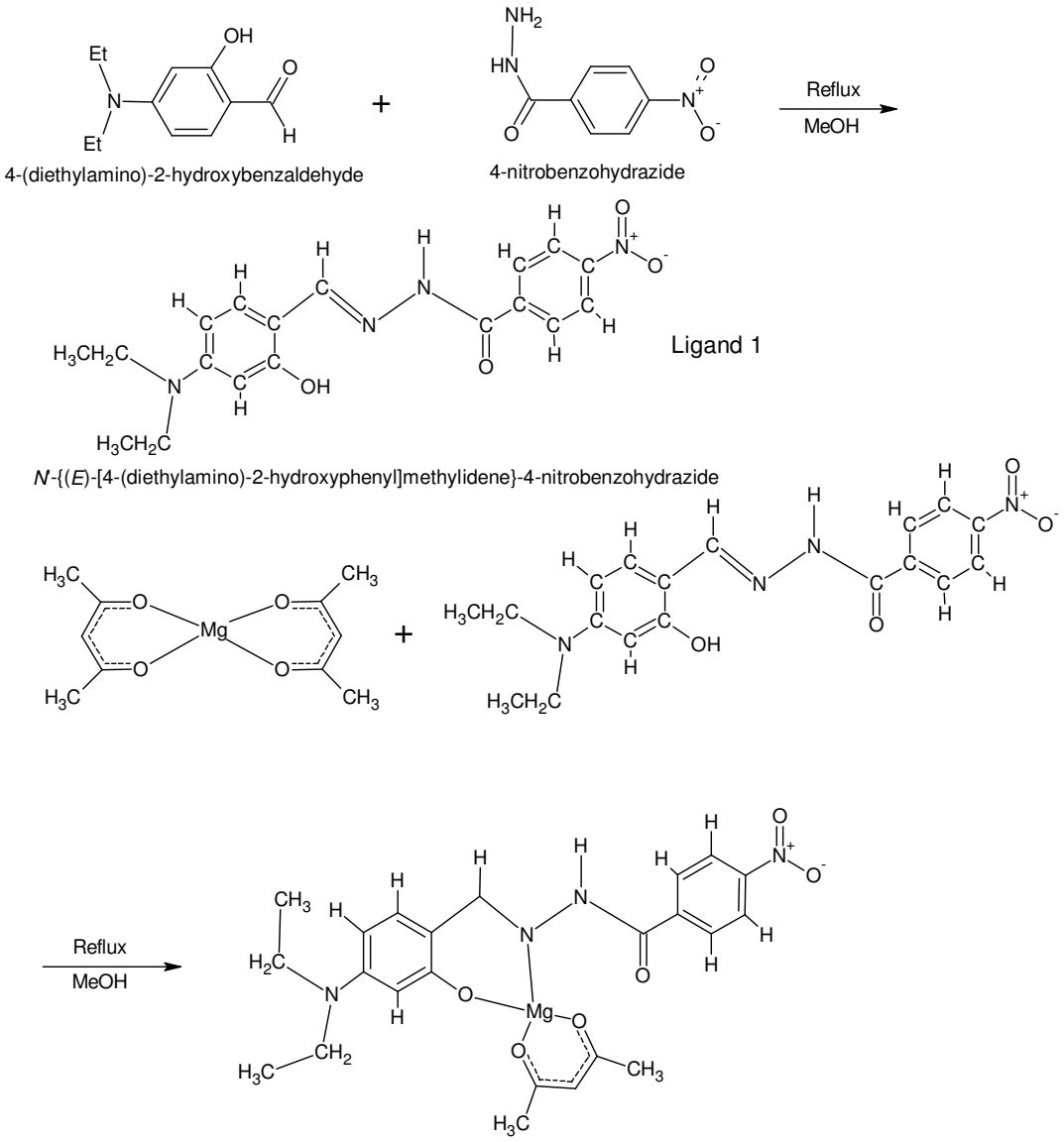

Schiff Base Complex 4A (SBC 4A)

3.3.3.2 Synthesis of Schiff base complexes 5-8

A stirred solution of L2 and $VO(acac)_2$, $Mn(acac)_3$, $Co(acac)_3$ and $Mg(acac)_2$, (0.01 mol) respectively were mixed in a 250 ml round bottom flask fitted with a water condenser. The mixture was refluxed over a steam bath for 1h. The resultant solution was left overnight in a fume cupboard at ambient temperature until all traces of the solvent had evaporated. The solid obtained was washed with methanol and dried in a vacuum desiccator over anhydrous calcium hydroxide for 48 hrs.

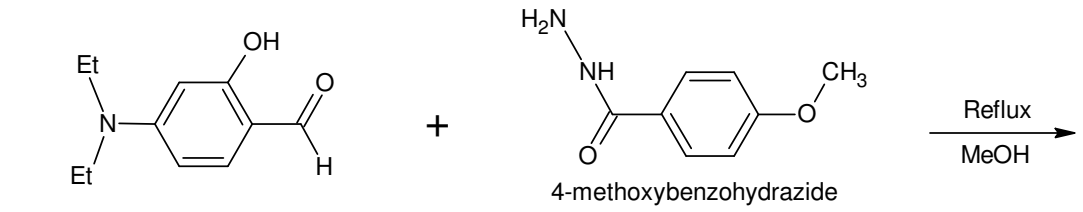

4-(diethylamino)-2-hydroxybenzaldehyde

4-methoxybenzohydrazide

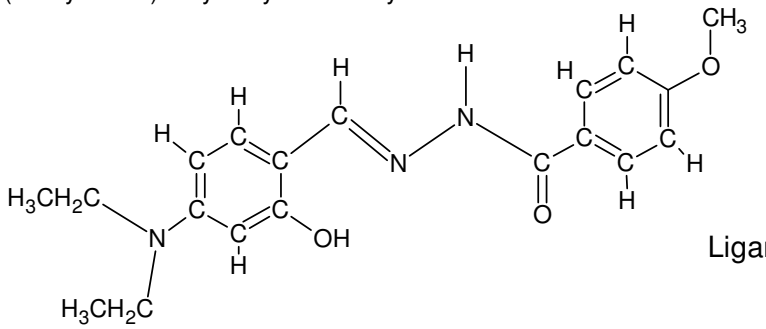

Ligand 2

N′-{(*E*)-[4-(diethylamino)-2-hydroxyphenyl]methylidene}-4-methoxybenzohydrazide

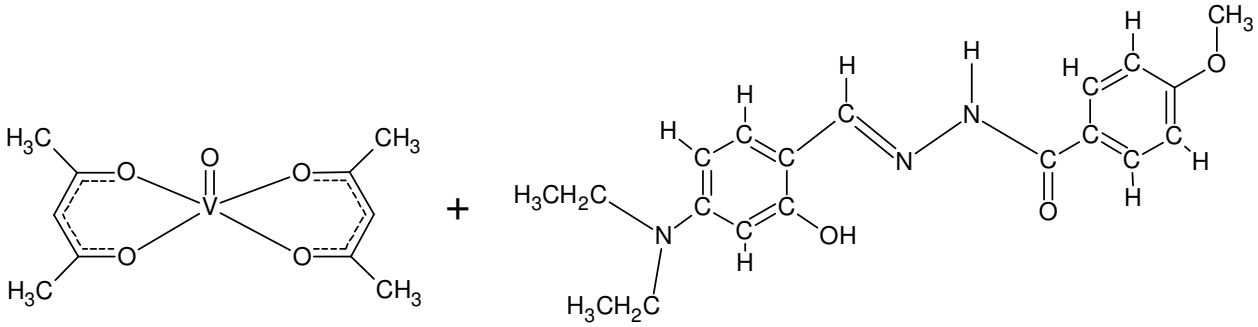

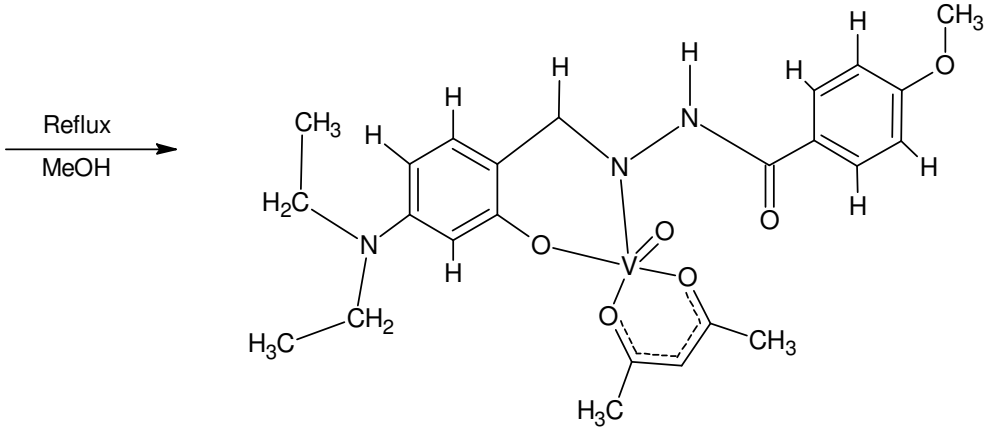

Schiff Base Complex 1B (SBC 1 B)

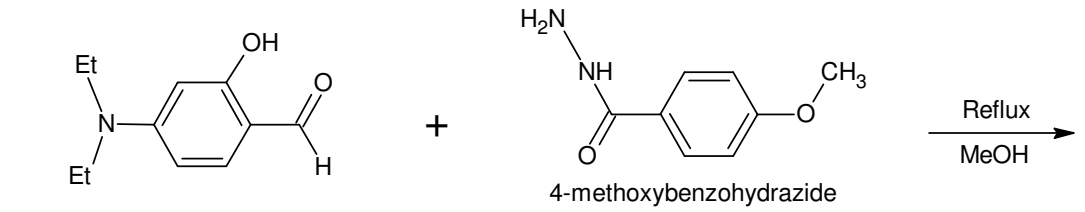

4-(diethylamino)-2-hydroxybenzaldehyde

4-methoxybenzohydrazide

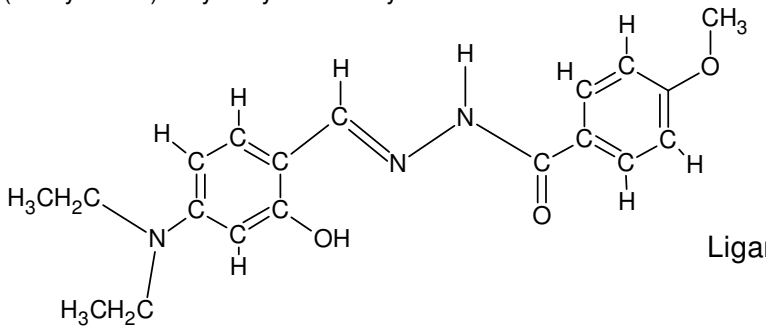

Ligand 2

N-{(*E*)-[4-(diethylamino)-2-hydroxyphenyl]methylidene}-4-methoxybenzohydrazide

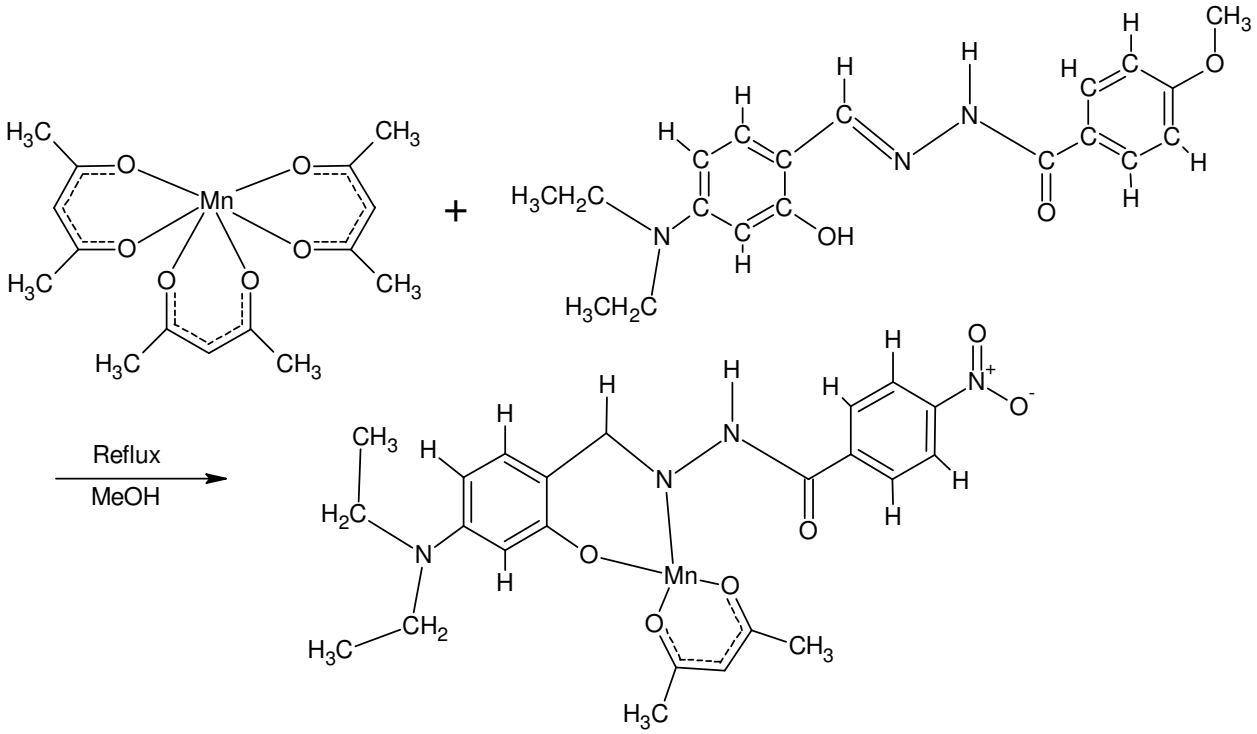

Schiff Base Complex 2B (SBC 2B)

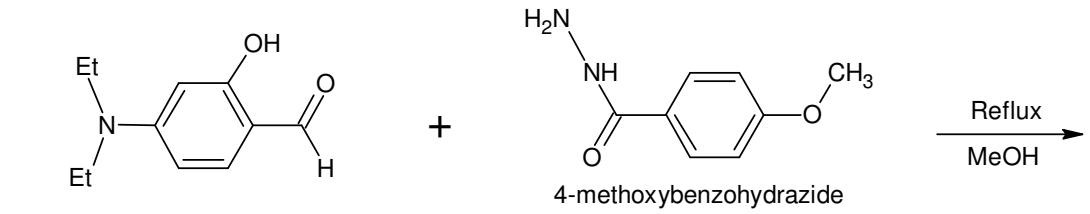

4-(diethylamino)-2-hydroxybenzaldehyde

4-methoxybenzohydrazide

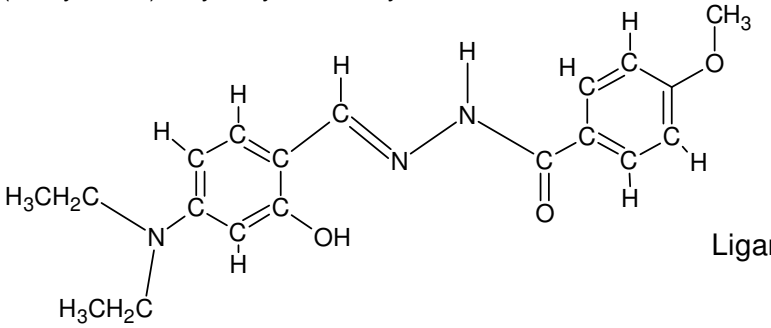

Ligand 2

N'-{(*E*)-[4-(diethylamino)-2-hydroxyphenyl]methylidene}-4-methoxybenzohydrazide

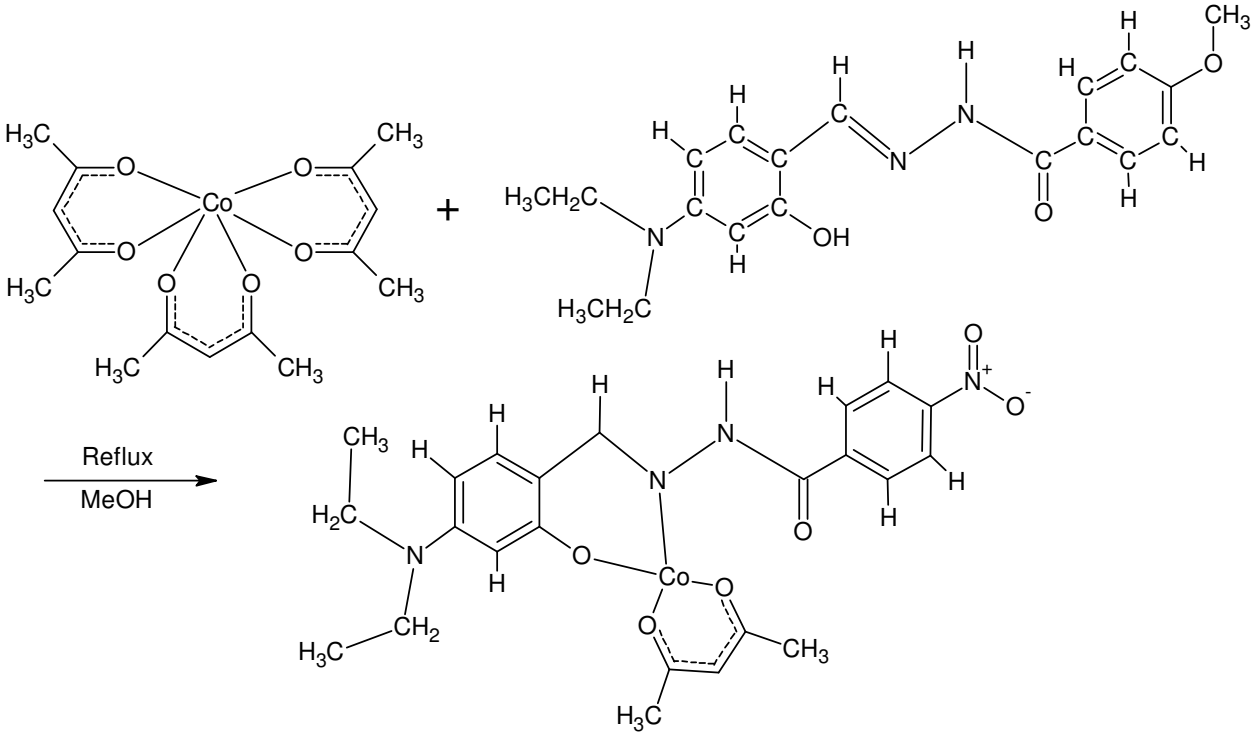

Schiff Base Complex 3B (SBC 3B)

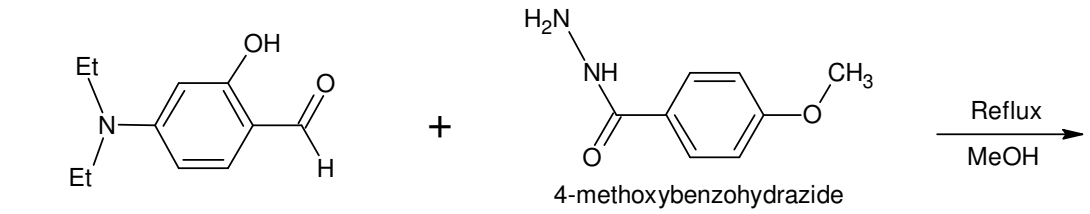

4-(diethylamino)-2-hydroxybenzaldehyde

4-methoxybenzohydrazide

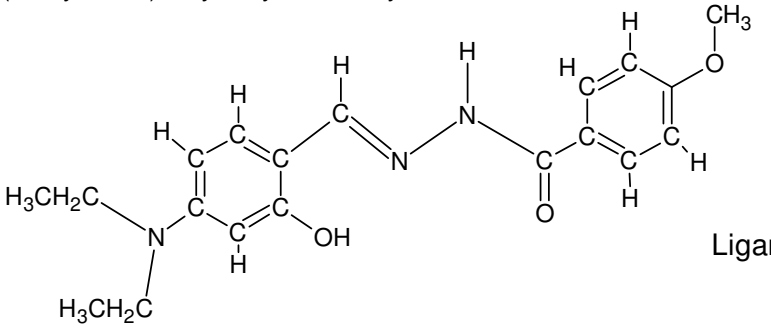

Ligand 2

N'-{(*E*)-[4-(diethylamino)-2-hydroxyphenyl]methylidene}-4-methoxybenzohydrazide

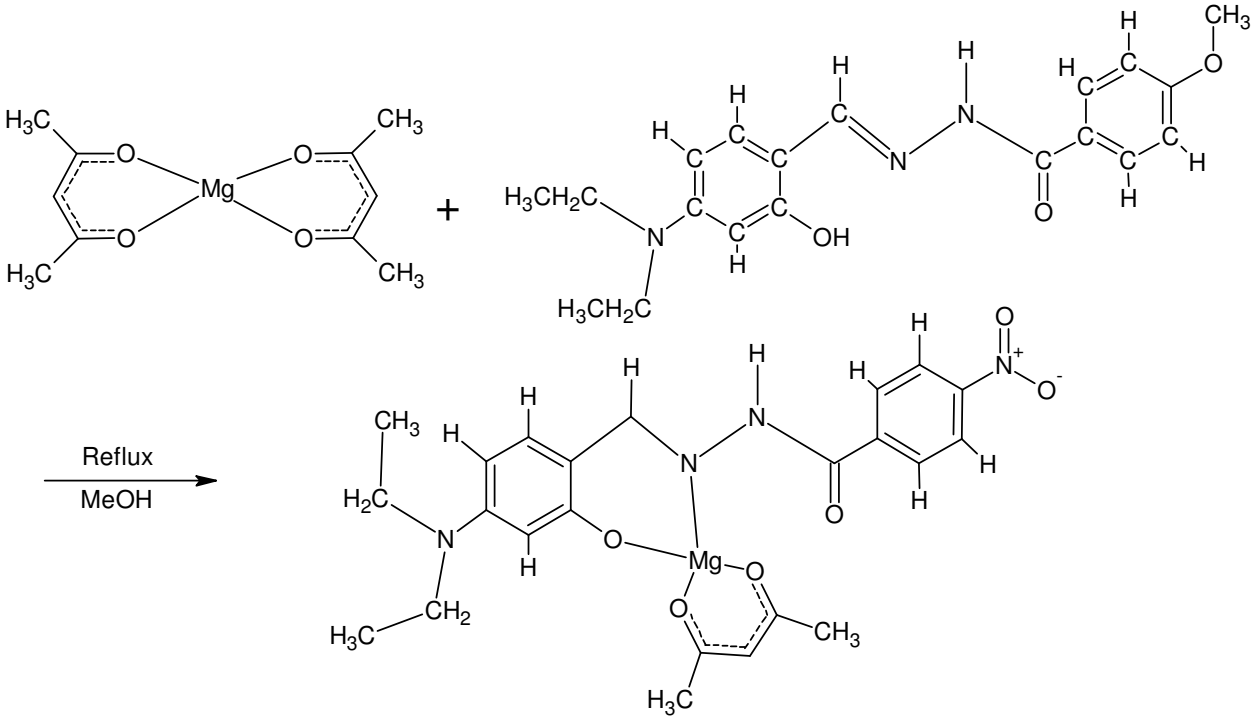

Schiff Base Complex 4B (SBC 4B)

3.3.3.3 Synthesis of Schiff base complexes 9-12

A stirred solution of L3 and $VO(acac)_2$, $Mn(acac)_3$, $Co(acac)_3$ and $Mg(acac)_2$, (0.01 mol) respectively were mixed in a 250 ml round bottom flask fitted with a water condenser. The mixture was refluxed over a steam bath for 1h. The resultant solution was left overnight in a fume cupboard at ambient temperature until all traces of the solvent had evaporated. The solid obtained was washed with methanol and dried in a vacuum desiccator over anhydrous calcium hydroxide for 48 hrs.

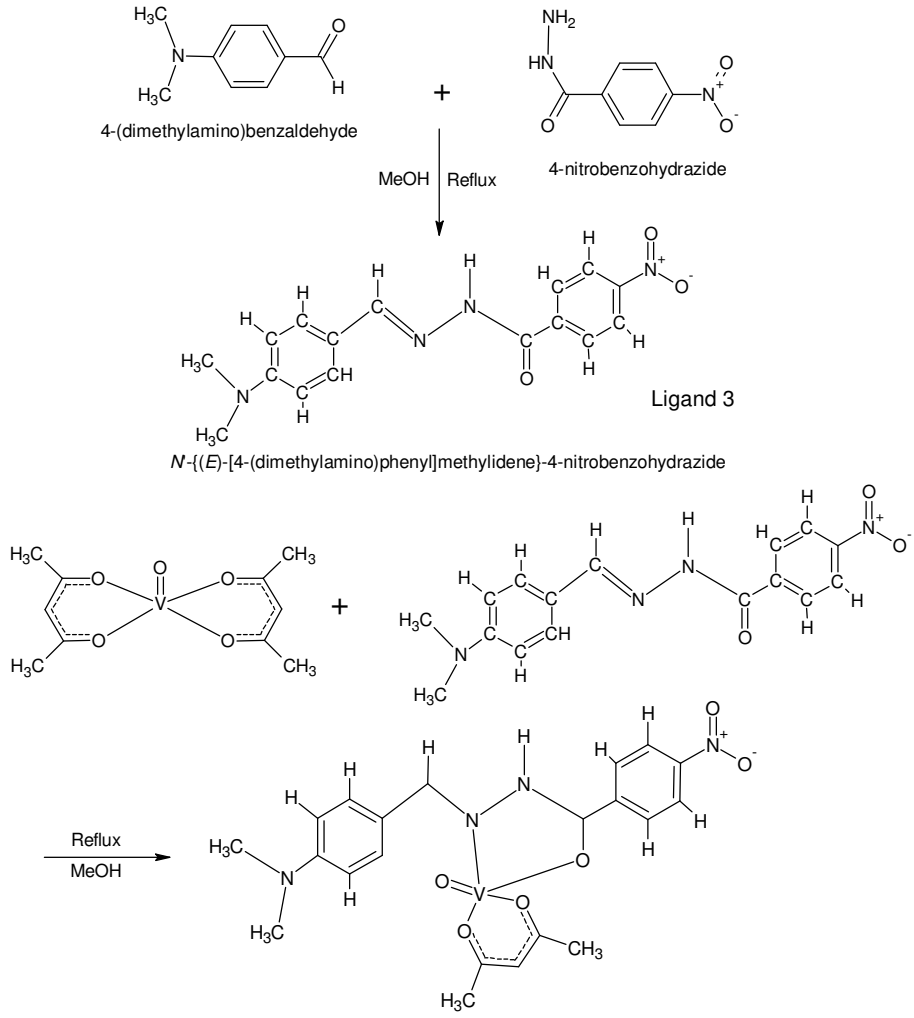

Schiff Base Complex 1C (SBC 1C)

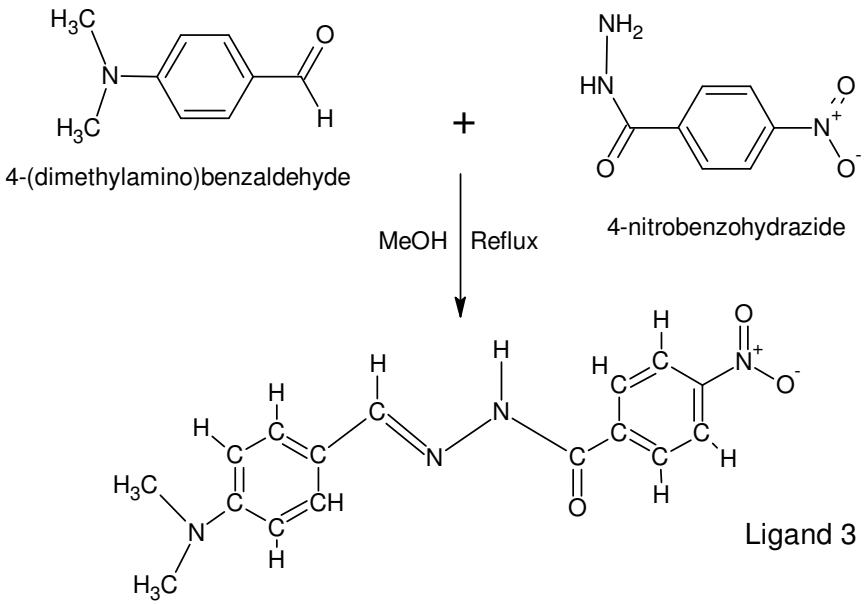

Ligand 3

N'-{(*E*)-[4-(dimethylamino)phenyl]methylidene}-4-nitrobenzohydrazide

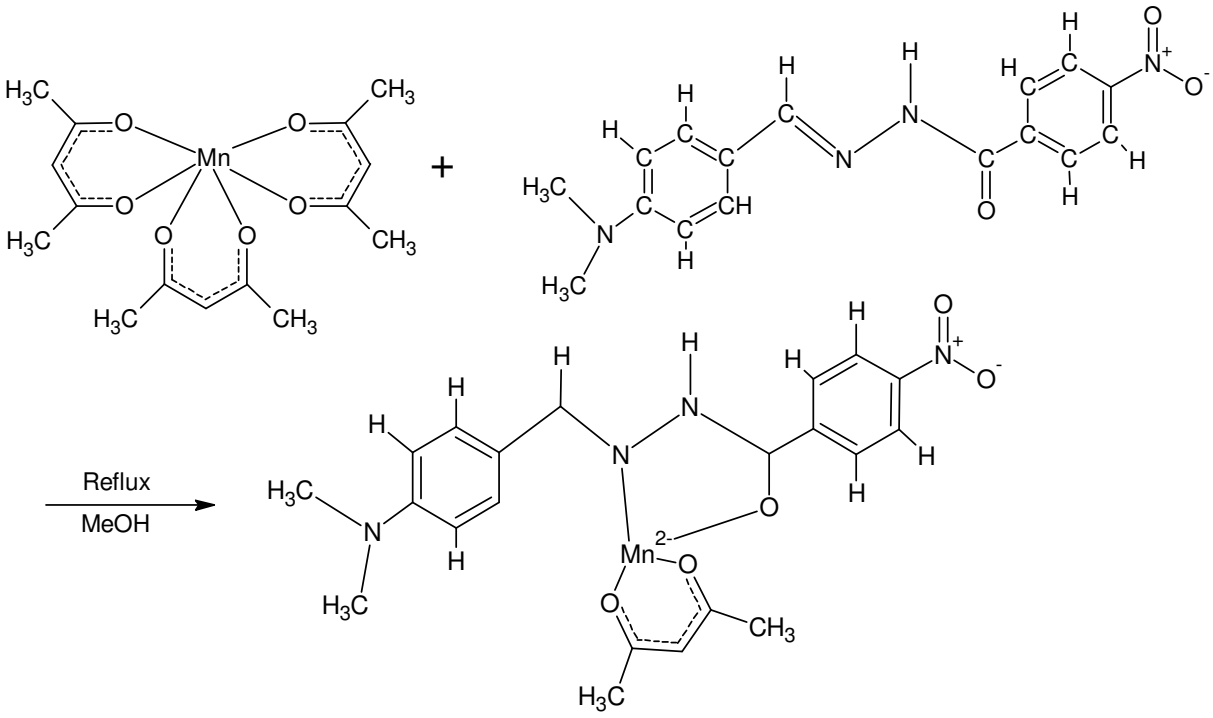

Schiff Base Complex 2C (SBC 2C)

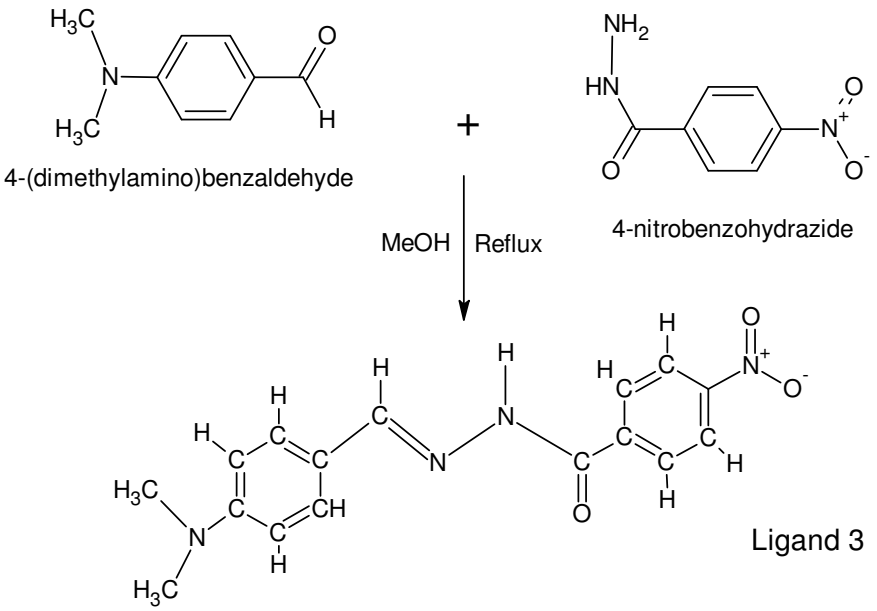

Ligand 3

N'-{(*E*)-[4-(dimethylamino)phenyl]methylidene}-4-nitrobenzohydrazide

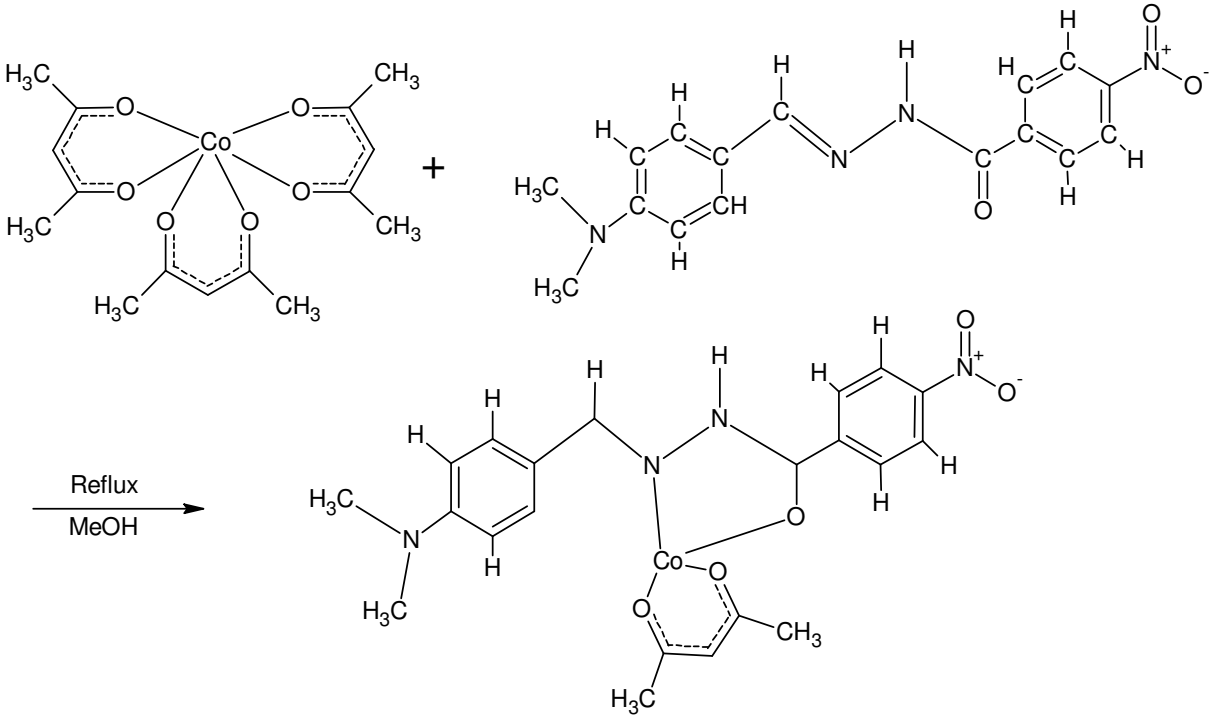

Schiff Base Complex 3C (SBC 3C)

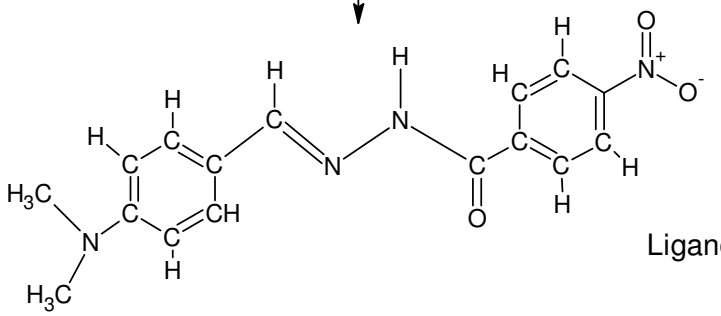

Ligand 3

N'-{(*E*)-[4-(dimethylamino)phenyl]methylidene}-4-nitrobenzohydrazide

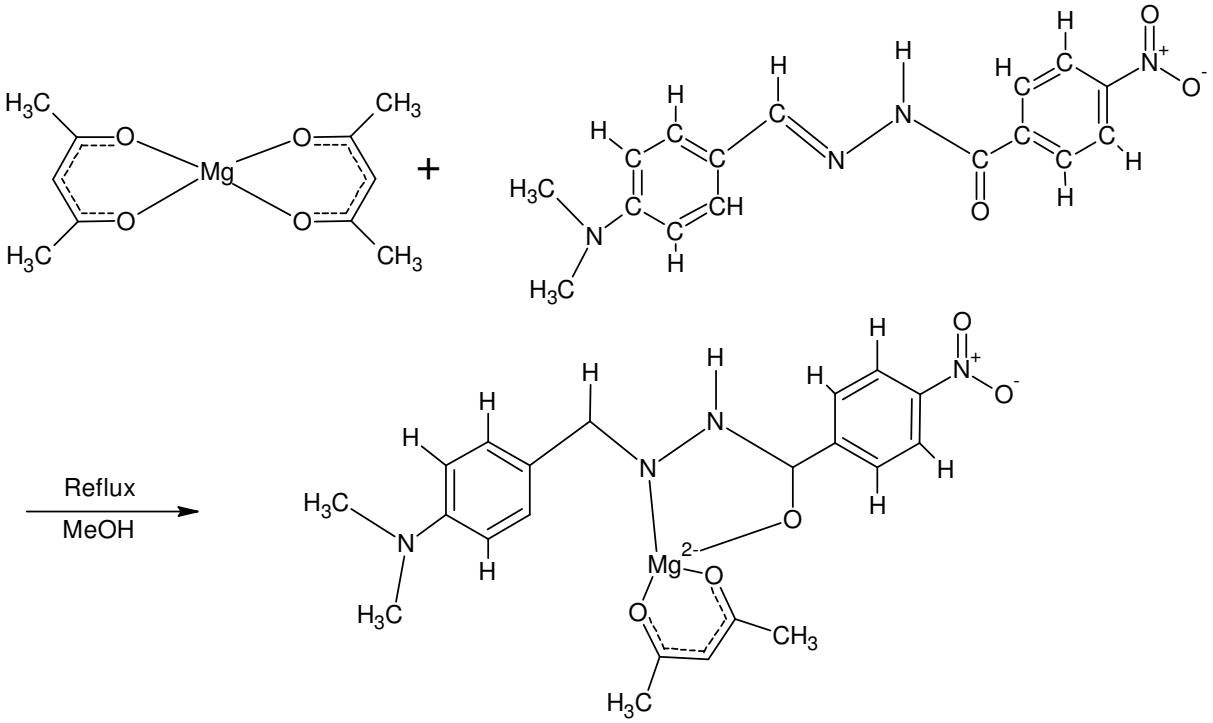

Schiff Base Complex 4C (SBC 4C)

3.3.3.4 SYNTHESIS OF SCHIFF BASE COMPLEXES 13-16

A stirred solution of L4 and $VO(acac)_2$, $Mn(acac)_3$, $Co(acac)_3$ and $Mg(acac)_2$, (0.01 mol) respectively were mixed in a 250 ml round bottom flask fitted with a water condenser. The mixture was refluxed over a steam bath for 1h. The resultant solution was left overnight in a fume cupboard at ambient temperature until all traces of the solvent had evaporated. The solid obtained was washed with methanol and dried in a vacuum desiccator over anhydrous calcium hydroxide for 48 hrs.

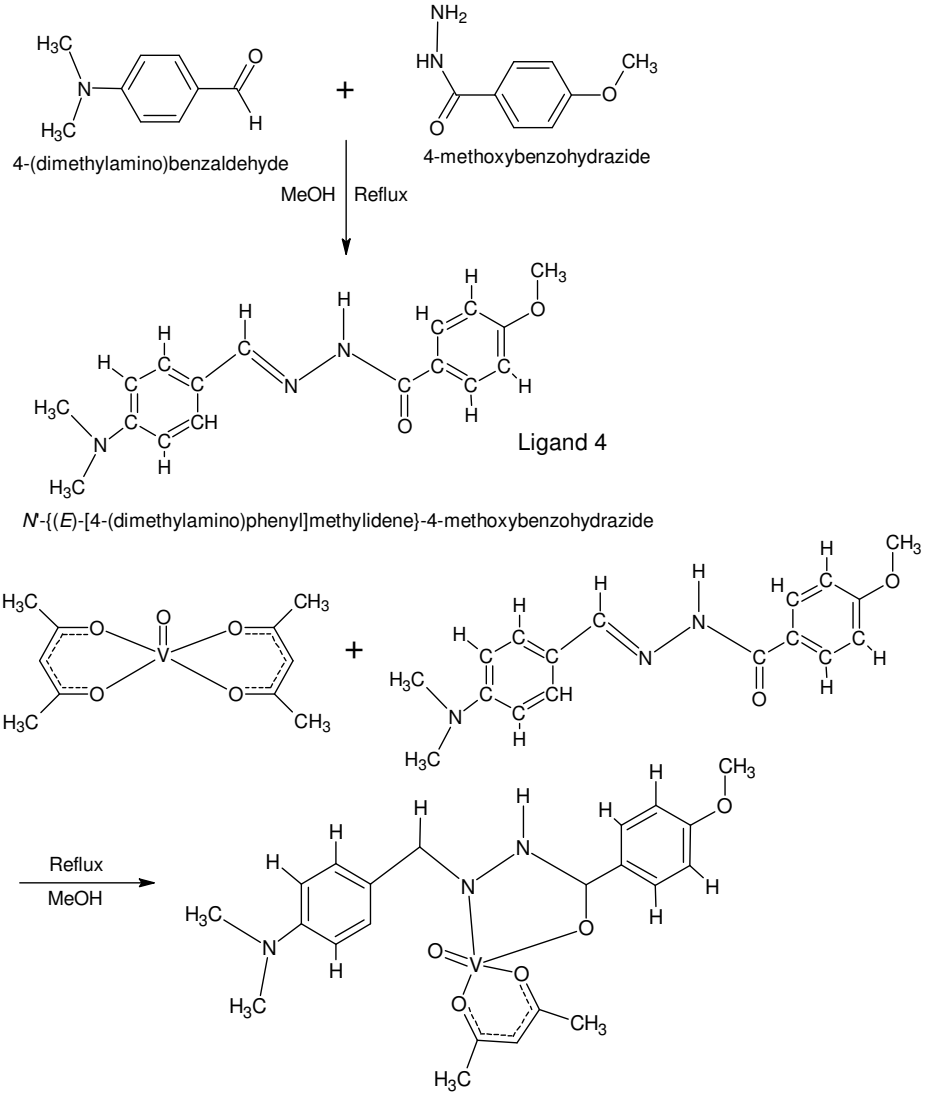

Schiff Base Complex 1D (SBC 1D)

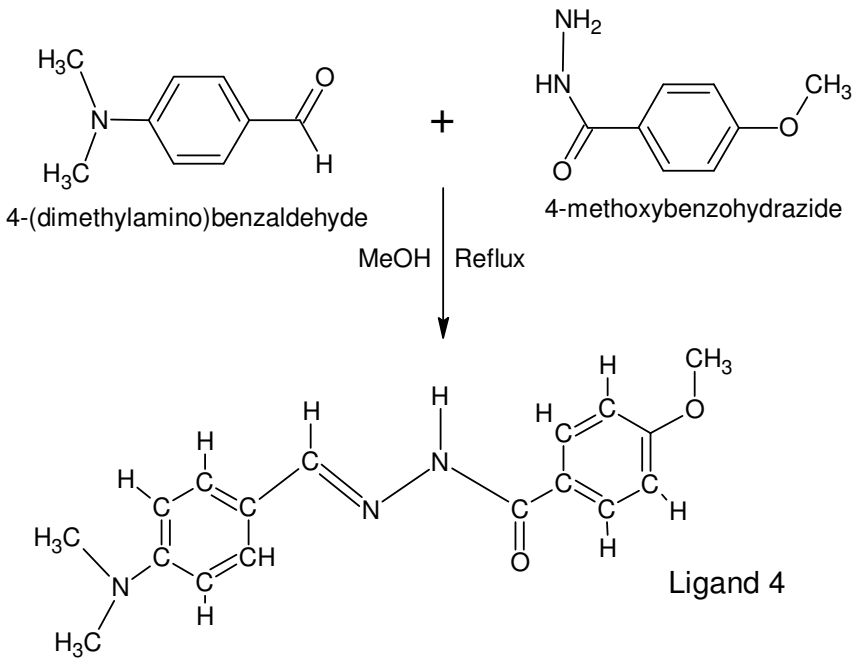

Ligand 4

N'-{(*E*)-[4-(dimethylamino)phenyl]methylidene}-4-methoxybenzohydrazide

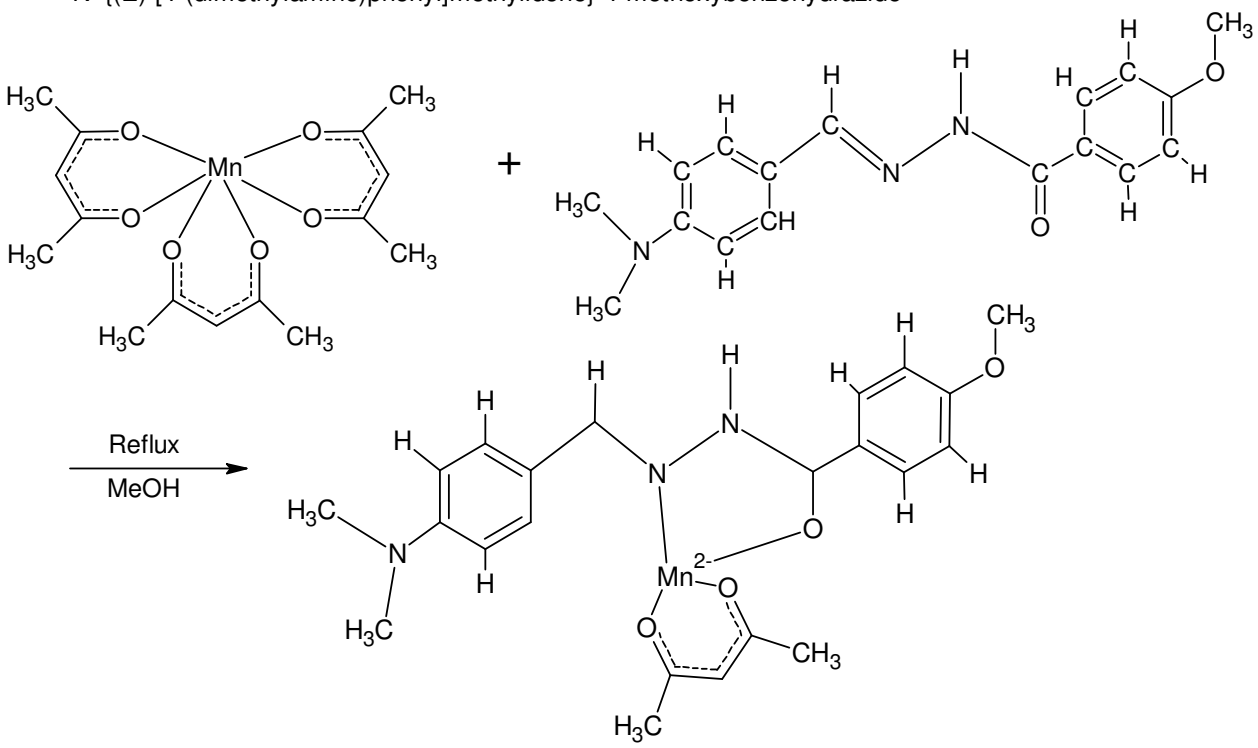

Schiff Base Complex 2D (SBC 2D)

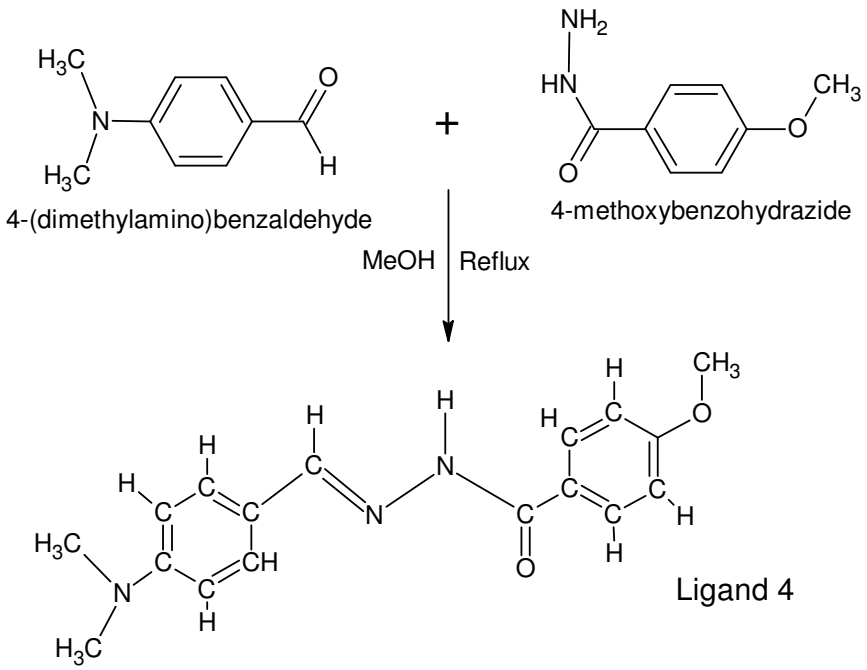

Ligand 4

N'-{(*E*)-[4-(dimethylamino)phenyl]methylidene}-4-methoxybenzohydrazide

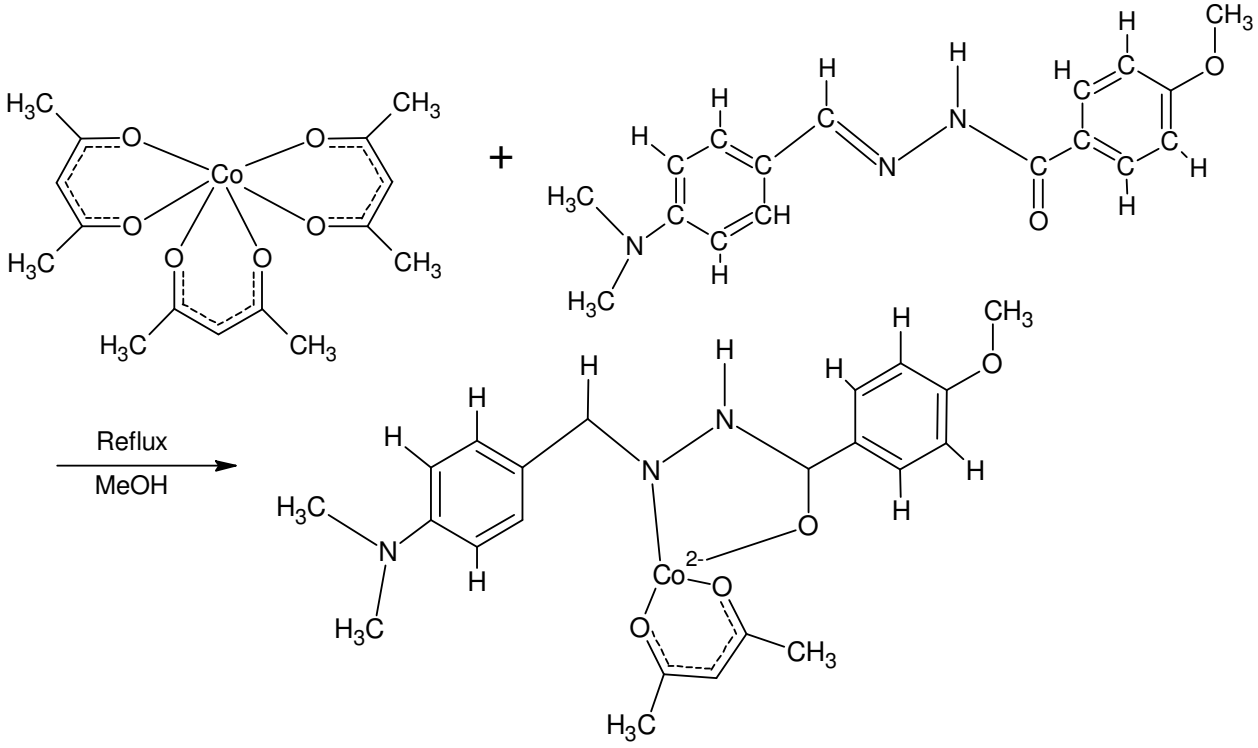

Schiff Base Complex 3D (SBC 3D)

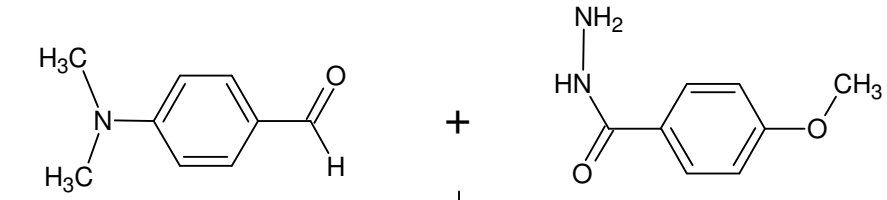

4-(dimethylamino)benzaldehyde + 4-methoxybenzohydrazide

MeOH | Reflux

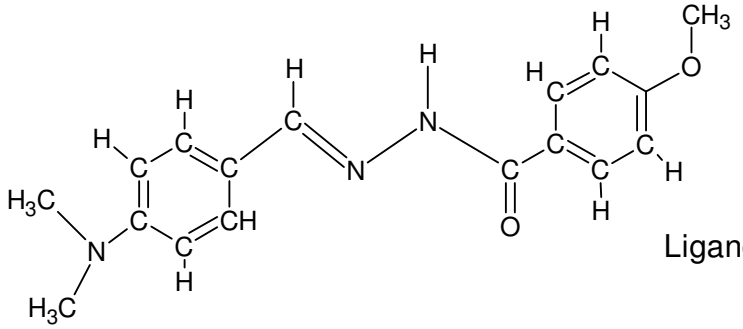

Ligand 4

N'-{(*E*)-[4-(dimethylamino)phenyl]methylidene}-4-methoxybenzohydrazide

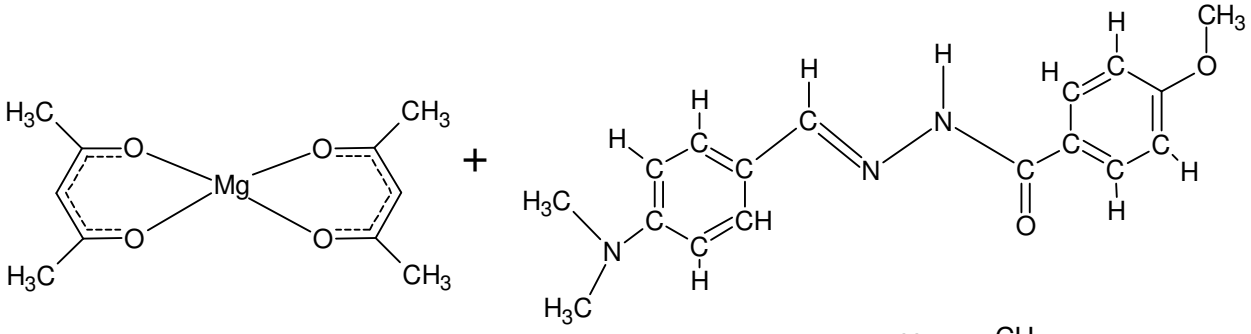

Reflux
MeOH

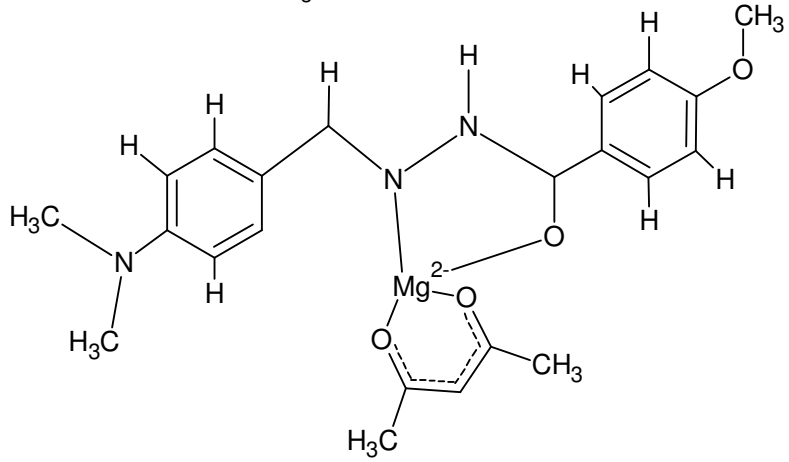

Schiff Base Complex 4D (SBC 4D)

3.4 Characterization Techniques

The synthesized Schiff base ligands and their metal complexes were characterized using the following techniques:- Fourier transform infrared (FT-IR), Ultraviolet Visible (UV-vis) Spectrometries, Thermogravimetric Analysis (TGA), Nuclear Magnetic Resonance (NMR) and Mass Spectrometry (MS).

3.4.1 Fourier Transform Infrared (FT-IR)

Fourier Transform Infrared Spectrophotometer will be used to detect the appearing or disappearing of peaks (functional groups) before and after synthesis.

FTIR relies on the fact that the most molecules absorb light in the infra-red region of the electromagnetic spectrum. This absorption corresponds specifically to the bonds present in the molecule. The frequency ranges are measured as wave numbers typically over the range 4000 – 600 cm-1.

The background emission spectrum of the IR source is first recorded, followed by the emission spectrum of the IR source with the sample in place. The ratio of the sample spectrum to the background spectrum is directly related to the sample's absorption spectrum. The resultant absorption spectrum from the bond natural vibration frequencies indicates the presence of various chemical bonds and functional groups present in the sample. FTIR is particularly useful for identification of organic molecular groups and compounds due to the range of functional groups, side chains and cross-links involved, all of which will have characteristic vibrational frequencies in the infra-red range.

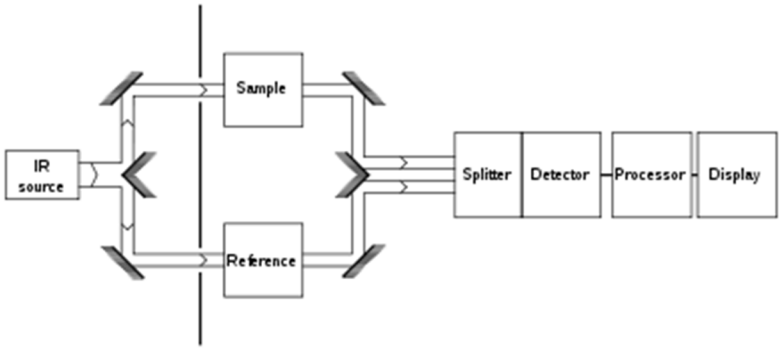

Figure 3.2: Diagram of FTIR instrument

3.4.2 ULTRA VIOLET- VISIBLE (UV-Vis)

A UV-vis Spectrometer comprises of the following main components; radiation source, monochromator, sample cell compartment, detector, and a display.

Ultraviolet-visible spectroscopy or ultraviolet-visible spectrophotometry (UV-Vis or UV/Vis) refers to absorption spectroscopy in the ultraviolet-visible spectral region. This means it uses light in the visible and adjacent (near-UV and near-infrared (NIR)) ranges. The absorption in the visible range directly affects the perceived color of the chemicals involved. In this region of the electromagnetic spectrum, molecules undergo electronic transitions. This technique is complementary to fluorescence spectroscopy, in that fluorescence deals with transitions from the excited state to the ground state, while absorption measures transitions from the ground state to the excited state. UV/Vis spectroscopy is routinely used in the quantitative determination of solutions of transition metal ions highly conjugated organic compounds, and biological macromolecules.

Solutions of transition metal ions can be colored (i.e., absorb visible light) because d electrons within the metal atoms can be excited from one electronic state to another. The colour of metal ion solutions is strongly affected by the presence of other species, such as certain anions or ligands. For instance, the colour of a dilute solution of copper sulfate is a very light blue; adding ammonia intensifies the colour and changes the wavelength of maximum absorption (λ_{max}).

Organic compounds, especially those with a high degree of conjugation, also absorb light in the UV or visible regions of the electromagnetic spectrum. The solvents for these determinations are often water for water soluble compounds, or ethanol for organic-soluble compounds. (Organic solvents may have significant UV absorption; not all solvents are suitable for use in UV spectroscopy. Ethanol absorbs very weakly at most wavelengths.) Solvent polarity and pH can affect the absorption spectrum of an organic compound. Tyrosine, for example, increases in absorption maxima and molar extinction coefficient when pH increases from 6 to 13 or when solvent polarity decreases. While charge transfer complexes also give rise to colours, the colours are often too intense to be used for quantitative measurement.

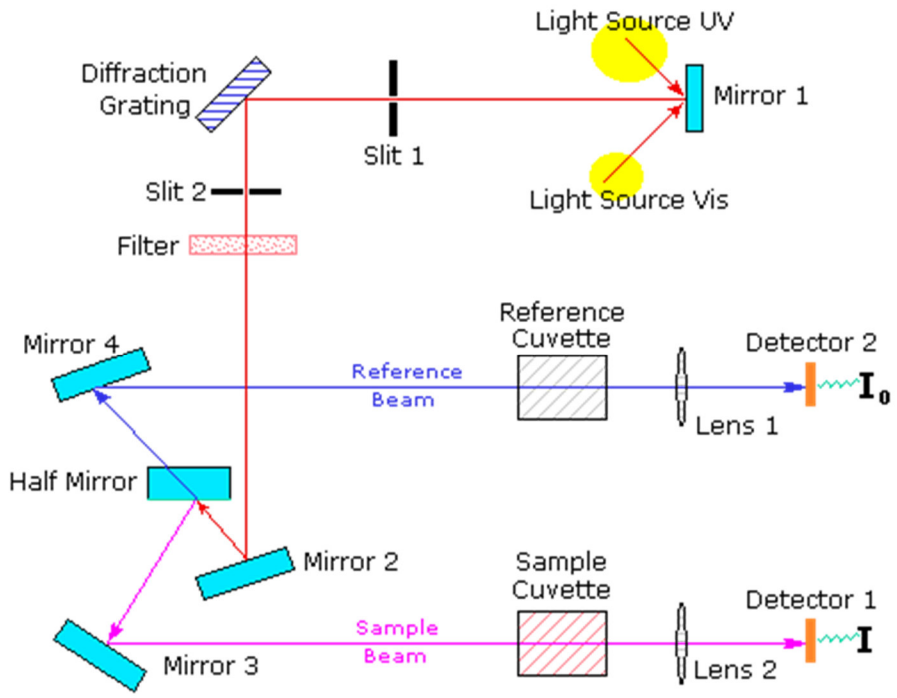

Figure 3.3: Diagram of UV-Vis Instrument

3.4.3. Proton and Carbon-13 Nuclear Magnetic Resonance (H-& C13 NMR)

Spectrophotometer will be used to collect spectra which will be used for the description of the chemical structure of compounds.

Proton NMR (also Hydrogen-1 NMR, or ^{1}H NMR) is the application of nuclear magnetic resonance in NMR spectroscopy with respect to hydrogen-1 nuclei within the molecules of a substance, in order to determine the structure of its molecules[1]. In samples where natural hydrogen (H) is used, practically all the hydrogen consists of the isotope ^{1}H (hydrogen-1; i.e. having a proton for a nucleus). A full ^{1}H atom is called protium.

Simple NMR spectra are recorded in solution, and solvent protons must not be allowed to interfere. Deuterated (deuterium = ^{2}H, often symbolized as D) solvents especially for use in NMR are preferred, e.g. deuterated water, D_2O, deuterated acetone, $(CD_3)_2CO$, deuterated methanol, CD_3OD, deuterated dimethyl sulfoxide, $(CD_3)_2SO$, and deuterated chloroform, $CDCl_3$. However, a solvent without hydrogen, such as carbon tetrachloride, CCl_4 or carbon disulphide, CS_2, may also be used.

Historically, deuterated solvents were supplied with a small amount (typically 0.1%) of tetramethylsilane (TMS) as an internal standard for calibrating the chemical shifts of each analyte proton. TMS is a tetrahedral molecule, with all protons being chemically equivalent, giving one single signal, used to define a chemical shift = 0 ppm [2]. It is volatile, making sample recovery easy as well. Modern spectrometers are able to reference spectra based on the residual proton in the solvent (e.g. the $CHCl_3$, 0.01% in 99.99% $CDCl_3$). Deuterated solvents are now commonly supplied without TMS.

The chemical shift of carbons is caused by the same phenomenon as the chemical shift of hydrogens, i.e., the electrons in the molecule generate small magnetic fields that affect the net field experienced by each carbon nucleus. In general, electrons surrounding an atom move in such a way so as to create a field at the atom that tends to counteract the applied magnetic field. The electrons thus "shield" the carbon nucleus from the applied magnetic field and this means that less energy is necessary to excite the carbon nucleus from one spin state to another and therefore its chemical shift comes at a lower frequency than it would otherwise. For example, the carbon atom in a carbonyl group has a relatively low electron density around it, and thus is relatively "deshielded" and consequently has a higher chemical shift than most other types of carbons.

Carbon-12 atoms do not have a nuclear spin, and hence don't show up in the NMR. When we take a carbon NMR we are looking only at carbon-13 atoms. Only 1% of naturally occuring carbon atoms are carbon-13, so the sensitivity of natural abundance carbon NMR is lower than that for proton NMR. Another consequence of this low abundance, is that we don't normally observe coupling between adjacent carbon atoms (like we do between adjacent protons in H-NMR) since 99% of the neighboring carbons are carbon-12 and don't have a nuclear spin. However, protons attached to a carbon atom will cause splitting of the carbon signal. This splitting will lower the signal to noise ratio, so carbon NMR spectra are usually obtained under conditions of proton decoupling. Under these conditions each nonequivalent carbon atom in a molecule will appear as a single peak in the carbon NMR.

Another difference between proton and carbon NMR is that carbon NMR spectra are not normally integrated. This is due to the fact that unless a long delay is introduced between acquisitions the carbon intensities don't accurately reflect the relative numbers of carbon atoms. For example, what you will usually observe is that carbon atoms with no hydrogens attached to them (e.g., carbonyl

carbons) will be less intense than those that do have hydrogens attached. Nevertheless, for carbon atoms that do have hydrogens attached the relative height of the NMR peak usually can be used to estimate the relative number of carbon atoms. For example, in the carbon NMR of isopropanol, the 2 methyl carbons are equivalent and will show up as a peak that is approximately twice as high as the methine (one H-attached) carbon peak.

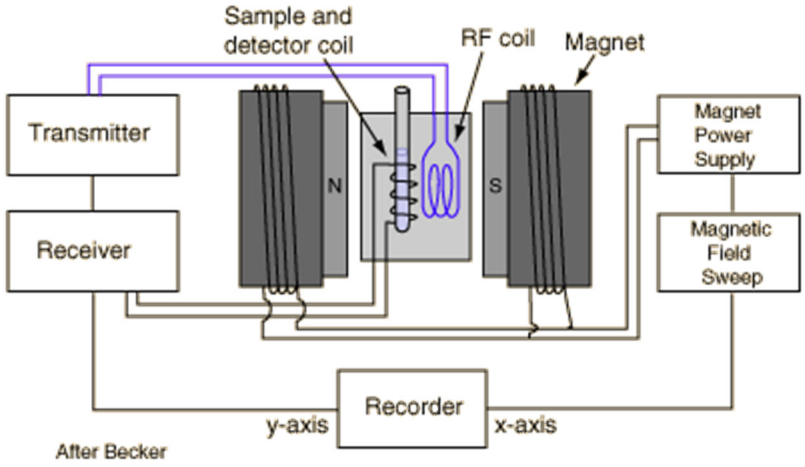

Figure 3.4: Diagram of Proton NMR instrument

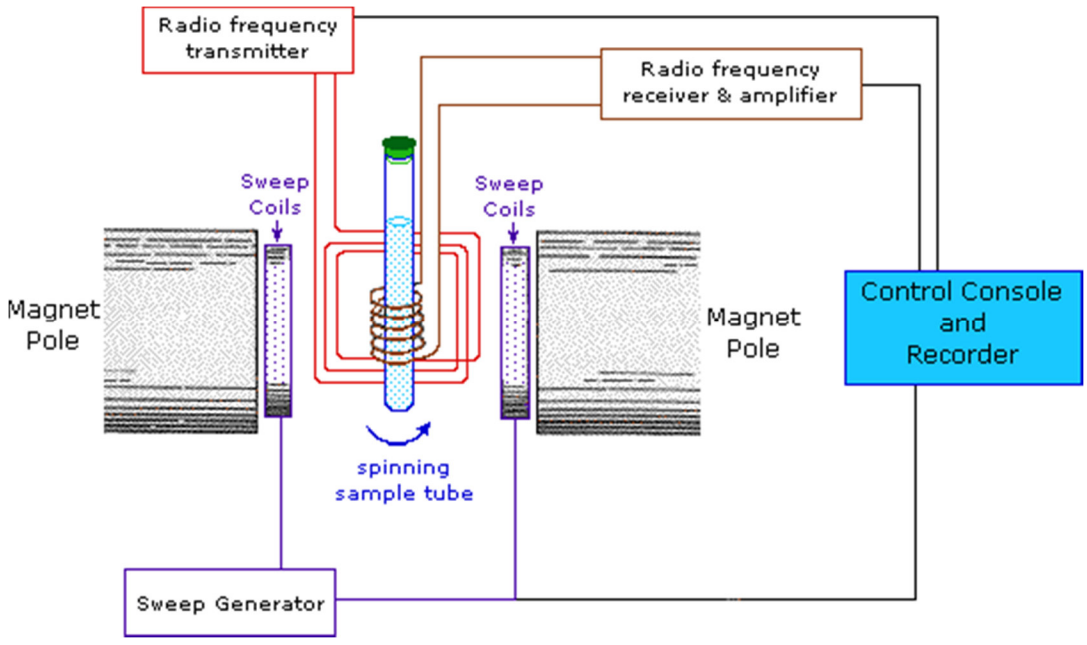

Figure 3.5: Diagram of Carbon-13 NMR instrument

3.4.4. Thermogravimetric Analysis (TGA)

Thermogravimetric analysis is an instrumental technique used to measure the weight loss of a sample as a function of temperature or time. The weight loss are often associated with chemical or physical processes such as dehydration, sublimation desorption, oxidation, vaporization and decomposition of the sample resulting from increase in temperature. [Tian]

A thermo gravimetric analyzer comprises of a thermo balance, furnace, purge-gas system, and a computer system. Thermogravimetric analysis is carried out by exponentially increasing the temperature of the furnace under an inert atmosphere. The sample is continuously weighed while being heated to higher temperatures. The data is plotted as mass or mass percentage as a function of temperature or time. This graph is called a thermogram or a thermal decomposition curve.

The new instruments facilitate studies by dynamic thermogravimetry in which the sample is heated at a uniform rate. Hence thermogravimetry has increased in recent years because of the commercial availability. Care must be taken to avoid errors, which may include the effect of changing air buoyancy and convection, the measurement of temperature, and the effects of atmosphere, heating rate, and heat of reaction. Thermogravimetric analysis is an invention of microbalance and minimization of effect of purge gas on the balance sensitivity during quantitative analysis.

TGA uses a sensitive balance. The thermobalance facilitates studies of a sample which is subjected to conditions of continuous increase in temperature, usually linear with time. The weight loss during the sample decomposition is measured with a thermogravimetric analyzer. It uses either inert or nitrogen gas or air atmosphere for a given specific chemical measured. A TGA experiment depends mainly on initial weight and temperature, heating rate, and gas flow (air, nitrogen, argon, etc.). The experimental conditions of every experiment are carried out with TGA to design, optimize, and test the sample. TGA experiments are performed using crucibles made of alumina (Al_2O_3) or platinum in the temperature range 23–930°C.

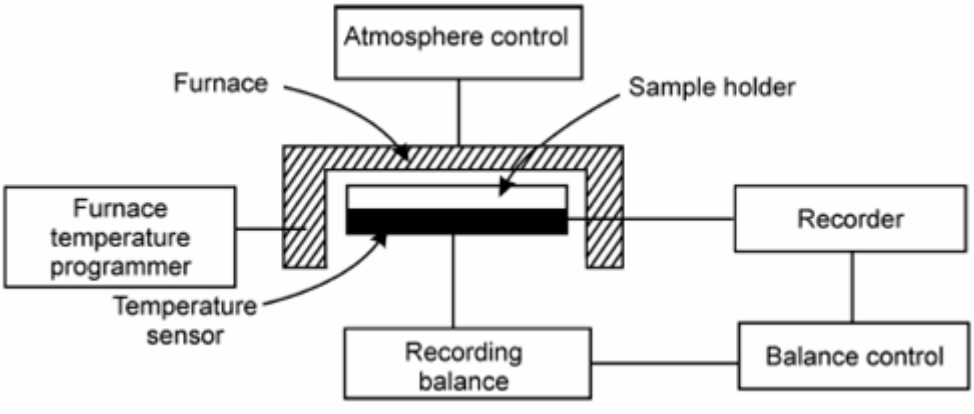

Figure 3.6: Diagram of TGA/DTA instrument

3.5 Biological Testing

The synthesized Schiff base ligands and their metal complexes were evaluated for their in vitro antibacterial activities. Antibacterial activity was tested against two gram positive bacterial strains:-*Staphylococcus aureus* and *Enterococcus faecalis* using a modification of the Kirby-Bauer disc diffusion technique [16].

References

[1] PRAKASH A., ADHIKARI D. **2011**. Application of Schiff bases and their metal complexes. A Review. *Int. J. Chem. Tech. Res.*, 3(4), 1891.

[2] IQBAL, J., SIDDIQUI, R., KAZMI, SU., KHAN, NA. **2013**. A simple assay to screen antimicrobial compounds potentiating the activity of current antibiotics. *BioMed Res Int.* DOI: 10.1155/927323, 4 pages

[3] RICE, LB. **2006**. Unmet medical needs in antibacterial therapy. *Biochem Pharmacol.*, 71(7), 995 – 1005.

[4] DA SILVA, CM., DA SILVA, DL., MODOLO, LV., ALVES, RB., DE RESENDE, MA., MARTINS, CVB., DE FATIMA, A. **2009**. Schiff bases: A short review of their antimicrobial activities. *J. Adv. Res.* 2, 1 – 8.

[5] JOSEPH, J., MARY, NL., SIDAMBARAM, R. **2010**. Synthesis, characterization and antibacterial activity of Schiff bases derived from thiosemicarbazide, salicylaldehyde, 5-bromosalicylaldehydeand their copper(II) and nickel(II) complexes. *Synth. React. Inorg. Met-Org. Chem.* 40, 930 – 933.

[6] ASHRAF, MA., MAHMOOD, K., WAJID, A. **2011**. Synthesis, characterization and biological activities of Schiff bases. *Int. Conf. Chem. Chem Proc*. 10, 1 – 7.

[7] ONAL, Z., YILDIRIM, I., KANDEMIRLI, F. & ARSLAN, T., **2010**. Experimental and theoretical studies on the reactions of 1-amino-5-benzoyl-4-phenyl-1H-pyrimidine-2-one/-thione compounds with ethylacetoacetate. *J. Struct. Chem.* 21, 809 – 816.

[8] MALHOTRA, E., KAUSHIK, NK., MALHORA, HS. **2006**. Synthesis and studies of ionic chelates of halfnocene with guanine. *Indian J. Chem*. 45A, 370 – 376.

[9] PRASHANTHI, Y., KIRANMAI, K., KUMAR, SK., CHITYALA, VK., SHIVARA, J. **2012.** Spectroscopic characterization and biological activity of mixed ligand complexes of Ni(II) with 1,10-Phenanthroline and heterocyclic Schiff bases. *Bioinorg. Chem. Appl.* DOI: 10.1155/948534, 8 pages.

[10] MOHAMED, G., OMAR, MM., IBRAHIM, AA. **2009**. Biological activity studies on metal complexes of novel tridentate Schiff base ligand. Spectroscopic and thermal characterization. *E. J. Med. Chem*. 44(12), 4801 – 4812.

[11] TIAN, ZQ. **2005**. Special issue on SERS. *J. Raman Spectros*. 36, 125.

[12] POURALIMARDAN, O., ANNE-CHRISTINE, C., JANIAK, C. & HOSSEINI-MONFARED, H. **2007**. Hydrazone Schiff base manganese(II) complexes: Synthesis, crystal structure and catalytic reactivity. *Inorg. Chim. Acta.* 360, 1599 – 1608.

[13] CANPLAT, E., SAHAL, H., KAYA, M., & GUR, S. **2014.** Synthesis, characterization, antibacterial and antifungal activities of copper(II), cobalt(II) and zinc(II) complexes of the Schiff base ligand derived from 4,4-diaminodiphenylether. *J. Chem. Soc. Pak.* 36(1), 106 – 112.

[14] SAM, N., AFFAN, M.A., SALAM, M.A., AHMAD, F.B. & ASARUDDIN, M.R. **2012.** Synthesis, special characterization and biological activities of organotin(IV) complexes with ortho-vanillin-2-hydrazinopyridine (VHP). *O. J. Inorg. Chem*. 2, 22 – 27.

[15] SHIVHARE, S., MISHRA, R., GHARIA, A. & GAUTAM, M.D., **2012**. Synthesis, characterization and antimicrobial studies of Cu(II) and Ni(II) complexes with Schiff base derived from N-aminorhodanine and salicylaldehyde. *Int. J. Pharm. Sci.* 4, 394 – 397.

[16] BARTYZEL, A. **2013.** Synthesis, crystal structure and characterization of manganses(III) complex containing a tetradentate Schiff base. *J. Coord. Chem*. 66(24), 4292 – 4303.

CHAPTER FOUR

RESULTS AND DICUSSIONS

In this chapter, we present the results obtained in the synthesis, characterization and antimicrobial study(ies) of hydrazide Schiff bases with acetylacetonates of the metals, zinc, copper, cobalt, iron, manganese, cadmium, vanadium, chromium, magnesium and nickel.

4.1 Metal Acetylacetonates

4.1.1 Synthesis

Acetylacetonates of the metals zinc, copper, cobalt, iron, manganese, cadmium, vanadium, chromium, magnesium and nickel were synthesized as described in chapter 3.

The metal acetylacetonates showed the characteristics shown in table 1.

Table 1: Characteristics of metal acetylacetones

	Metal Acetylacetonates	**Crystalline/ powder**	**Colour**
1	Bis-(acetylacetonatato) zinc(II)	Crystalline	White
2	Bis-(acetylacetonato) oxovandium(IV)	Crystalline	Green
3	Bis-(acetylacetonato) cadmium(II)	Crystalline	White
4	Bis-(acetylacetonato) magnesium(II)	Crystalline	White
5	Bis-(acetylacetonato) nickel(II)	Crystalline	Green
6	Bis-(acetylacetonato) copper(II)	Crystalline	Blue
7	Tris-(acetylacetonato) ferric(III)	Crystalline	Red/Wine
8	Tris-(acetylacetonato) cobalt(III)	Crystalline	Green
9	Tris-(acetylacetonato) cobalt(II)	Crystalline	Pink
10	Tris-(acetylacetonato) manganese(III)	Crystalline	Black

4.1.2 FTIR

Synthesized metal acetylacetonates were characterized by Fourier transform infrared spectroscopy (FTIR). Crystalline or powders samples of the metal acetylacetonates were analyzed by placing a

small quantity of the solid in the sample holder of the FTIR and then pressing it with the handle into the light path of the instrument and then running the instrument.

Pure liquid acetylacetonate sample was also introduced into the sample holder of the instrument and run. The results obtained are presented in table 4.2 with the individual FTIR spectra presented in figures 4.1 to 4. 5

Table 4.2: Characteristic peaks of pure acetylacetone and metal acetylacetonates and their assignments.

Acac	Mg	Cd	Mn	Co(II)	VO	Zn	Ni	Co(III)	Cu	Assignment
2964				2950	2989	2985			2967	$\nu(CH_3)$
2917				2904						$\nu(CH_3)$
2877				2871	2892	2896			2881	$\nu(CH_3)$
1704										$\nu(C{=}O)$
1600	1604	1601			1670	1633				
	1520			1527		1581	1584	1570	1573	$\nu(CO)_{(acac)}$
		1505	1502	1515	1515	1511	1511	1513	1515	$\nu(CO)_{(acac)}$
1411										$\delta(CH_3)_{as}$
1357		1379	1339	1349	1382	1392		1360	1348	$\delta(CH_3)_{as}$
1243	1259	1245	1255	1272	1286	1257	1256	1278	1274	$\nu(C{-}C{-}C)_s$
	1020	1017	1016	1012		1016	1023	1015	1014	ν(M-O)
912	919	919	921	927	993	929	922		935	ν(M-O)
777	762	782	778	769	798	767	765	765	781	γ(C-H)
				665	682	655	660		651	δ(ring)

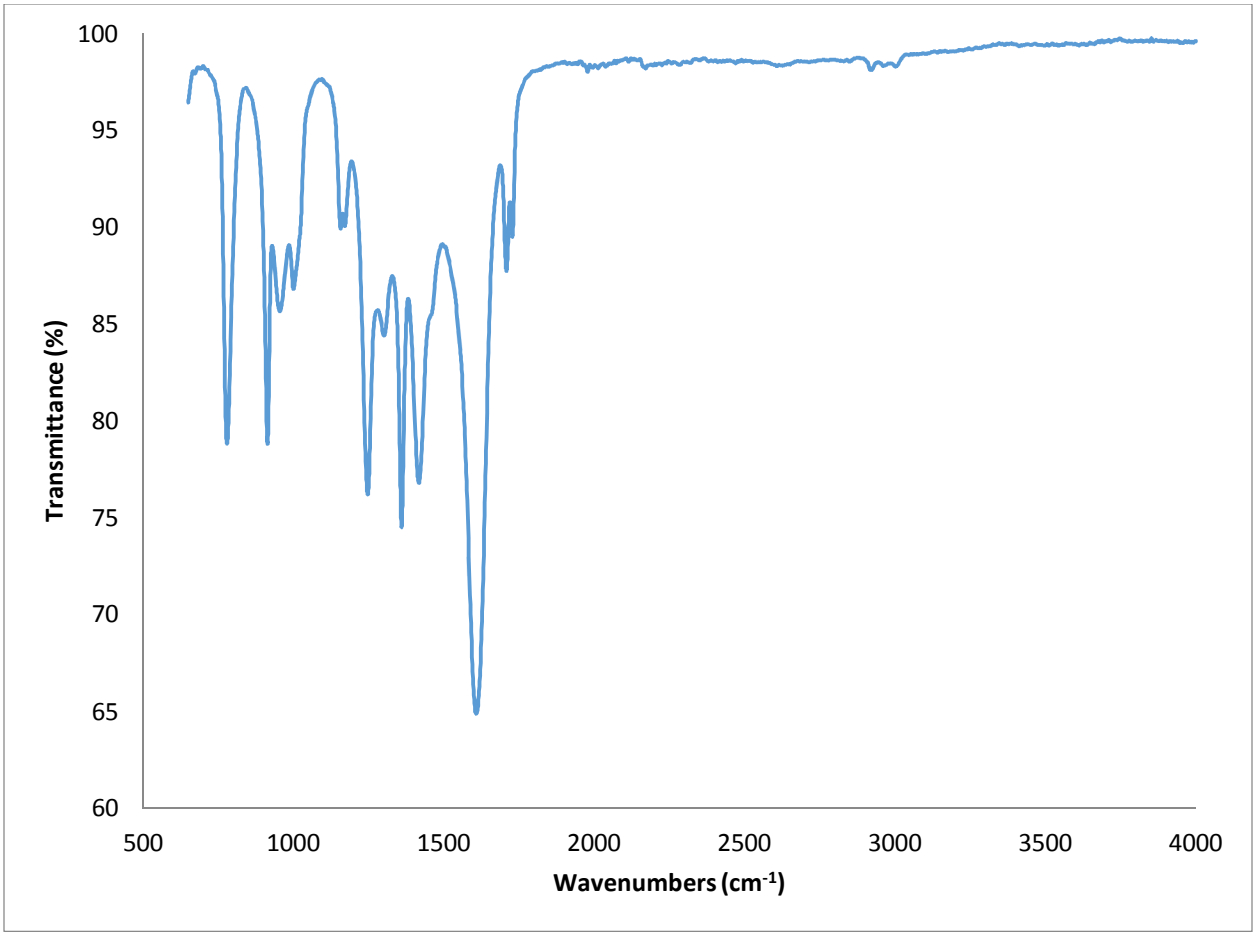

Figure 4.1: FTIR spectra of pure acetylacetone.

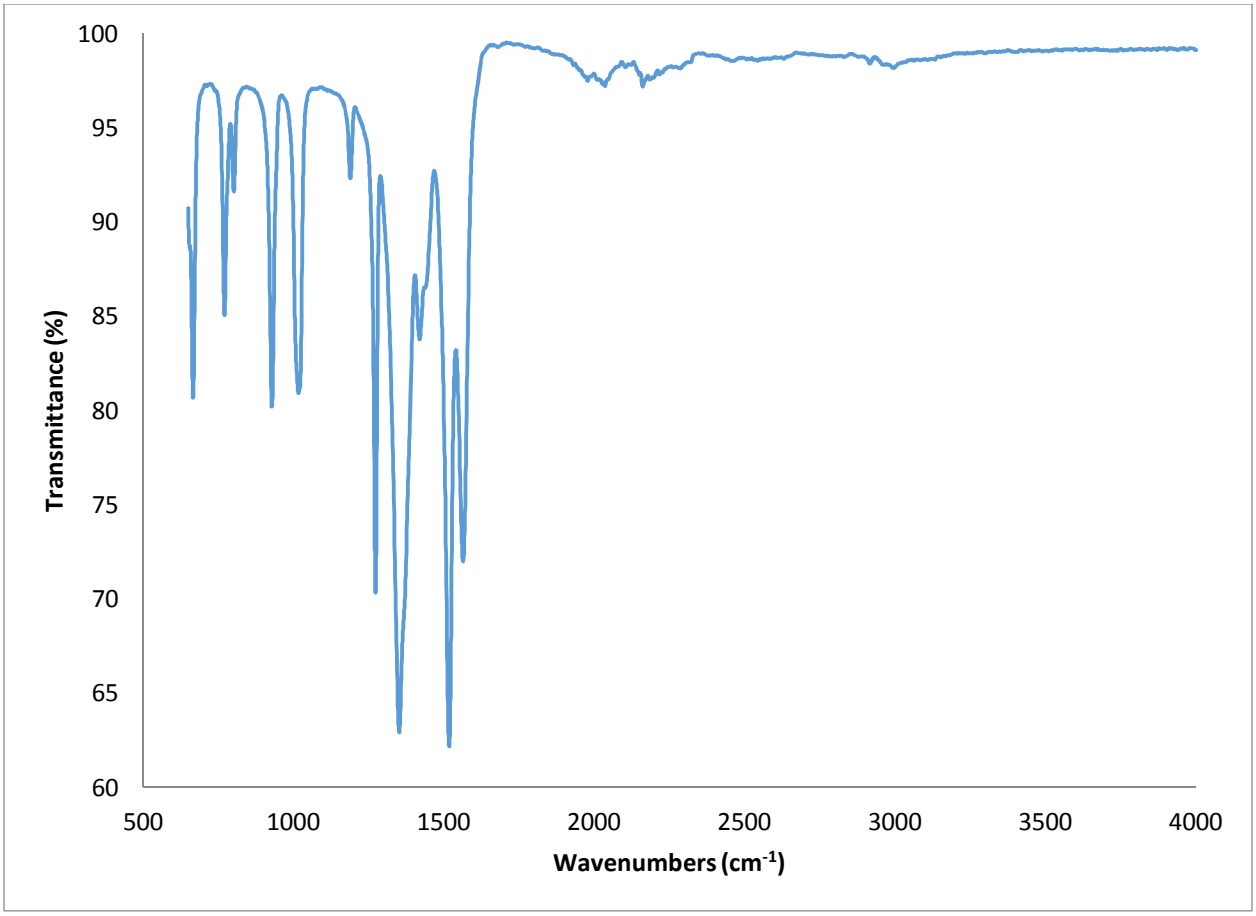

Figure 4.2: FTIR spectra of Cobalt(II) acetylacetonate

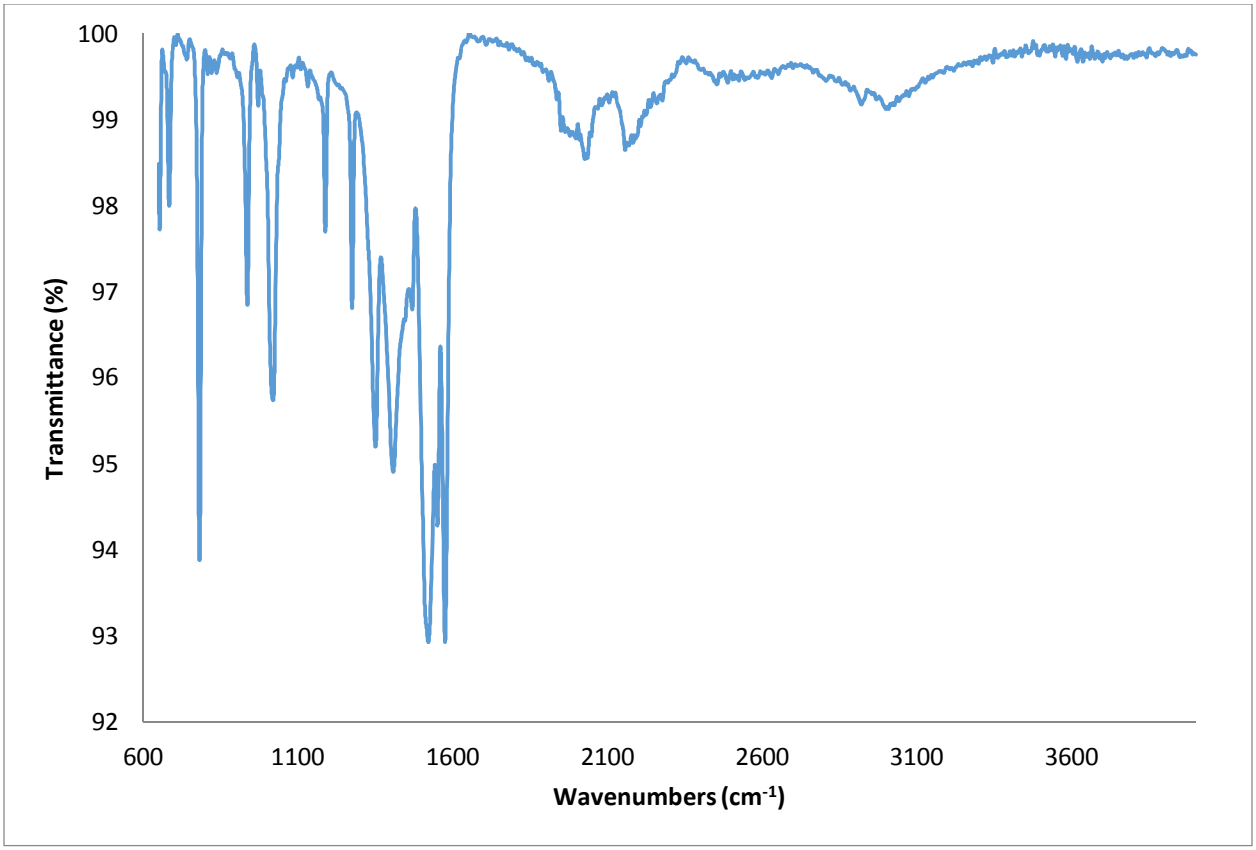

Figure 4.3: FTIR spectra of copper(II) acetylacetonate.

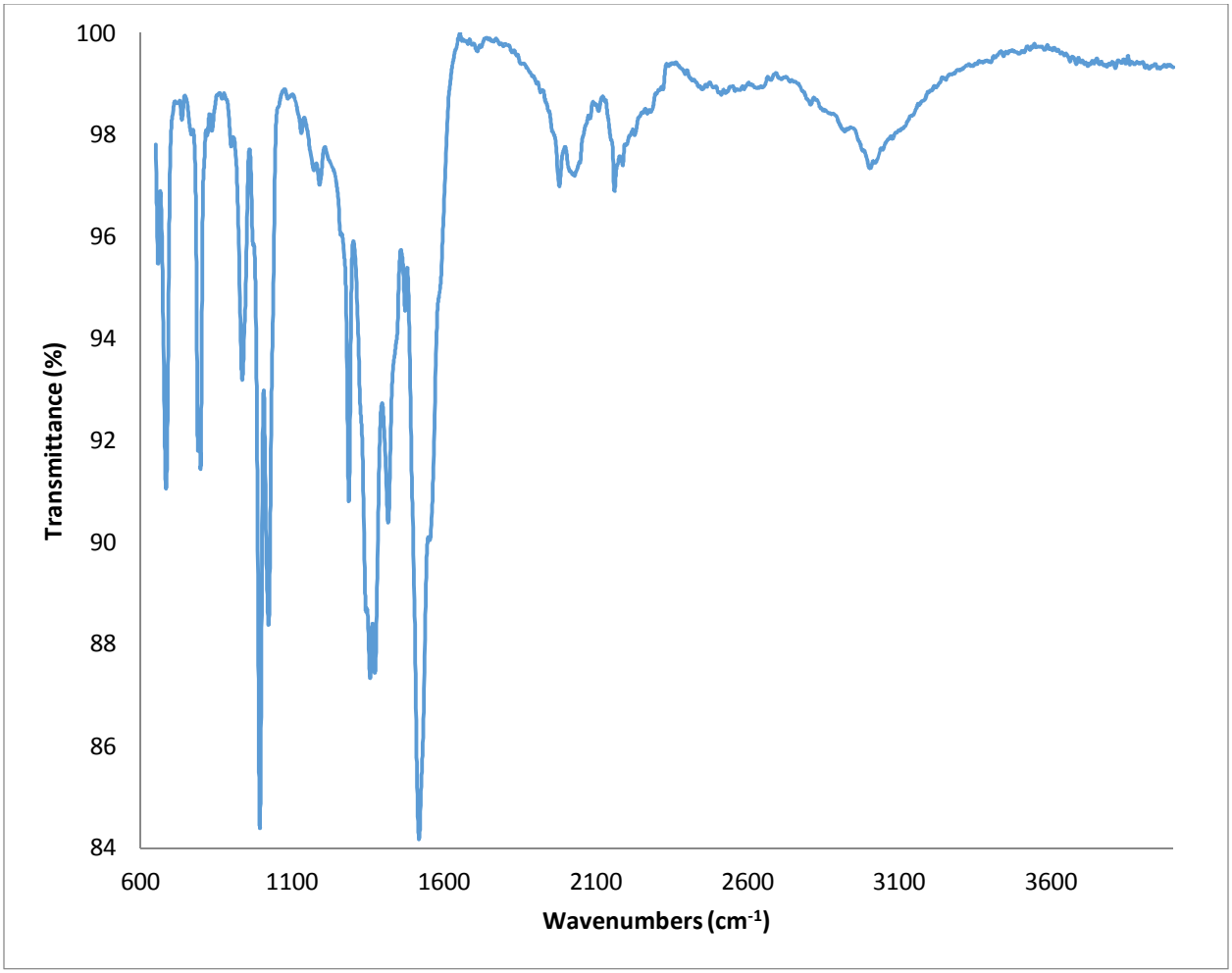

Figure 4.4: FTIR spectra of vanadium acetylacetonate.

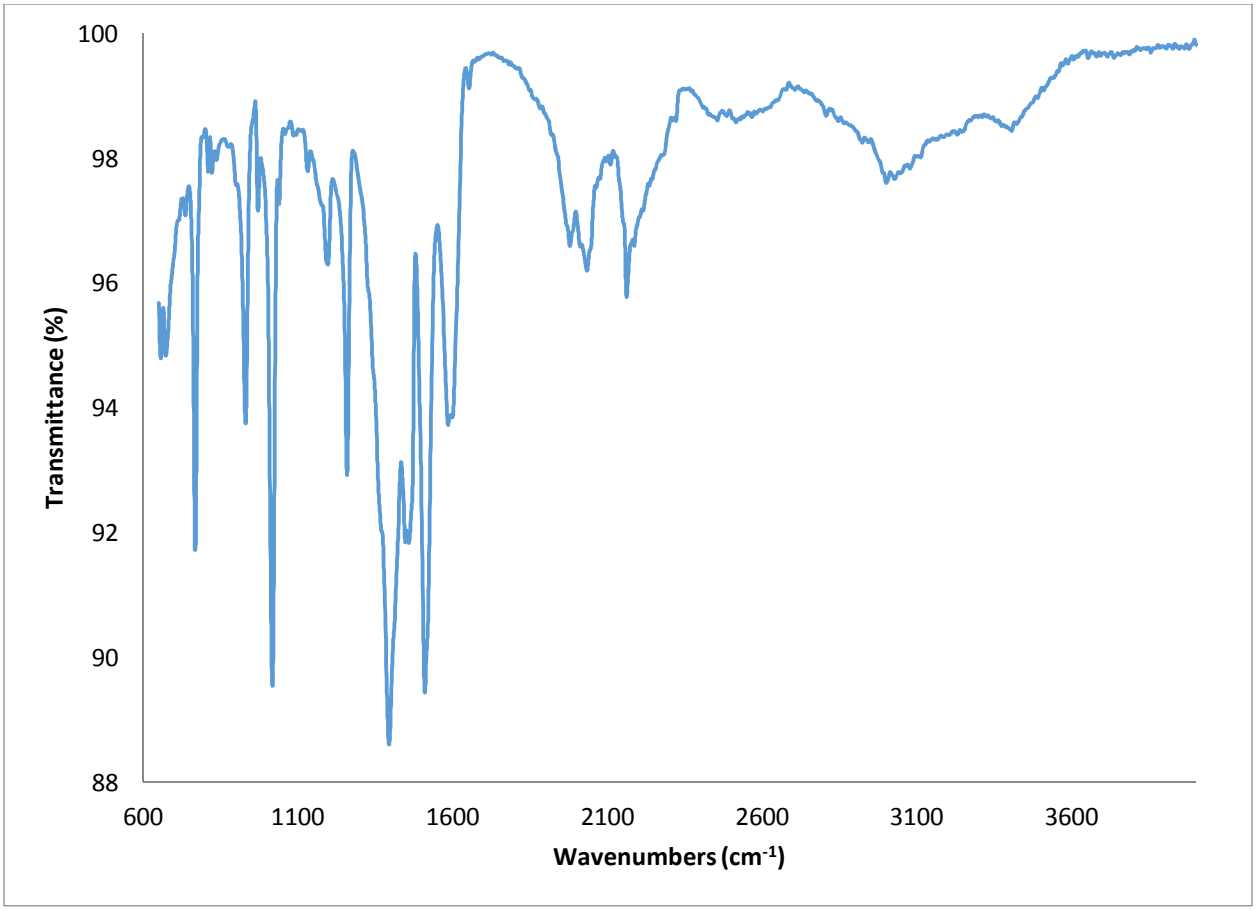

Figure 4.5: FTIR spectra of zinc(II) acetylacetonate.

DISCUSSION

The FTIR of pure acetylacetone (acac), figure 4.1, show vibrational peaks at 2964 to 2877 cm^{-1} due to methyl and methylene groups in the acetylacetone [1]. The peak at 1704 cm^{-1} is assigned as a carbonyl stretching vibration in the acetylacetone molecule. Acetylacetones exist in two forms due to tautomerization as diketone (keto-) and as an alcohol (enol). The percentage of these forms of acetylacetone show the purity of the substance at any time. A pure acetylacetone should have about 99% keto form while an impure acetylacetone should have an appreciable percentage of enol form which can be observed by FTIR as shown in scheme 4.1. The vibrational peak at 1704 cm^{-1} is therefore due to the carbonyl of the keto-form. The FTIR of pure acetylacetone presented does not any vibrational peak at 3300 cm^{-1} due to O-H stretching vibration. This is an indication that a large percentage of the acetylacetone used in the synthesis was pure acetylacetone.

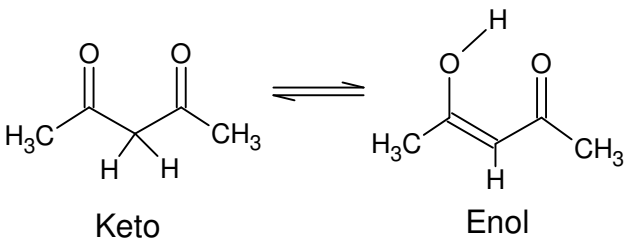

Scheme 4.1: Tautomeric forms of acetylacetone

An important observation in the FTIR of pure acetylacetone is the absence of a metal to oxygen vibrational peak observed at about 1020 to 935 cm^{-1}.

In the FTIR of metal acetylacetonates of zinc, cobalt(II), cobalt(III), magnesium, manganese, copper, oxo-vanadium, nickel and cadmium, figure 4.5, stretching vibrations due to the methyl group vibrational frequencies (2877 to 2964 cm^{-1}) are observed at different vibrational frequencies compared to pure acetylacetone [2-6].

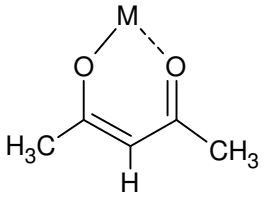

The vibrational frequency of the carbonyl, 1700 cm^{-1}, is conspicuously absent from the FTIR spectra of metal acetylacetonates indicating the formation of metal acetylacetonates bonds in our synthesis reaction. The metal oxygen vibrational frequency, ν(M-O), is observed at different wavenumbers which depends on the metal inserted in the acetylacetonate. The metal acetylacetonate frequency is observed from 1020 to 922 cm^{-1}. Among the metal acetylacetonates synthesized, only Bis-(acetylacetonato) oxovandium(IV) did not show a metal oxygen bond frequency between 1012 to 1023 cm^{-1}. The metal oxygen bond for Bis-(acetylacetonato) oxovandium(IV) is found at 993 cm^{-1}.

4.2 Schiff Base Ligands

4.2.1 Synthesis

Schiff base ligands were prepared as described in chapter 3, by reacting 4-(diethylamina)-2-hydroxybenzaldehyde with 4-Nitrobenzohydrazide and 4-methoxybenzohydrazide to form two ligands. 4-(dimethylamino)benzaldehyde was also reacted with 4-Nitrobenzohydrazide and 4-methoxybenzohydrazide to form two ligands. The Schiff base ligand are *N*'-{(*E*)-[4-(diethylamino)-2-hydroxyphenyl]methylidene}-4-nitrobenzohydrazide, ($C_{18}H_{20}N_4O_4$), hereafter called Ligand 1. *N*'-{(*E*)-[4-(diethylamino)-2-hydroxyphenyl]methylidene}-4-methoxybenzohydrazide, ($C_{19}H_{23}N_3O_3$) ligand 2. *N*'-{(*E*)-[4-(dimethylamino)phenyl]methylidene}-4-nitrobenzohydrazide, ($C_{16}H_{16}N_4O_3$), Ligand 3 and *N*'-{(*E*)-[4-(dimethylamino)phenyl]methylidene}-4-methoxybenzohydrazide, ($C_{17}H_{19}N_3O_2$), Ligand 4.

4.2.2. FTIR

The FTIR of all Schiff base ligands were measured at room temperature. The FTIR of these ligands are presented in figure 4.6 to 4.9 and a summary of the important absorption bands and their assignments presented in table 4.3.

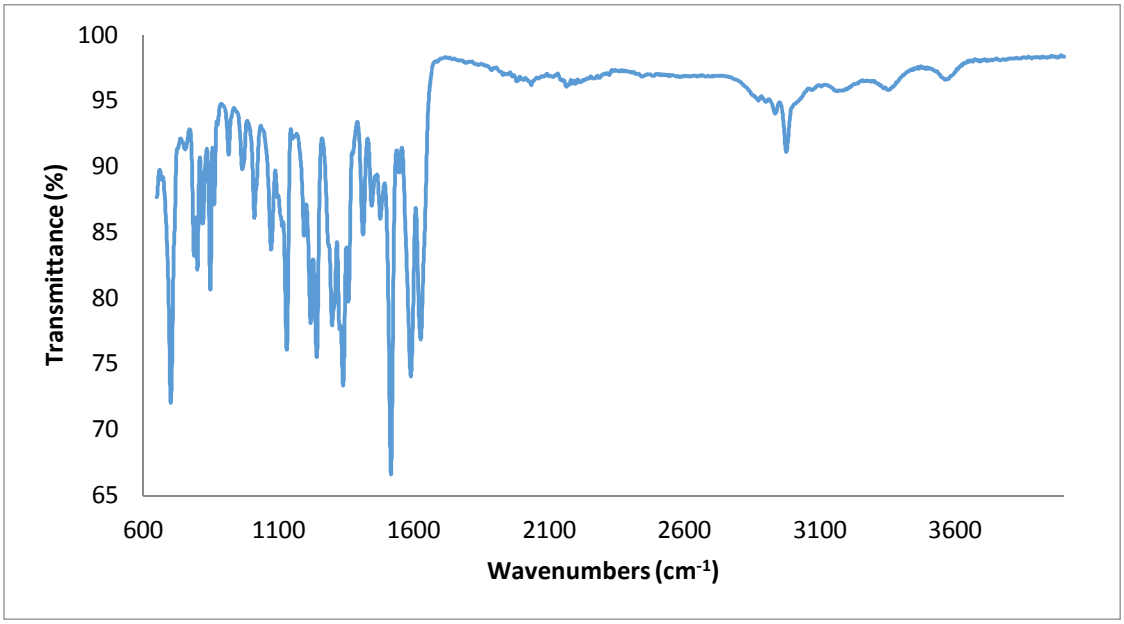

Figure 4.6 FTIR spectrum of Ligand 1

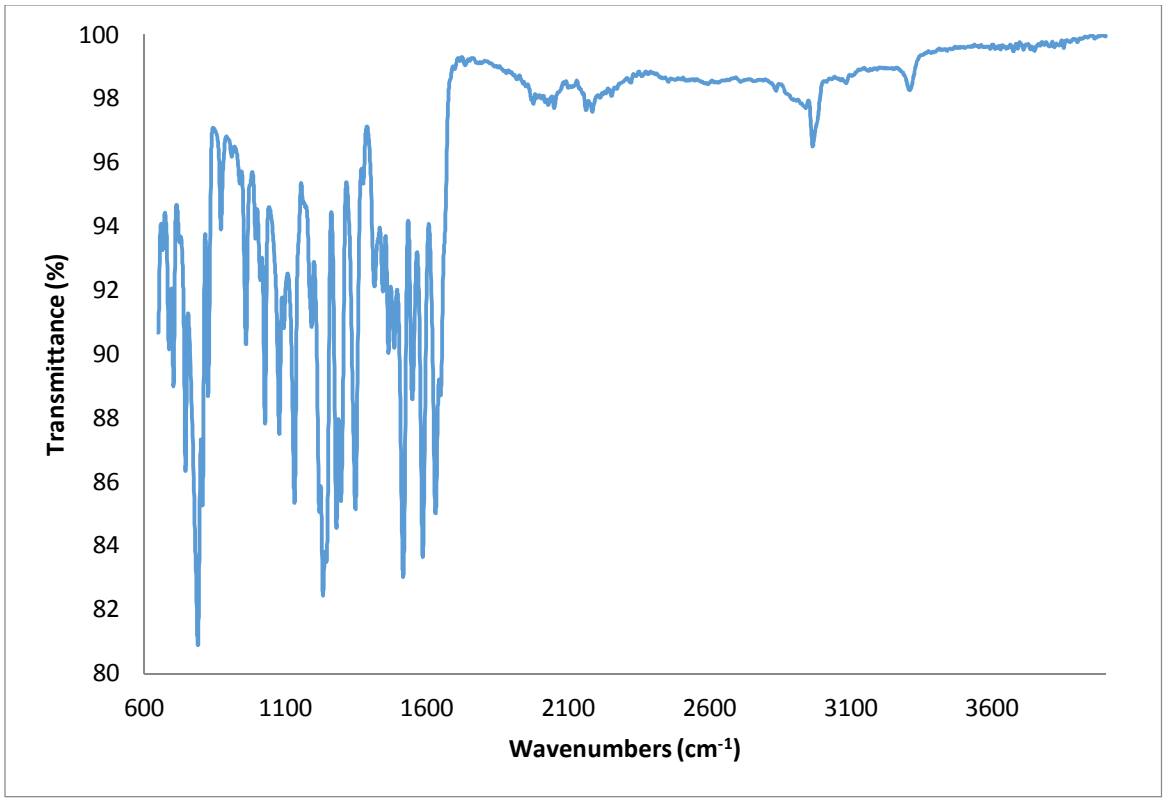

Figure 4.7: FTIR spectrum of Ligand 2

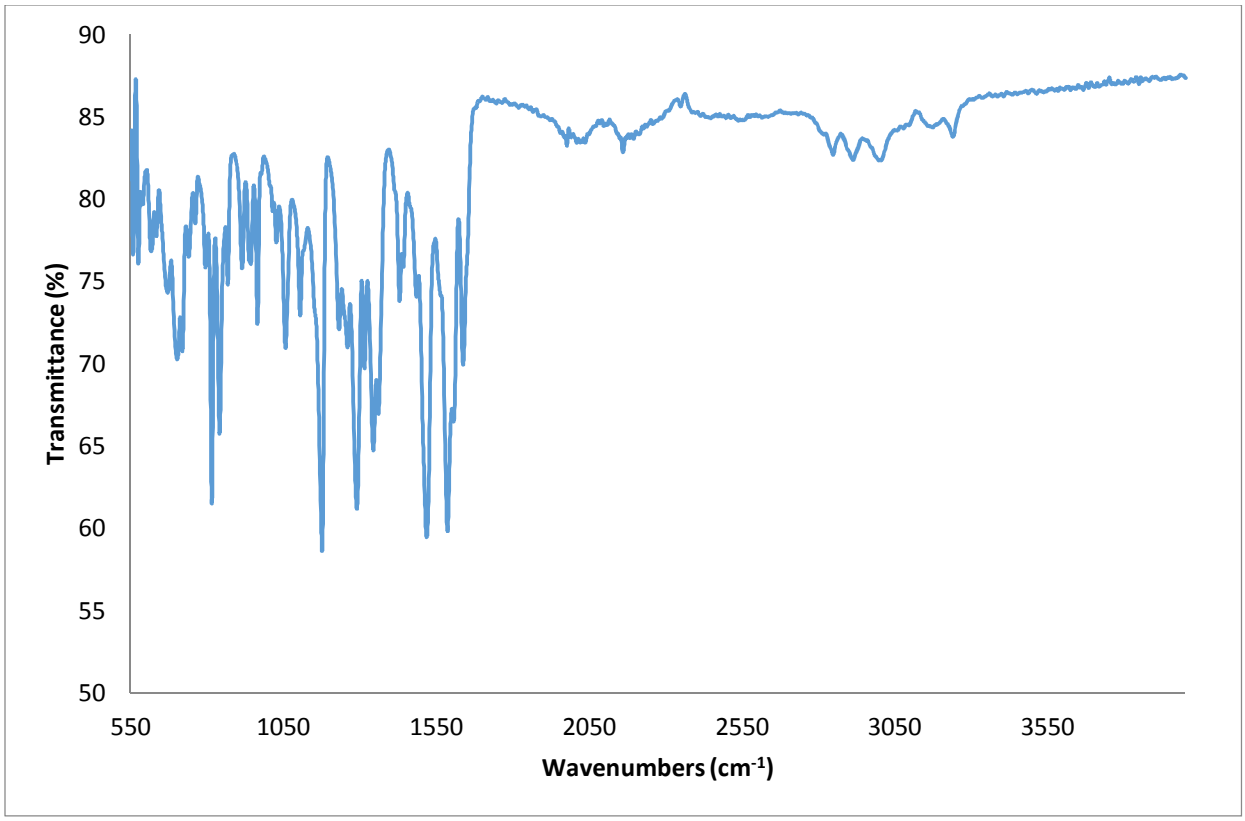

Figure 4.8: FTIR spectrum of Ligand 3

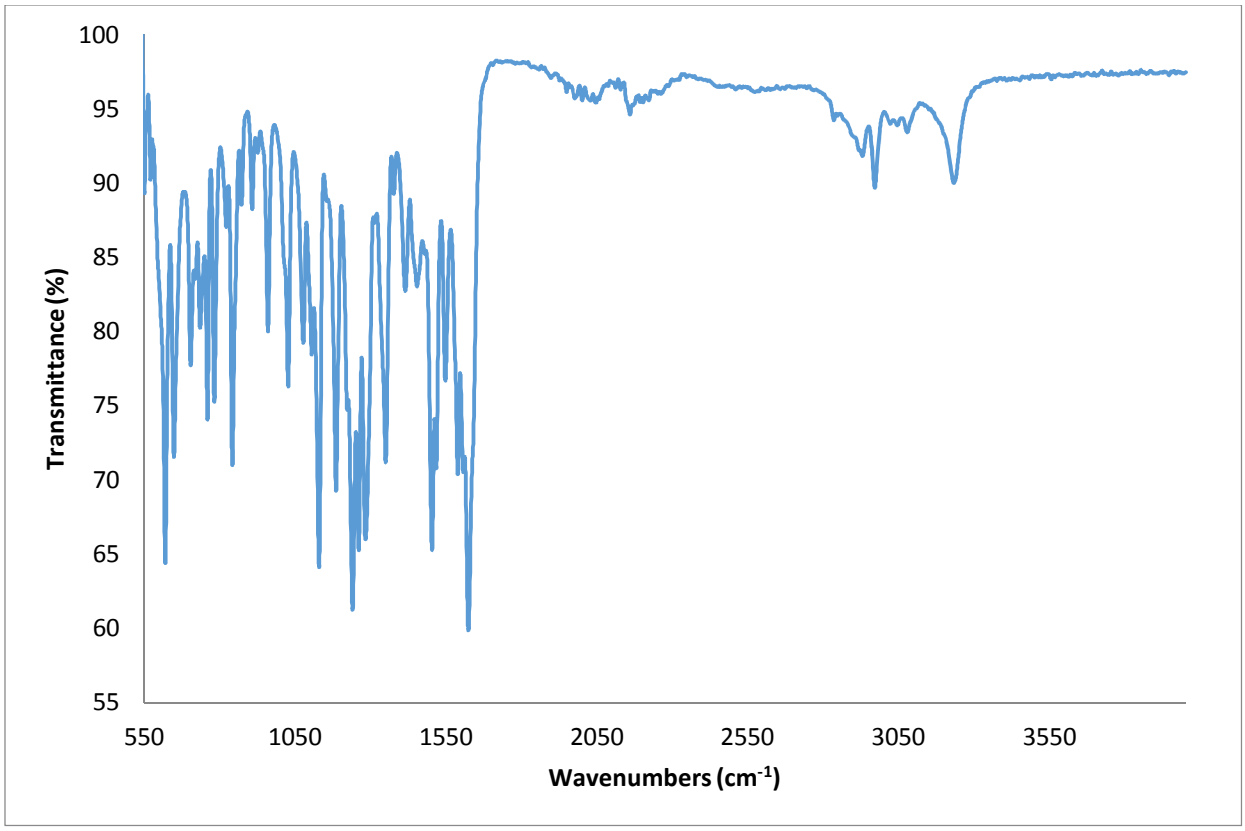

Figure 4.9: FTIR spectrum of Ligand 4

Table 4.3: FTIR absorption bands of ligands 1 to 4.

Ligand 1	Ligand 2	Ligand 3	Ligand 4	Assignment
3558				ν(N-H) stretching
3344			3224	ν(O-H)
3174	3288	3189	3033	
2973	2960	2977	2967	ν(C-H) stretching
2927			2913	
	2890	2890	2827	
1623	1687	1612	1623	ν(N-H) bending ν(C=N) stretching
1589	1589	1585		ν(C=C) aromatic
	1585			
1515	1515	1515	1502	ν(C-H) bending
1413		1429		
1340			1349	ν(C-C) skeletal
1240	1297	1297	1240	
	1232	1288		
1130	1130	1176	1128	ν(C-O) stretch
1074	1027	1054	1025	
1012	1025			ν(C-C) skeletal
964	958	964	960	
914				
848	835	815	842	Ring inplane and
800				Ring out of plane
	788			bending
701	703	696	619	

Discussion

The FTIR of the ligands show some interesting absorption bands. The bands at 3174 to 3558 cm^{-1} are assigned as N-H and O-H stretching vibrations. These are week bands resulting from the formation of an azomethine bond characteristic of Schiff bases. The absorption band at 1612 to 1687 cm^{-1}, assigned as a ν(N-H) or ν(C=N) stretching vibration originates from the nitrogen of the hydrazide linked to form the Schiff base. The other absorption bands observed are basically expected absorption bands due to the benzene rings, the methyl and carbonyl groups stretching, bending and skeletal vibrations [3-5].

4.2.3 Thermogravimetric Analysis of Schiff base Ligands

Thermogravimetric analysis (TGA) and Derivative thermogravimetric analysis (DTA) of Schiff base ligands were measured in a nitrogen atmosphere from 0°C to 900°C. The results obtained are displayed in figures 4.10 to 4.13. The TGA result is plotted as percentage weight loss against temperature and provides information such as vaporization, sublimation, phase transition etc while the DTA is plotted as percentage derivative weight against temperature. Changes in the sample in the DTA curve show either exothermic or endothermic reaction taking place in the sample [5].

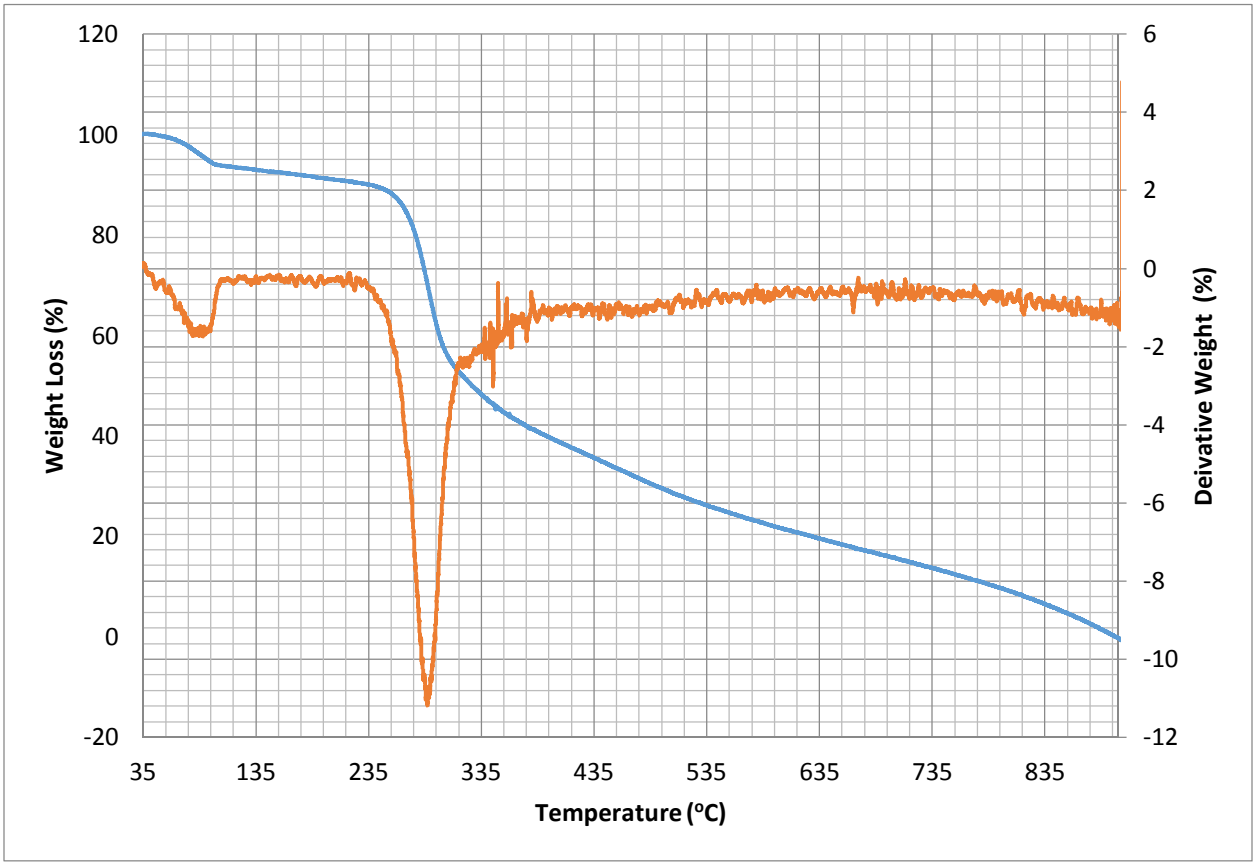

Figure 4.10: Thermogravimetric and derivative thermogravimetric analysis of Ligand 1

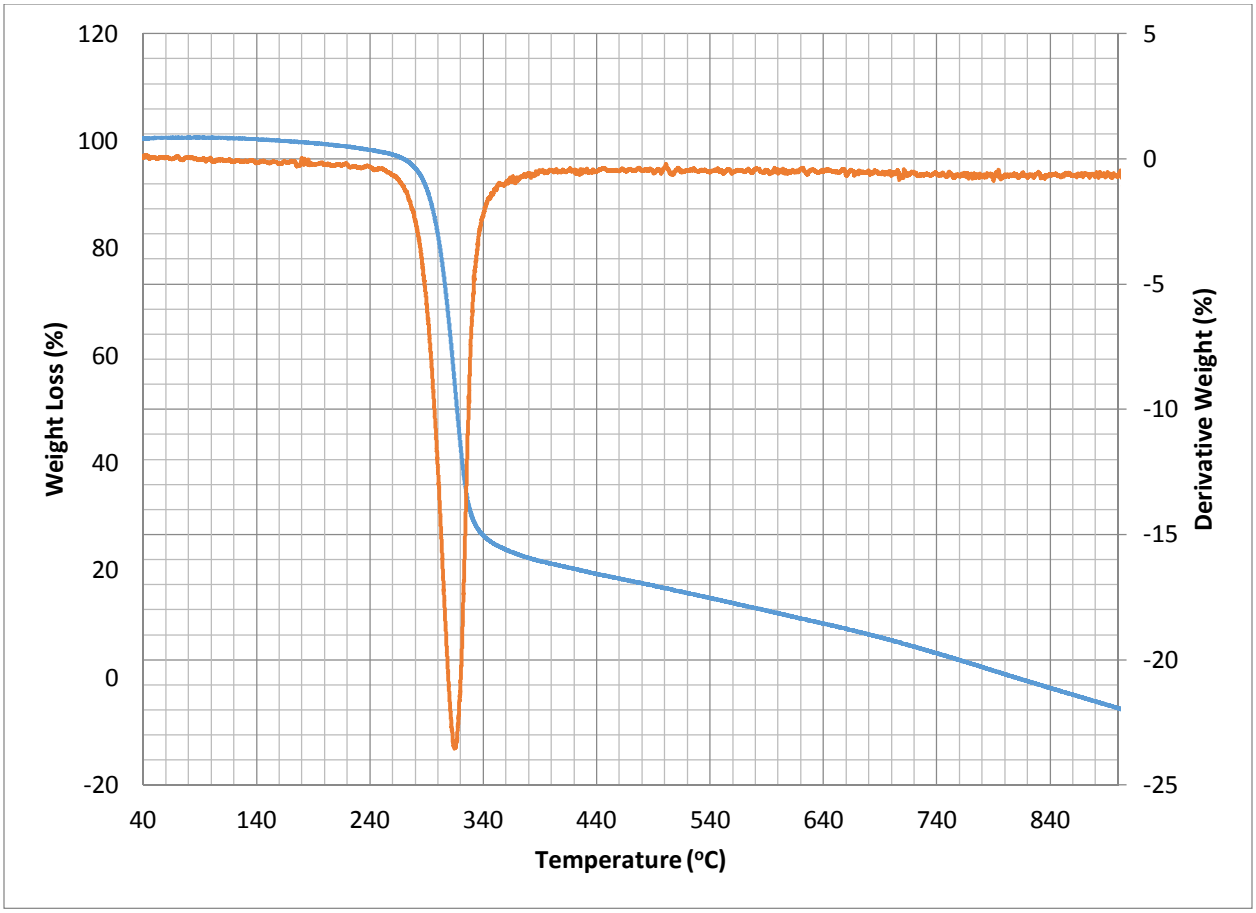

Figure 4.11: Thermogravimetric and derivative thermogravimetric analysis of Ligand 2

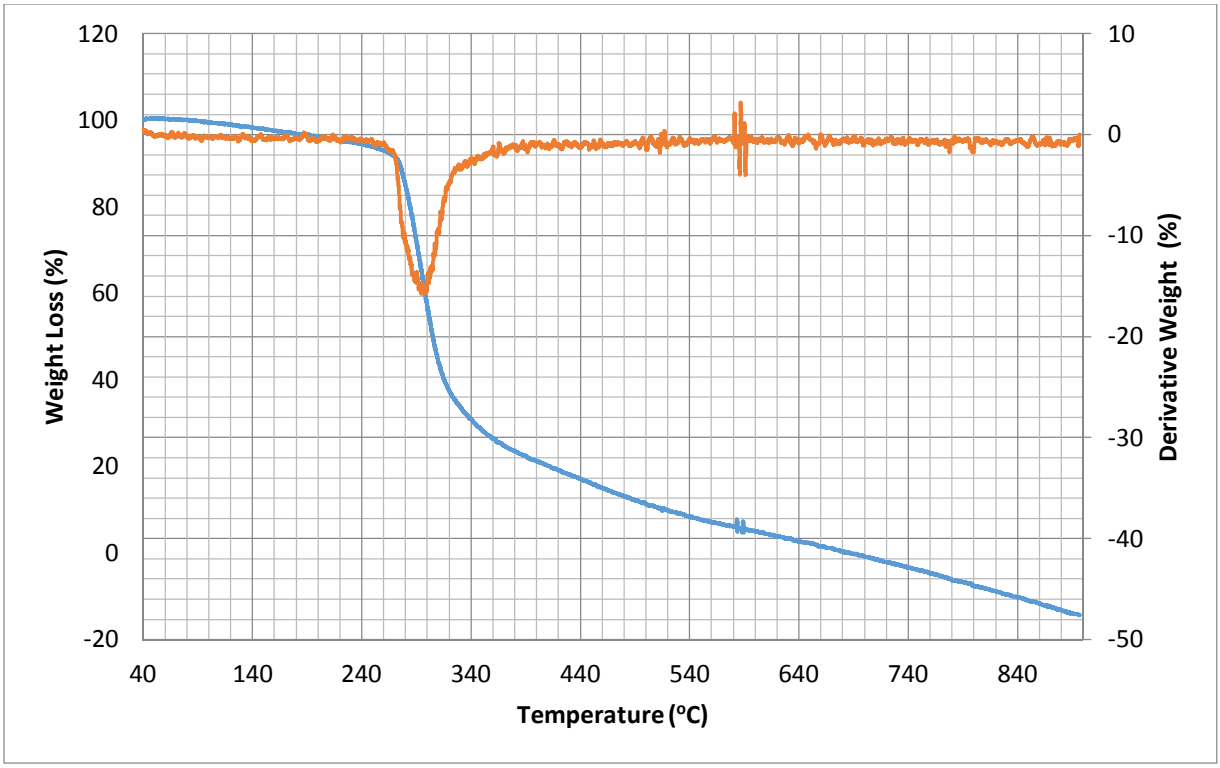

Figure 4.12: Thermogravimetric and derivative thermogravimetric analysis of Ligand 3

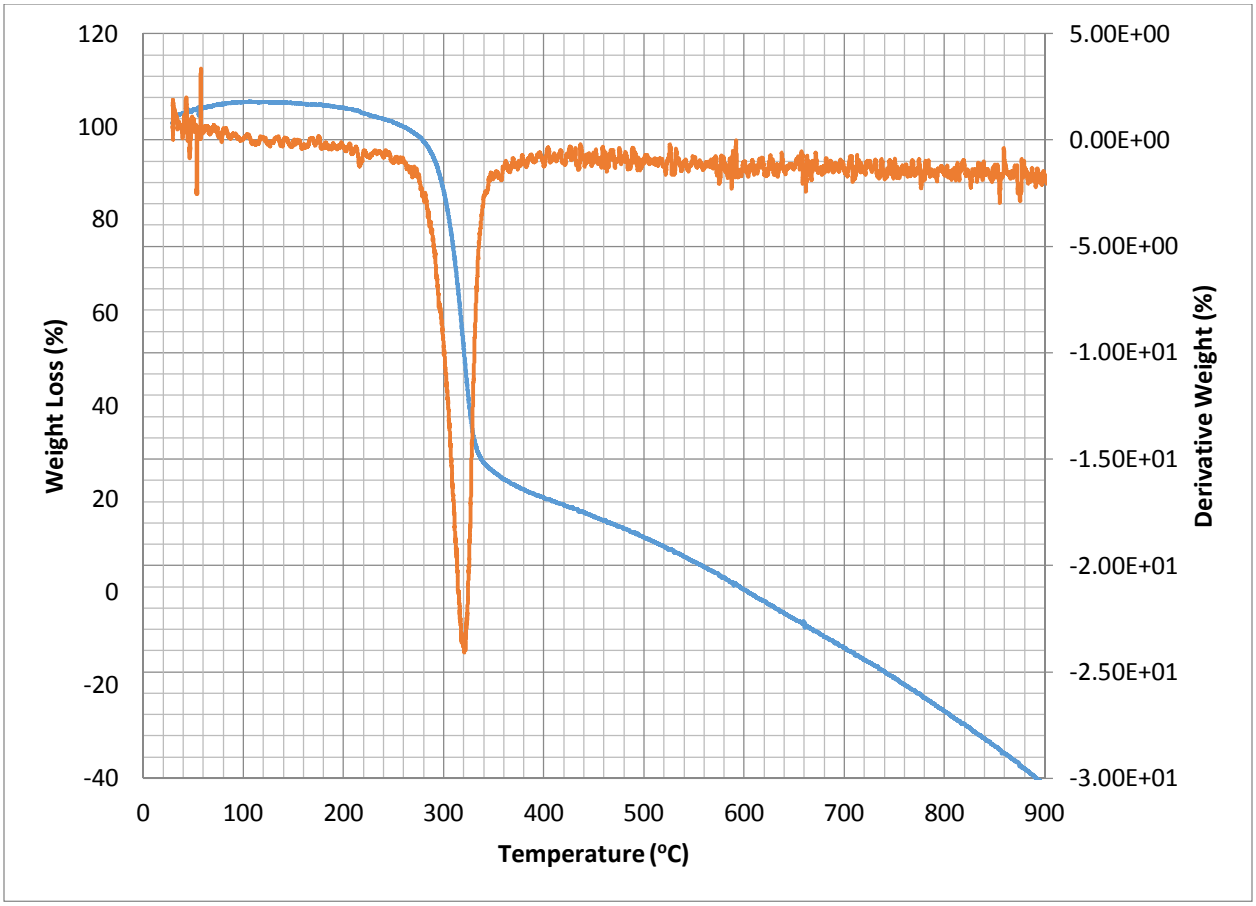

Figure 4.13: Thermogravimetric and derivative thermogravimetric analysis of Ligand 4

Discussion

The TGA and DTA of ligand 1, figure 4.10, show two reaction peaks. The peak at about 42.83^{o}C could be assigned as the vaporization of methanol solvent used in the synthesis while the peak at 223.83^{o}C is the temperature at which the ligand melts. No other reaction peaks is observed indicating the sample prepared is a pure sample.

The TGA and DTA of ligand 2, figure 4.11, show only a single reaction taking place. The synthesized sample begins to melt at 248.9^{o}C. The presence of a single peak is an indication that the substance synthesized was pure.

The TGA and DTA of ligand 3, figure 4.12, show only a single reaction taking place. The synthesized sample begins to melt at 251.41^{o}C. The presence of a single peak is an indication that the substance synthesized was pure.

The TGA and DTA of ligand 4, figure 4.13, show only a single reaction taking place. There is a gain in mass from the on-set indicating a reaction with the atmosphere characteristic of oxidation of a metal. The synthesized sample begins to melt at 266.42^{o}C. The graph shows a single stage decomposition indicating that the substance synthesized was pure.

4.2.4 Proton and Carbon-13 NMR of Ligands

Proton and carbon-13 nuclear magnetic resonance spectroscopy (NMR) of ligands were measured in d_6-dimethylsulphoxide (DMSO) solution using tetramethylsilane (TMS) as internal standard. The proton and carbon-13 spectra of the ligands are presented in figures 4.14 to 4.17 and the chemical shifts of the different types of protons and carbon are presented in table 4.4. [4-8]

The proton NMR of ligand 1 to 4 shows eleven proton environments at different chemical shifts. The area under each peak indicates the number of protons in the environments. The splitting of the peak indicates the number of hydrogen atoms at each environment. The structure and formula of ligand 1, page 45 and 82, show two benzene rings and hydrogen atoms at different environments. The chemical shifts and assignments are presented in table 4.4 [1].

The carbon-13 NMR spectra provide further support for the structural characterization of the Schiff base ligands synthesized. Carbon-13 NMR spectral data are presented in table 4.5. The number of signals found corresponds to the presence of magnetically non-equivalent carbon atoms which were assigned by comparison with literature.

Table 4.4: Chemical shifts of proton NMR of ligands 1 to 4.

Chemical Shift (δ) (ppm)				**Assignment**
Ligand 1	**Ligand 2**	**Ligand 3**	**Ligand 4**	
1.114	1.109		1.107	Aliphatic hydrogen
2.5	2.5	2.5	2.5	CH_3 of solvent
3.338 – 3.386	3.332 – 3.836	2.996 – 3.325	3.322 – 3.836	Amino hydrogen
6.133 – 6.292	6.130 – 6.281	6.770 – 6.787	6.125 – 6.273	Aromatic ring hydrogen
7.229 – 7.246	7.145 – 7.503	7.563 – 7.580	7.054 – 7.912	Aromatic ring hydrogen
8.144 – 8.457	8.431	8.133 – 8.377	8.409	Azomethine hydrogen
11.319	11.466 – 11.758	11.835	11.534 – 11.671	Carbonyl
12.068				Phenolic hydrogen

Table 4.5: Chemical shifts of Carbon-13 NMR of ligands 1 to 4.

Chemical Shift (δ) (ppm)				Assignment
Ligand 1	Ligand 2	Ligand 3	Ligand 4	
13.01	13.02		13.02	Methyl Car
44.29	44.27 – 55.82		44.26 – 55.90	Methylene carbon
97.91	97.99		98.03	Methoxy carbon
		112.27		
104.26 – 106.79	104.13 – 106.92		104.06 – 107.01	Aromatic carbon
124.11 – 132.11	113.23 – 120.1	121.72 – 124.07	114.22 – 125.68	Aromatic carbon
139.39	130.13 – 135.05	129.12 – 129.50	129.82 – 132.04	
149.65 – 151.24	150.54 – 150.66	140.01	149.96 – 150.52	Azomethine carbon
160.29 – 160.96	159.71 – 162.41	149.57 – 152.19	160.17 – 162.43	Phenolic carbon

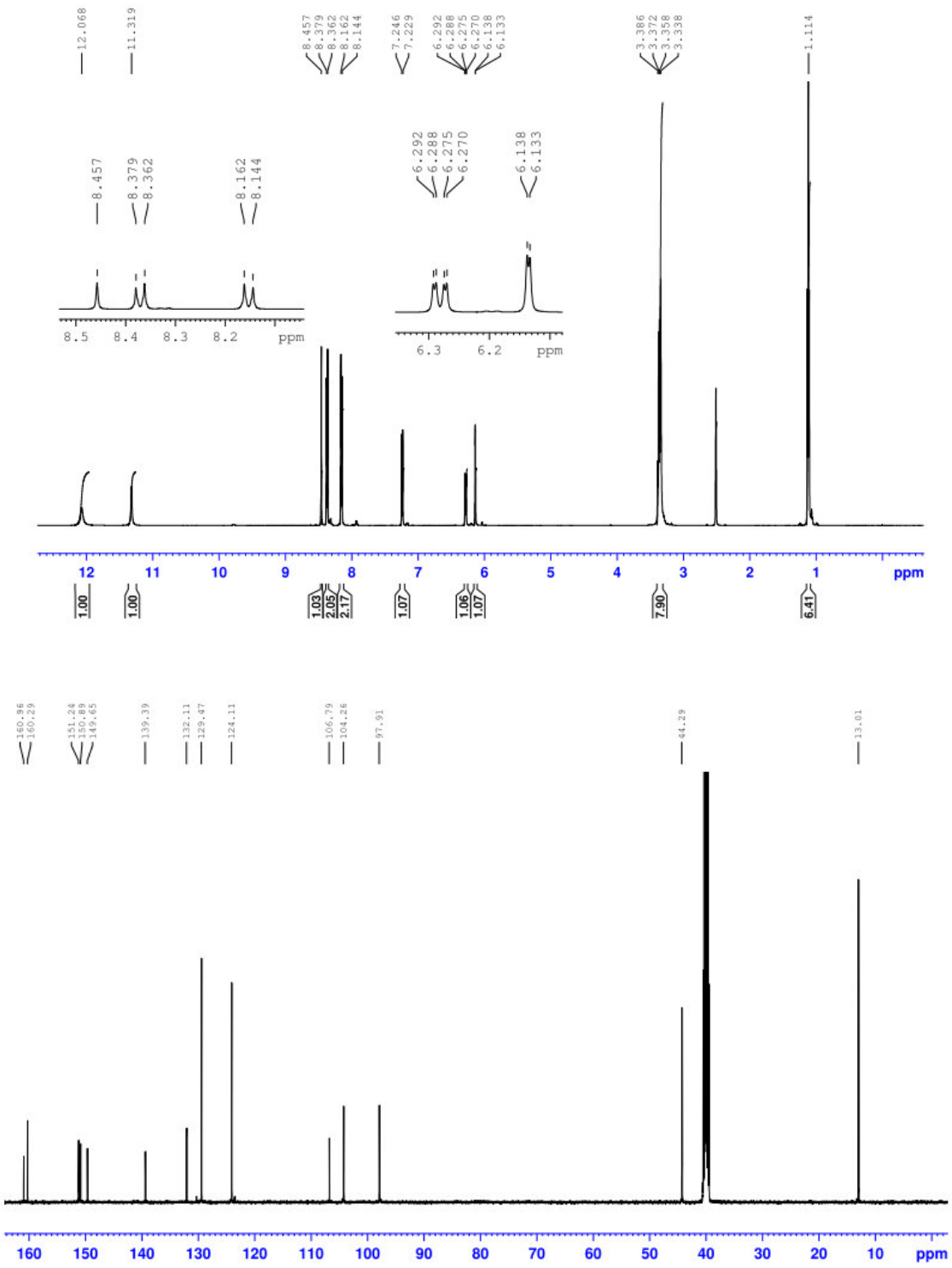

Figure 4.14: Proton and Carbon-13 NMR of Ligand 1.

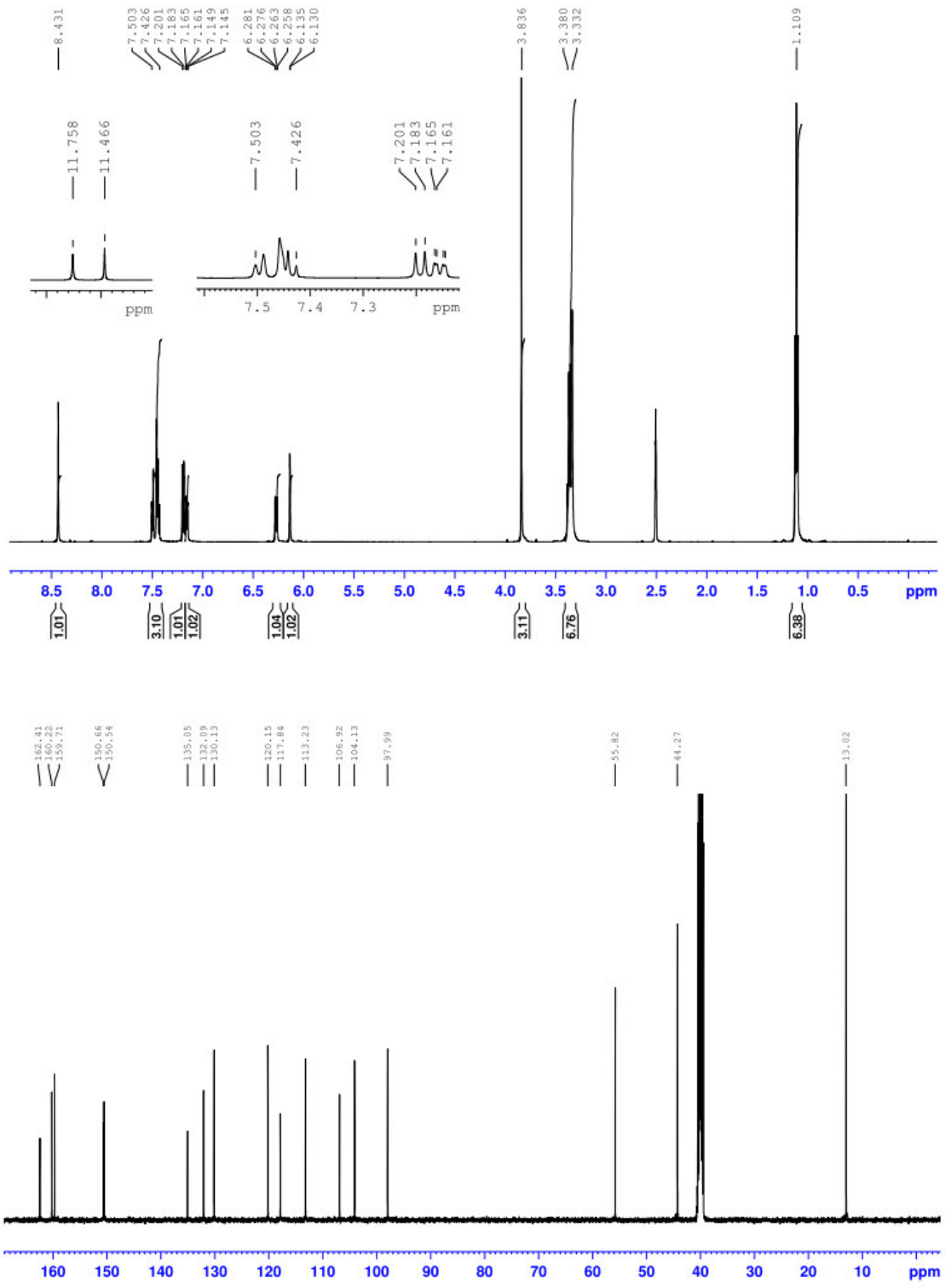

Figure 4.15: Proton and Carbon-13 NMR of Ligand 2.

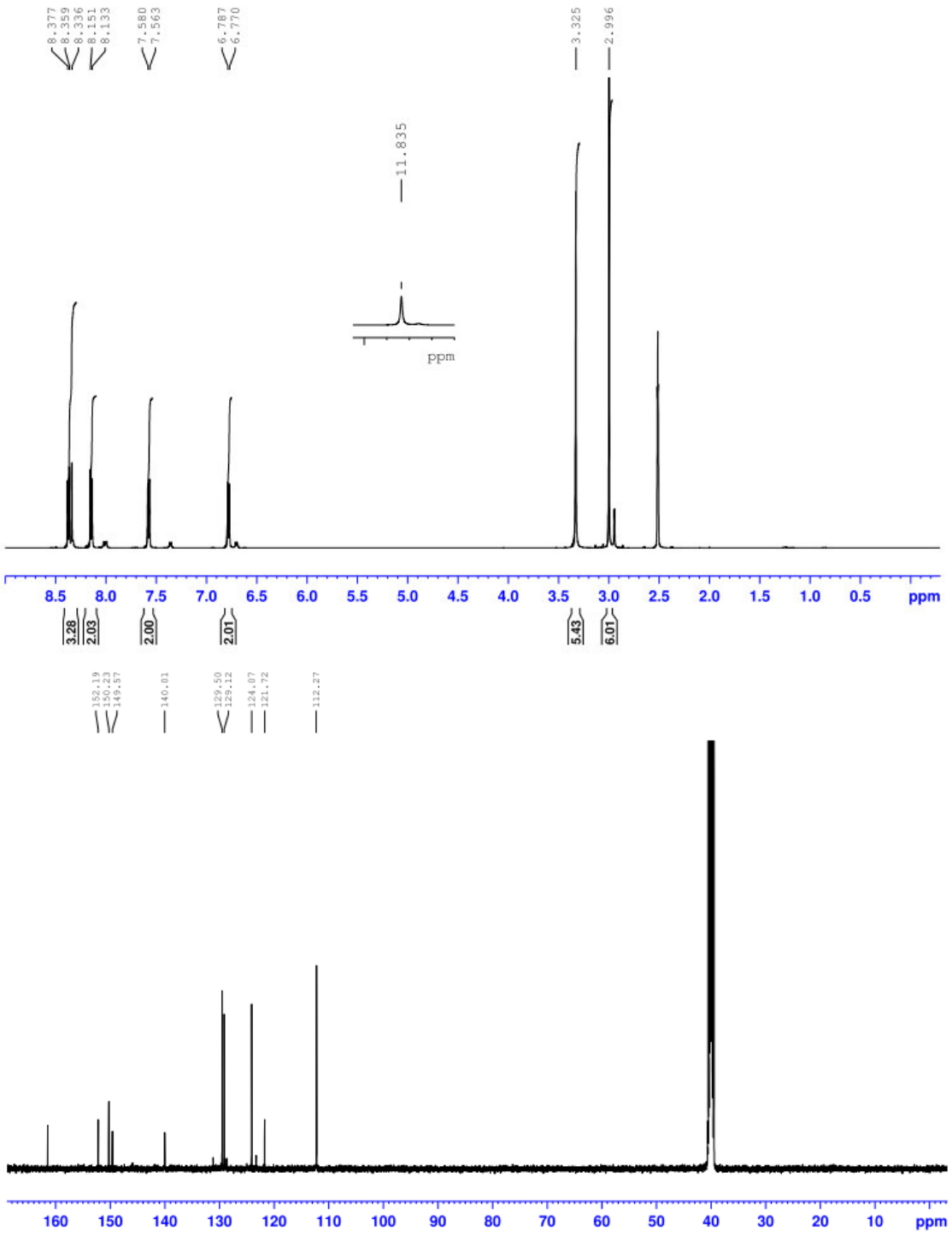

Figure 4.16: Proton and Carbon-13 NMR of Ligand 3.

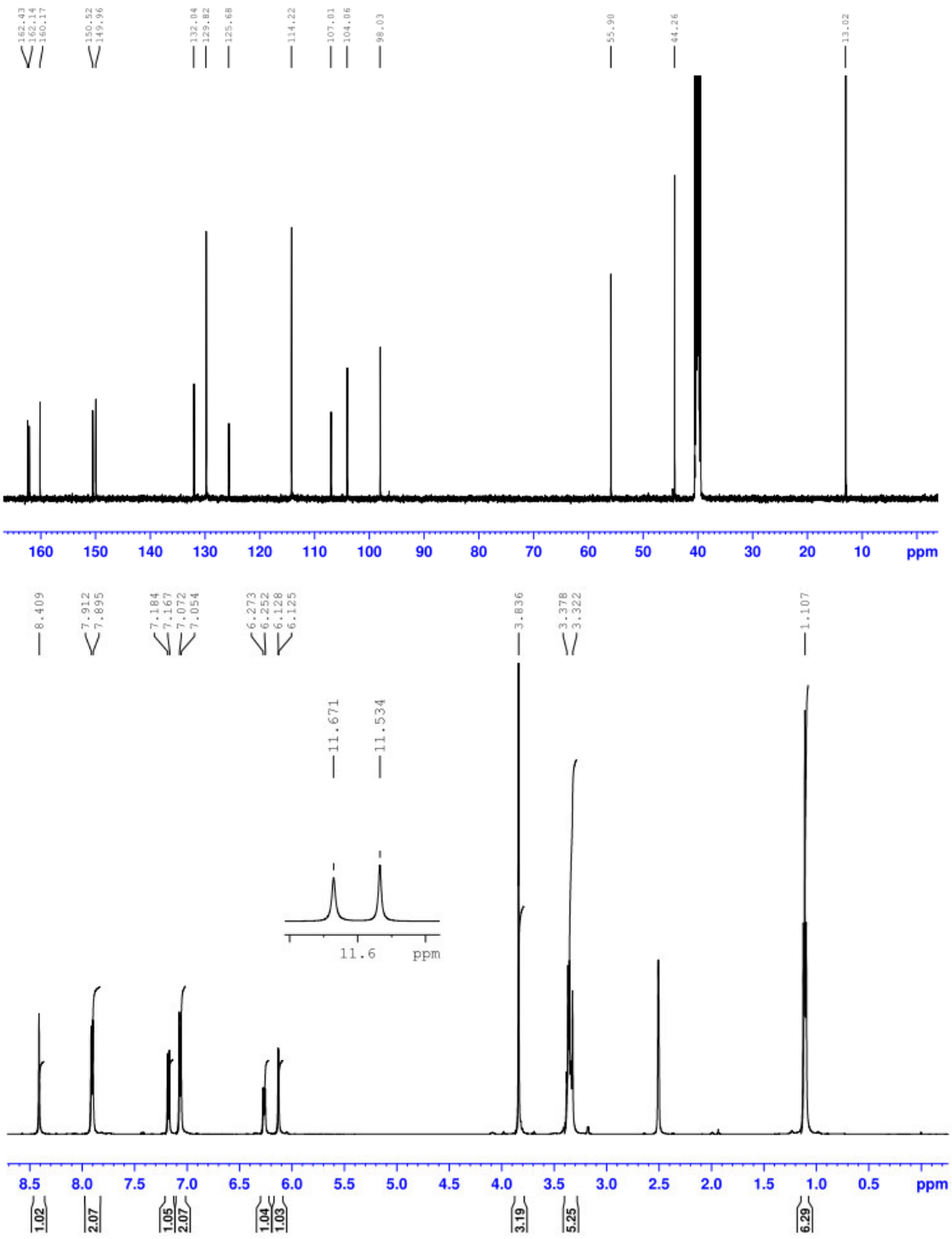

Figure 4.17: Proton and Carbon-13 NMR of Ligand 4.

4.3 Schiff Base Complexes

Schiff base complexes were synthesized as described in chapter 3. Four metal acetylacetonates, $VO(acac)_2$, $Mn(acac)_3$, $Co(acac)_3$, and $Mg(acac)_2$, were reacted with each of ligands 1, 2, 3 and 4 to form Schiff Base Complexes, (SBC), as shown in table 4.6

Table 4.6: Reaction of Schiff base ligands and metal acetylacetonates to form Schiff Base Complexes

Schiff Base Complex	Ligand	Metal Acetylacetonate	Comment
1A	Ligand 1	$VO(acac)_2$	Ligand 1 was formed by reacting 4-(diethylamino)-2-hydroxy benzaldehyde with 4-nitrohydrazide
2A		$Mn(acac)_3$	
3A		$Co(acac)_3$	
4A		$Mg(acac)_2$	
1B	Ligand 2	$VO(acac)_2$	Ligand 2 was formed by reacting 4-(diethylamino)-2-hydroxy benzaldhyde with 4-methoxyhydrazide
2B		$Mn(acac)_3$	
3B		$Co(acac)_3$	
4B		$Mg(acac)_2$	
1C	Ligand 3	$VO(acac)_2$	Ligand 3 was formed by reacting 4-(dimethylamino) benzaldehyde with 4-nitrohydrazide
2C		$Mn(acac)_3$	
3C		$Co(acac)_3$	
4C		$Mg(acac)_2$	
1D	Ligand 4	$VO(acac)_2$	Ligand 4 was formed by reacting 4-(dimethylamino) benzaldehyde with 4-methoxyhydrazide.
2D		$Mn(acac)_3$	
3D		$Co(acac)_3$	
4D		$Mg(acac)_2$	

4.3.2 FTIR

The FTIR of these Schiff Base Complexes are presented in figures 4.18 to 4.33 and important absorption bands and their assignments are presented in table 4.7. The absorption bands show the presence of N-H and O-H stretching vibrations in SBC 1B, 1C 2A, 2B, 3A, 3B, 4A to 4C. Carbonyl stretching vibration (C=O) is observed SBC 1B, 2A and 2B showing that the reaction of metal acetylacetonates with the ligands did not take place at the carbonyl oxygen. The other absorption bands shown in the table are mostly from finger print regions.

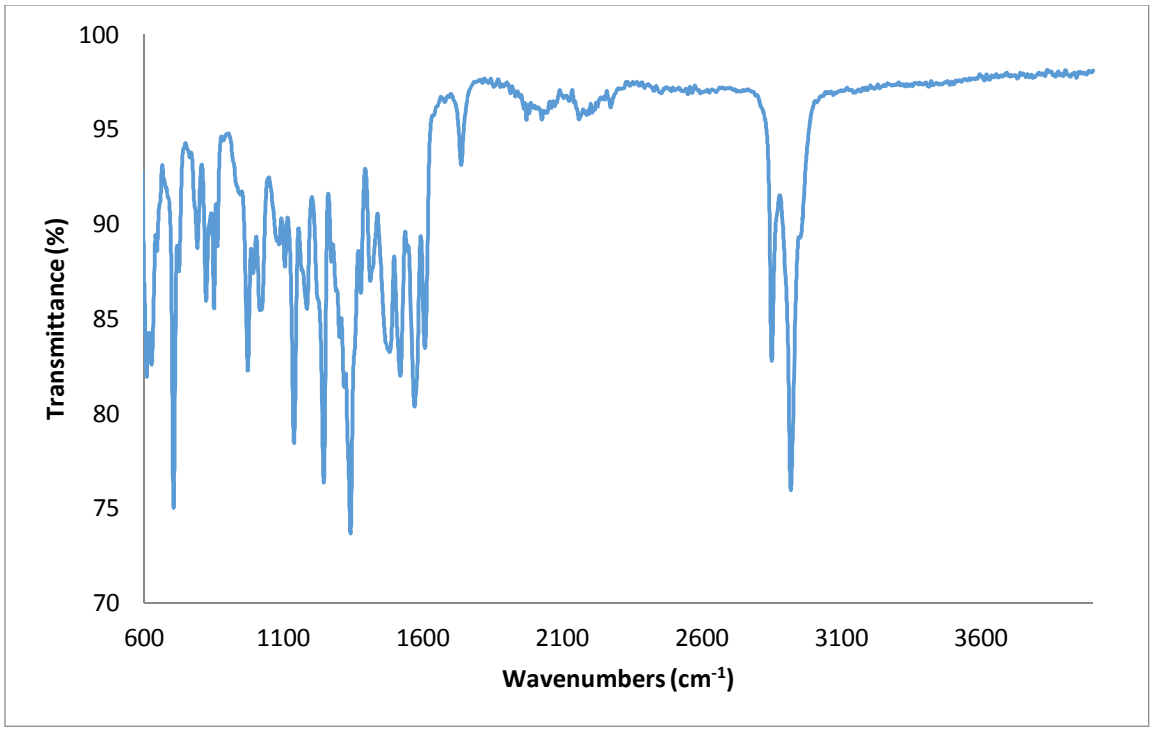

Figure 4.18: FTIR spectrum of Schiff base complex 1A.

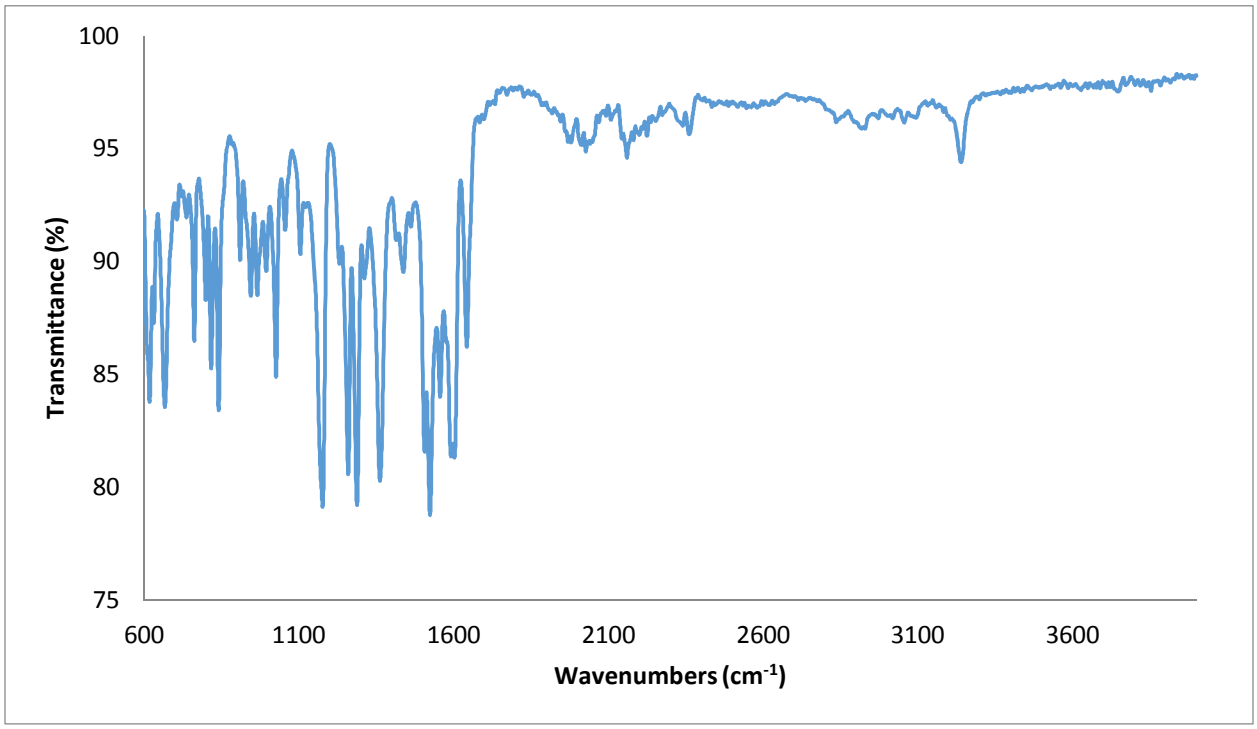

Figure 4.19: FTIR spectrum of Schiff base complex 1B.

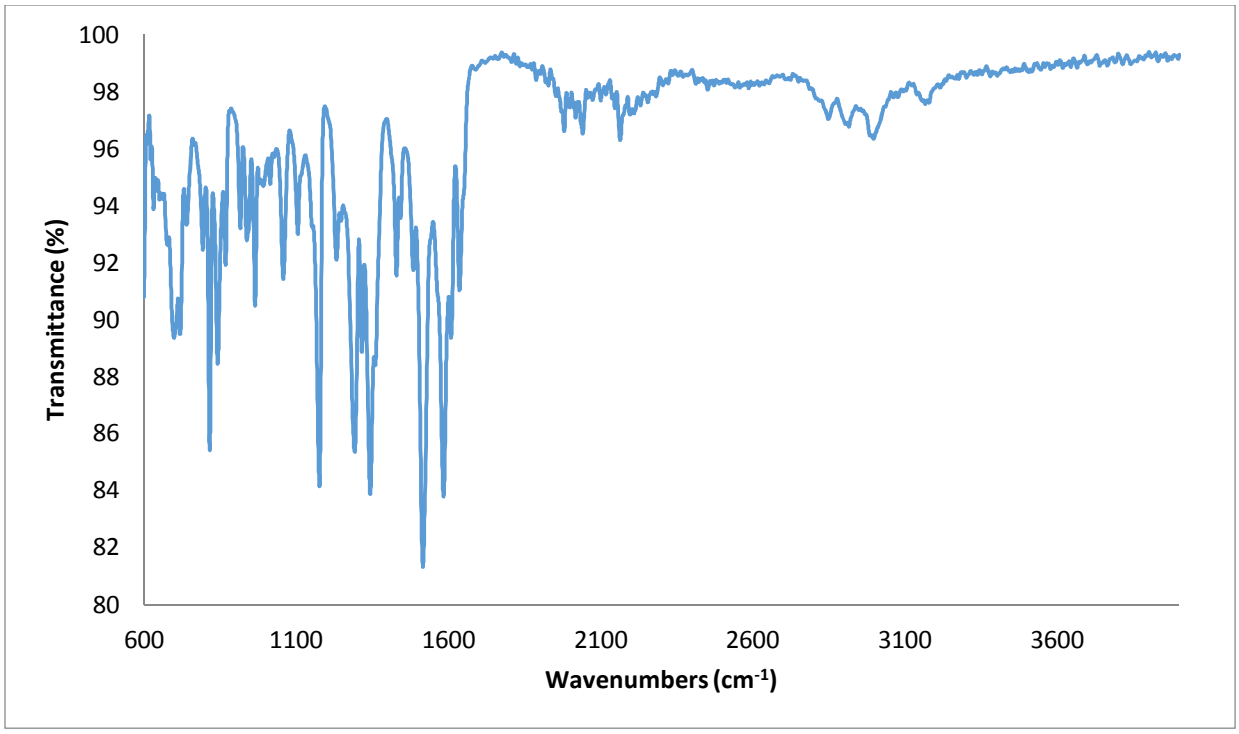

Figure 4.20: FTIR spectrum of Schiff base complex 1C

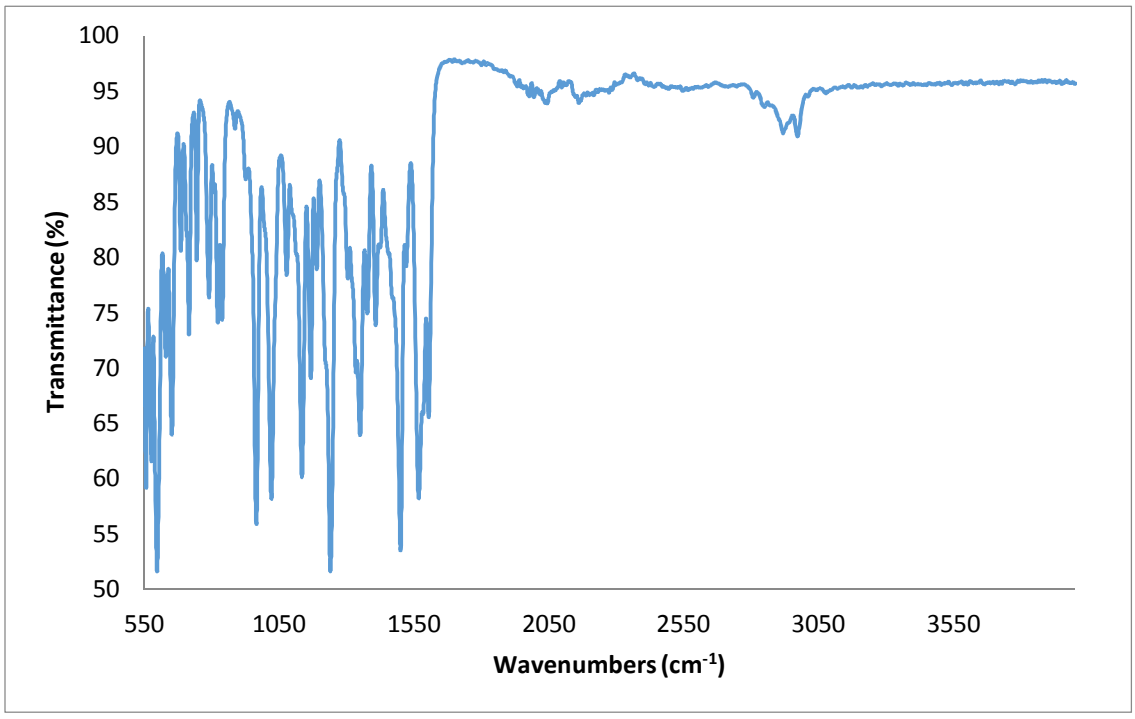

Figure 4.21: FTIR spectrum of Schiff base complex 1D

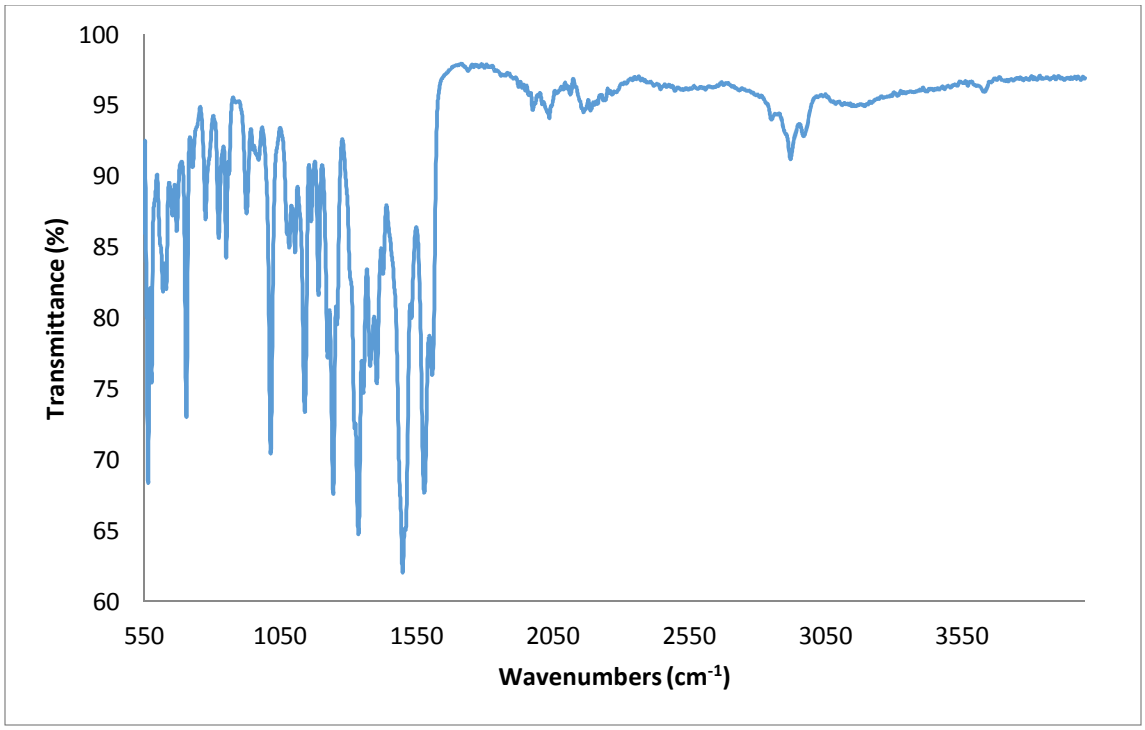

Figure 4.22: FTIR spectrum of Schiff base complex 2A

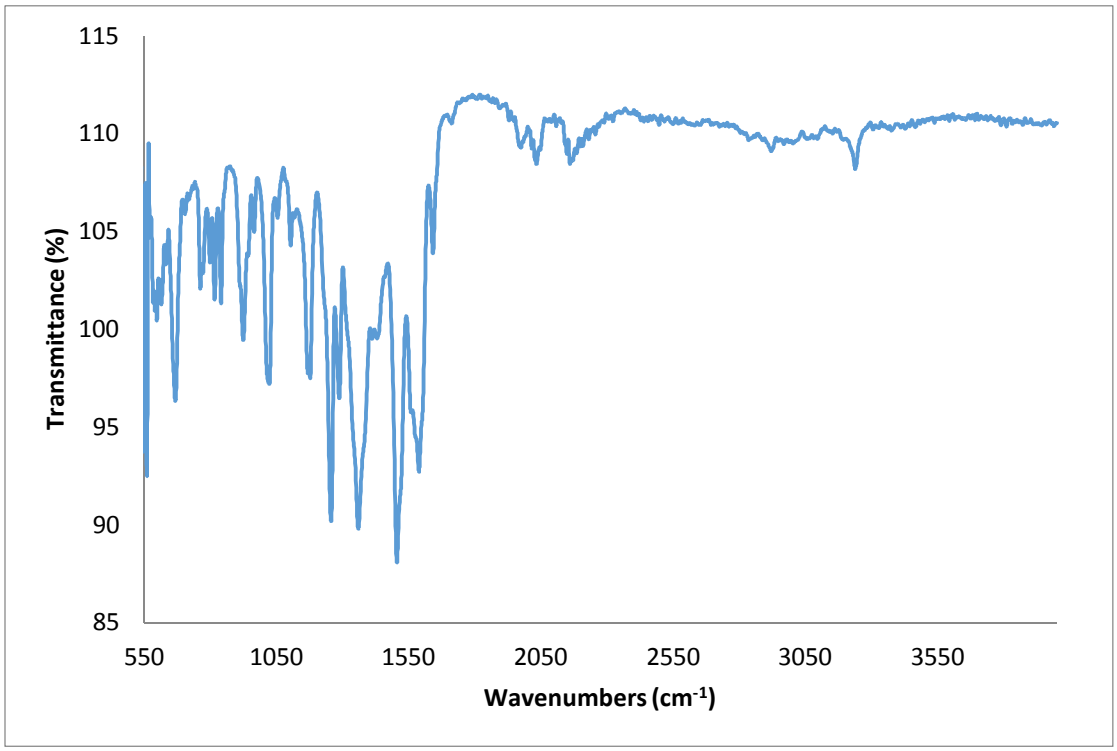

Figure 4.23: FTIR spectrum of Schiff base complex 2B

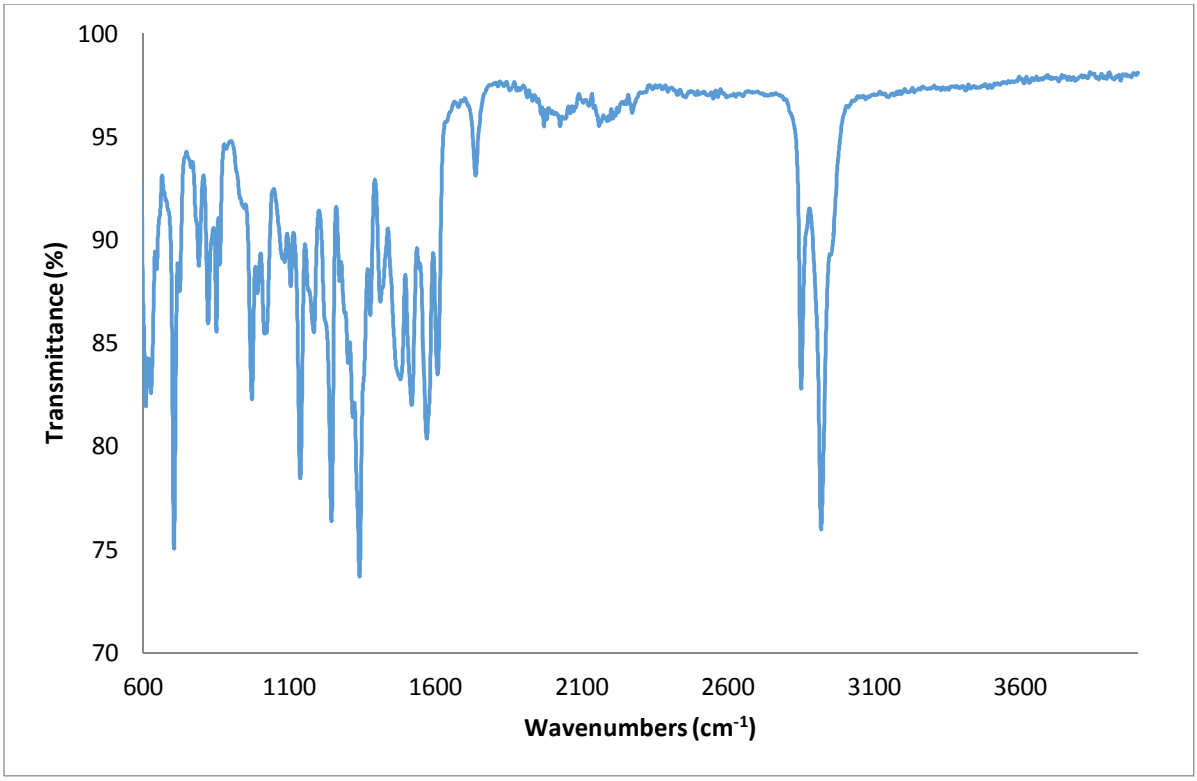

Figure 4.24: FTIR spectrum of Schiff base complex 2C

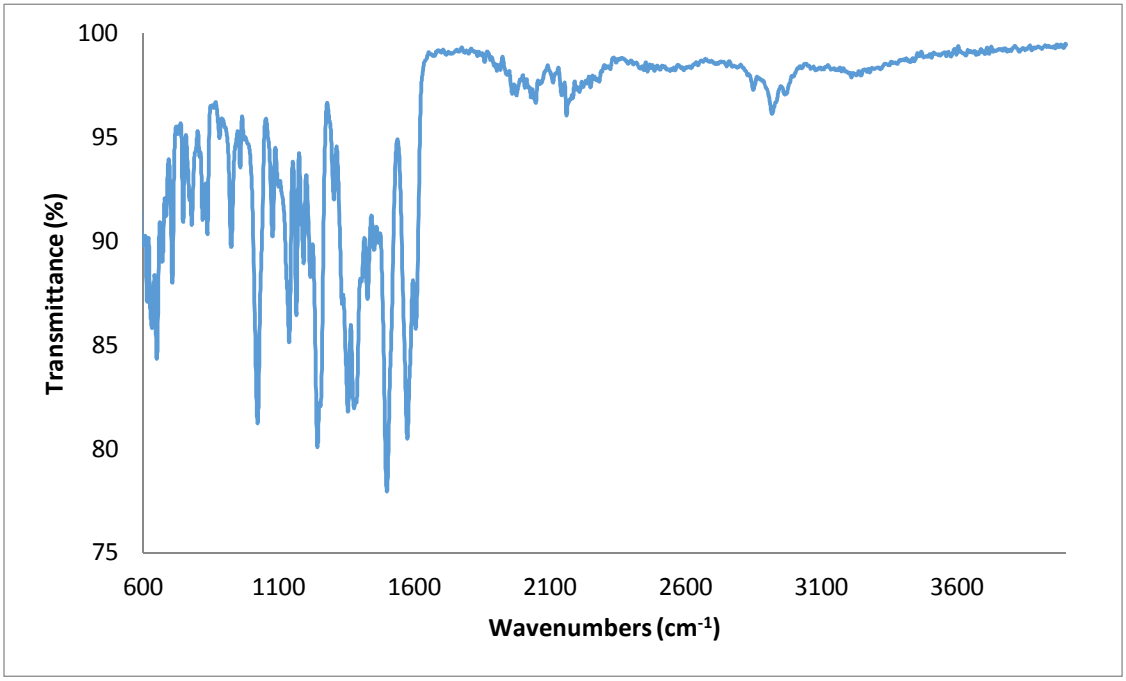

Figure 4.25: FTIR spectrum of Schiff base complex 2D

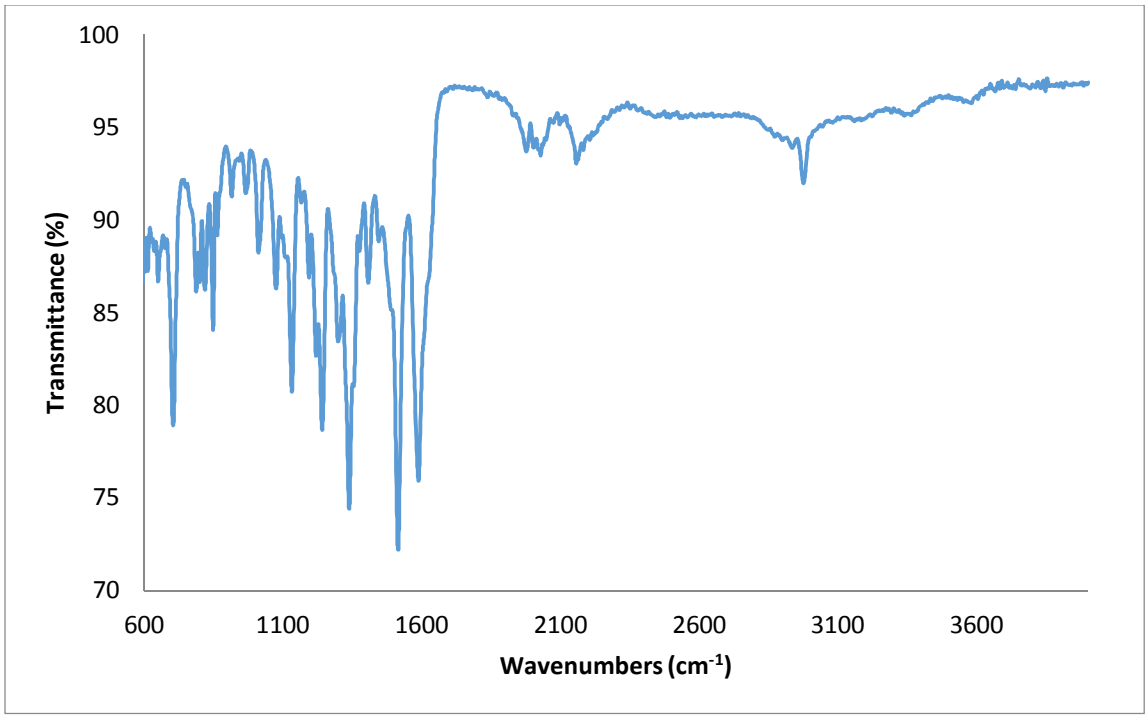

Figure 4.26: FTIR spectrum of Schiff base complex 3A

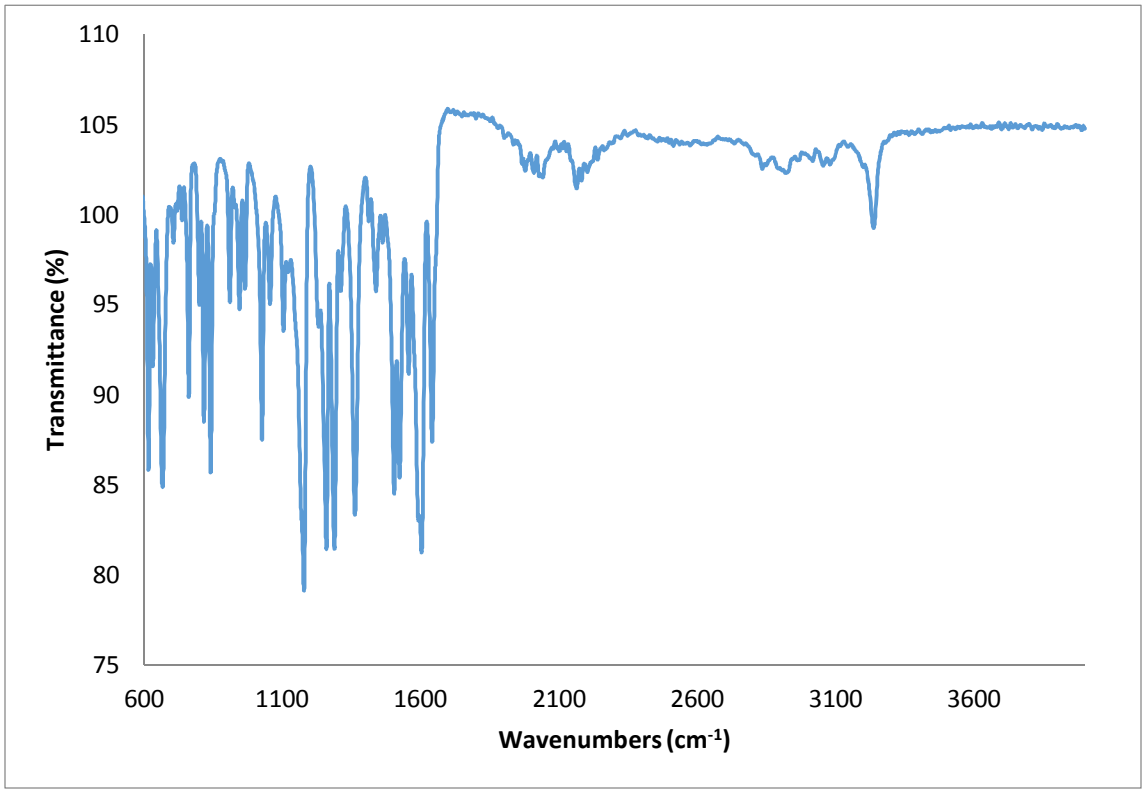

Figure 4.27: FTIR spectrum of Schiff base complex 3B

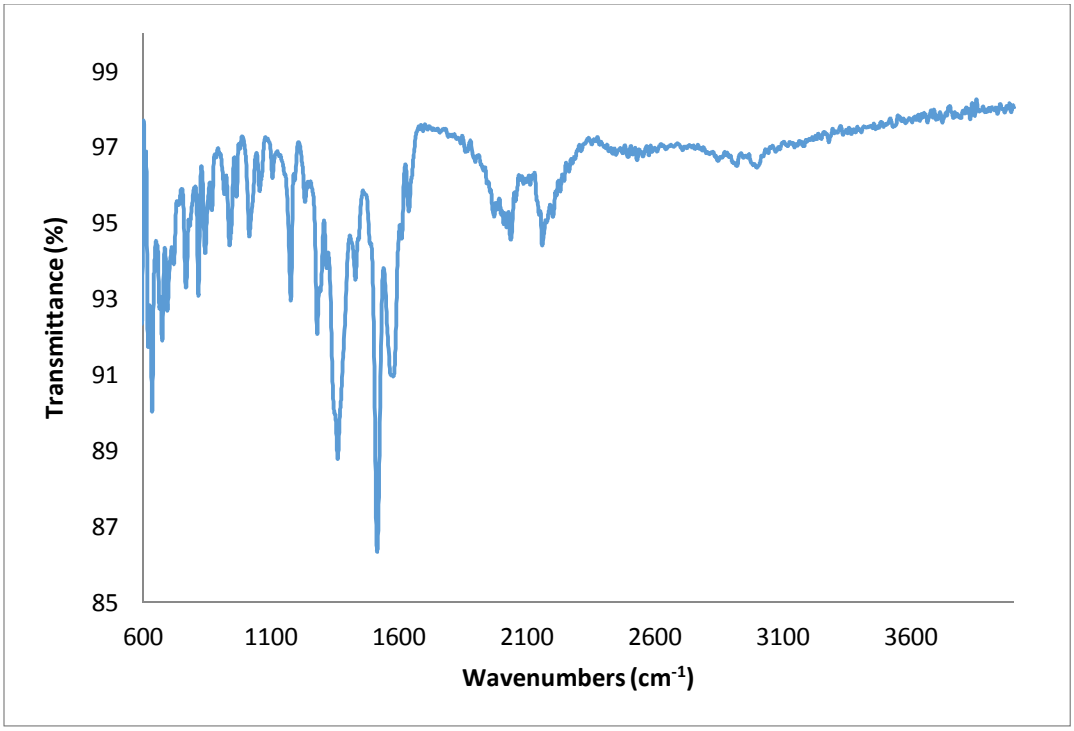

Figure 4.28: FTIR spectrum of Schiff base complex 3C

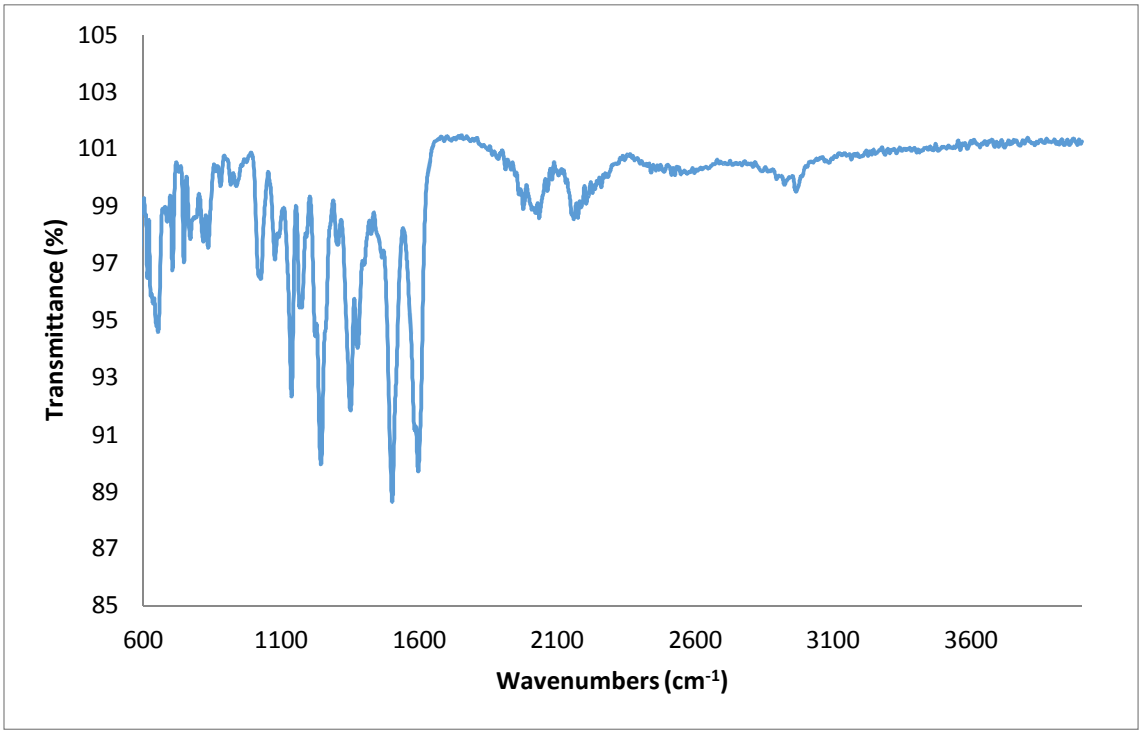

Figure 4.29: FTIR spectrum of Schiff base complex 3D

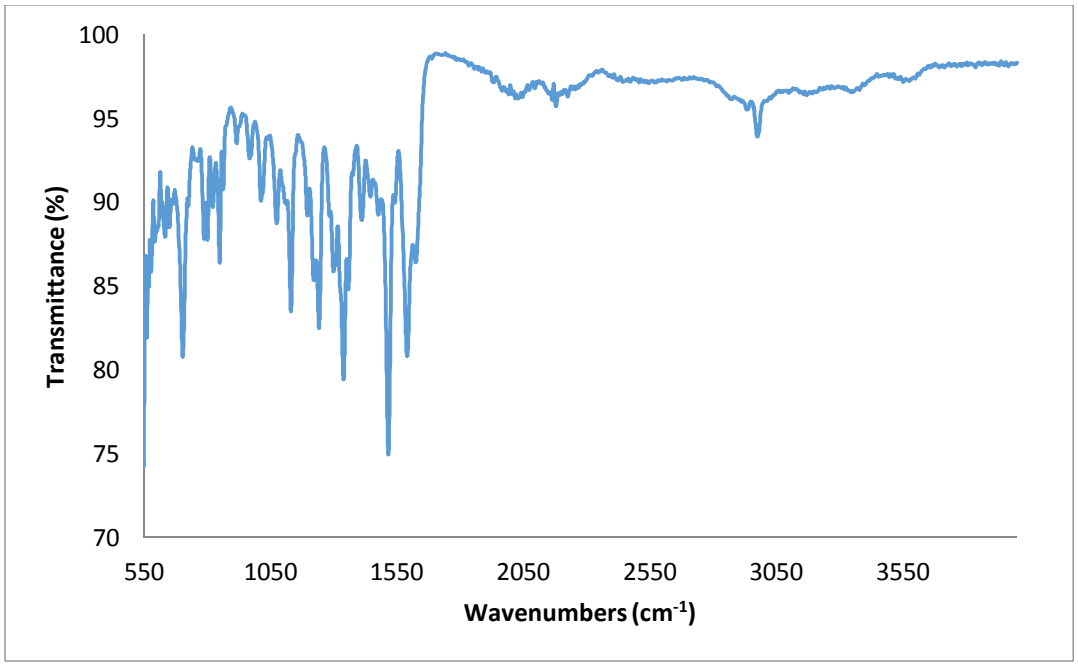

Figure 4.30: FTIR spectrum of Schiff base complex 4A

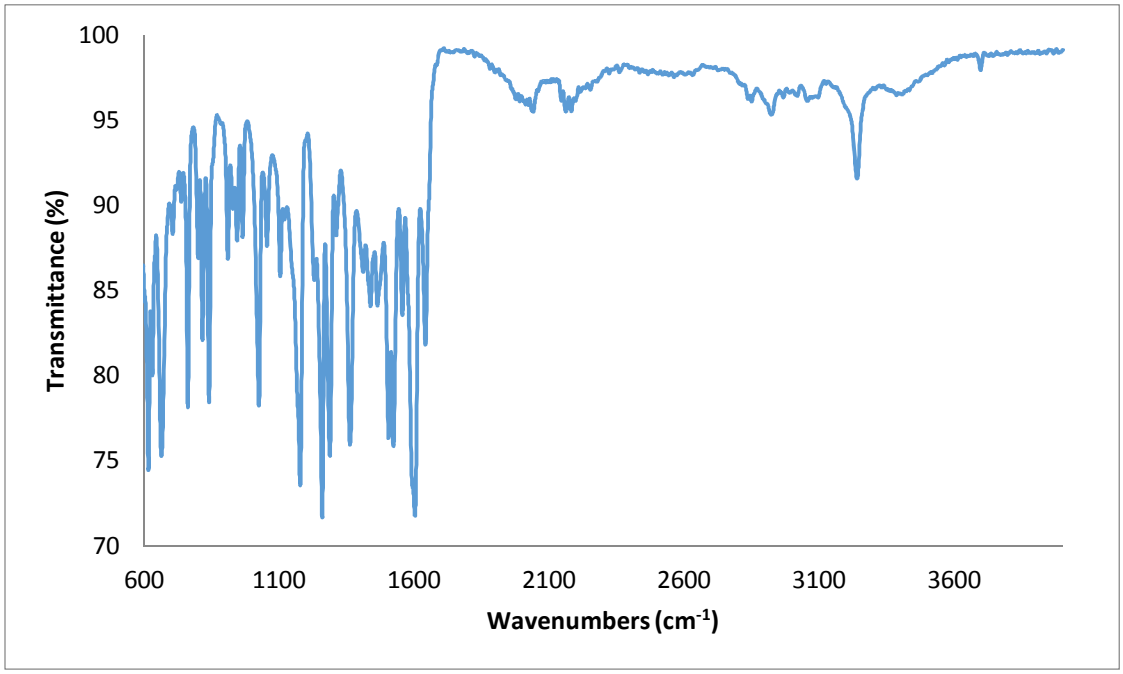

Figure 4.31: FTIR spectrum of Schiff base complex 4B

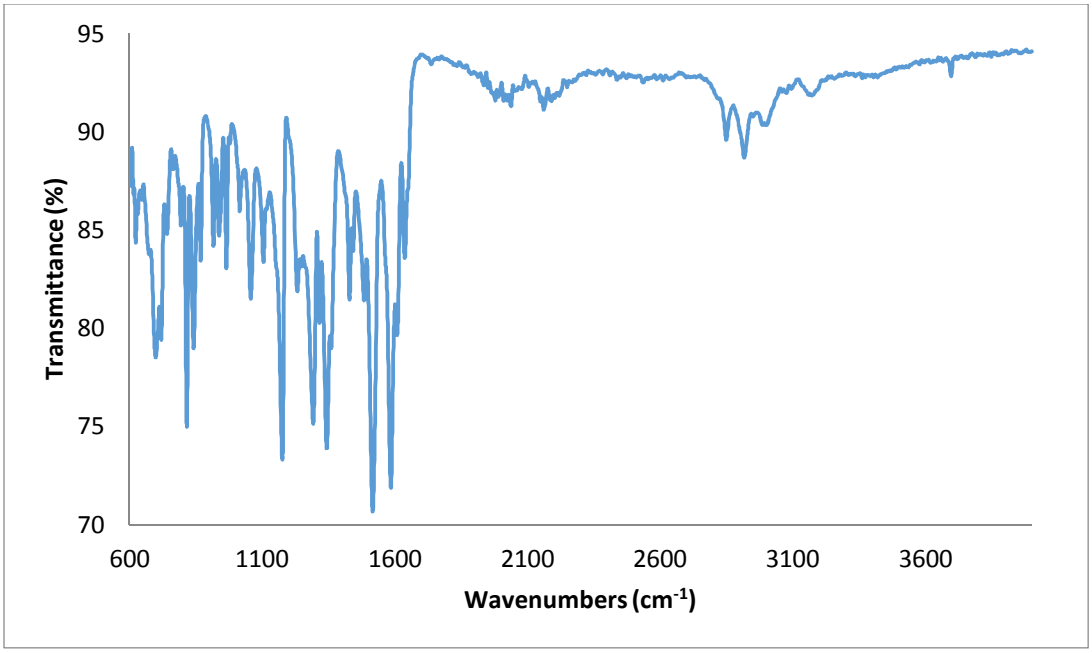

Figure 4.32: FTIR spectrum of Schiff base complex 4C

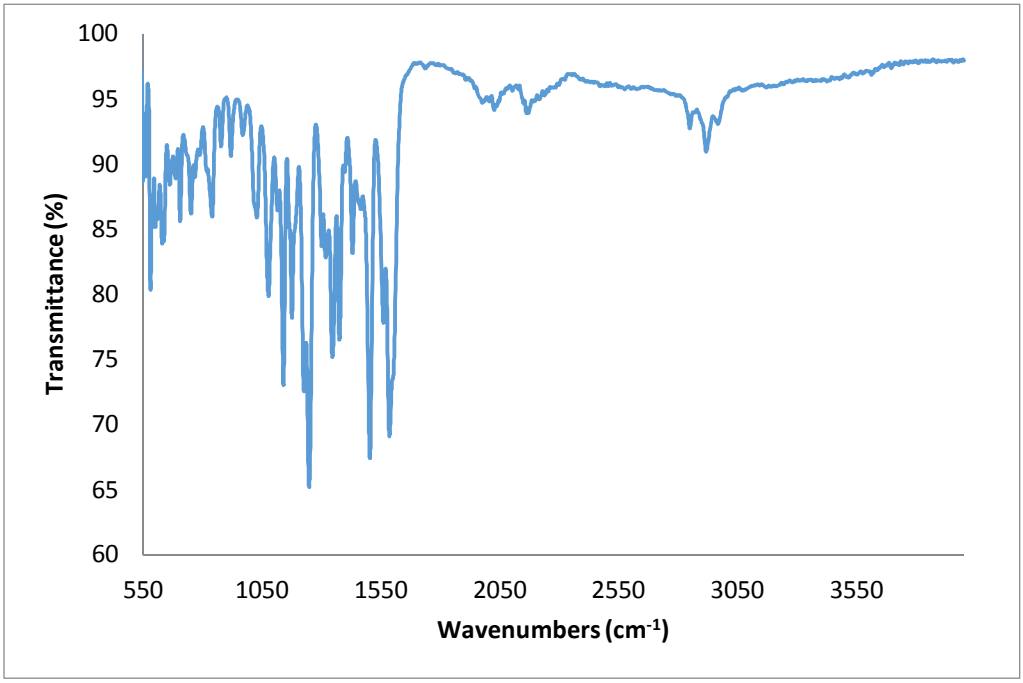

Figure 4.33: FTIR spectrum of Schiff base complex 4D

Table 4.7: FTIR absorption bands of Schiff base complexes

SBC 1A	SBC 1B	SBC 1C	SBC 1D	SBC 2A	SBC 2B	SBC 2C	SBC 2D	SBC 3A	SBC 3B	SBC 3C	SBC 3D	SBC 4A	SBC 4B	SBC 4C	SBC 4D	Assignment
	3228			3590				3558				3565	3689	3693		ν(N-H) stretching
		3160			3236			3353	3232			3349	3357			ν(O-H)
		2983	2964	2931	2921		2975	2971		2971	2925	3174	3234	3158		
2915	2929	2910	2902	2915		2915	2923	2927				2971		2987	2933	ν(C-H) stretching
2848	2883	2844	2802	2829	2832	2848	2848	2892		2877	2890	2929	2910	2915	2912	
										2800	2848	2865	2829	2848	2842	
1731				1735	1706	1731										(C=O) stretching
	1610	1635		1608	1643		1673		1639	1614		1633	1612	1637	1695	ν(N-H) bending
1581	1589	1585	1577	1577	1591	1581	1575	1587	1556	1564	1594	1589	1600	1585	1583	ν(C-H) bending
1565			1565			1565									1558	(C=C) aromatic
1513	1521	1515			1504	1513		1513	1504	1511	1500	1515	1504	1515	1502	
1461	1430	1429	1498	1498		1461	1498						1434	1429	1429	(C-O-C) stretching
			1376	1403				1409	1436			1365	1359	1342	1342	(C-O) bending
1338	1359	1344	1348	1336	1357	1338	1353	1340	1361	1357	1348	1336				
	1286	1290			1286				1286	1278						ν(C-C) skeletal
1241	1259	1230	1240	1243	1255	1241	1241	1240	1259		1241	1240	1259	1292	1247	ν(C=N) stretching
	1174	1176	1133	1137	1170		1137	1130	1178	1176			1176	1176	1135	ν(C-C) skeletal
1135	1103				1103	1135			1105		1135	1128	1103	1105		
	1025	1058	1039				1076	1072				1070	1024	1054	1074	ν(C-C) skeletal
			1020	1041	1018		1020	1014	1025	1012	1014	1010	1012		1018	
977	941	964	964			977		971	944	935		962	943	964		ν(C-H) bending
970						970							908		877	ν(C-C) skeletal
	908			927		908	923	914				869				ν(C-H) bending
	840	840		850	840		836	848	840			848	840	840	836	ν(C-C) skeletal
821	815	815	821	823	817	821		817		815	815			815		
	761		788	773	763	703	779	788	761	765	707	784	761		748	Ring-in-plane and
	665		607	703	667	605	746		665	640	646	700	619	696	703	out-of-plane
							707	701		634				622	628	bending

4.3.3 Proton and Carbon-13 NMR of Schiff base complexes

Proton and carbon-13 nuclear magnetic resonance spectroscopy of Schiff base complexes were measured in d_6 dimethyl sulphoxide (DMSO) solution using tetramethylsilane (TMS) as internal standard. The characteristic proton and carbon-13 NMR spectra of the Schiff base complexes are presented in figures 4.34 to 4.49. A summary of the peaks observed and their assignment are presented in table 4.8 and 4.9.

The most important proton and carbon-13 NMR peak that could confirm the formation of a Schiff base complex, among others, is the azomethine hydrogen peak. The azomethine proton NMR peak is expected to resonate at between δ (7.66 – 9.10). We find from the table that SBC 1C, 2A to 2D and 3C could not have formed Schiff base complexes due to the absence of this important peak. Proton NMR of the Schiff base ligands, table 4.4, showed the presence of the azomethine hydrogens at different chemical shift environments indicating the formation of Schiff base ligands.

Two groups of aromatic carbons are expected to be formed in the synthesis of the Schiff base ligands and complexes. Table 4.4 and 4.8 shows the presence of two sets of aromatic carbons from the two benzene rings of the Schiff base ligand and complex structures. While Schiff base ligands used in the preparation of Schiff base complexes have two aromatic carbons, Schiff base complexes 2A to 2D do not show the presence of these two sets of aromatic carbons indicating that these complexes did not form.

Carbon-13 NMR of the Schiff base complexes shows carbon from different environments. Again, the azomethine carbon (δ 121.46 to 151.92) is the most important carbon. The presence of this carbon in the spectra is a strong indication that a Schiff base complex was formed. All Schiff base complexes show the presence of azomethine carbon at different chemical shifts except SBC 1A, 2D, 3B and 4D.

Aromatic carbon atoms (δ 111.54 – 114.28, and 126.33 – 131.81) from the two aromatic rings in the complexes were not also observed in all Schiff base complexes. SBC 1A, 1C, 1D, 2A, 2D, 3A, 4A, 4B and 4D did not show the presence of two sets of aromatic carbon. We could therefore conclude from the C-13 NMR that these Schiff base complexes did not form. What we have from the proton NMR and carbon-13 NMR of these complexes are fragments. The carbon-13 NMR of

these Schiff base ligands however formed ligands as could be observed by the presence of the azomethine carbon and the aromatic carbons in their respective spectra.

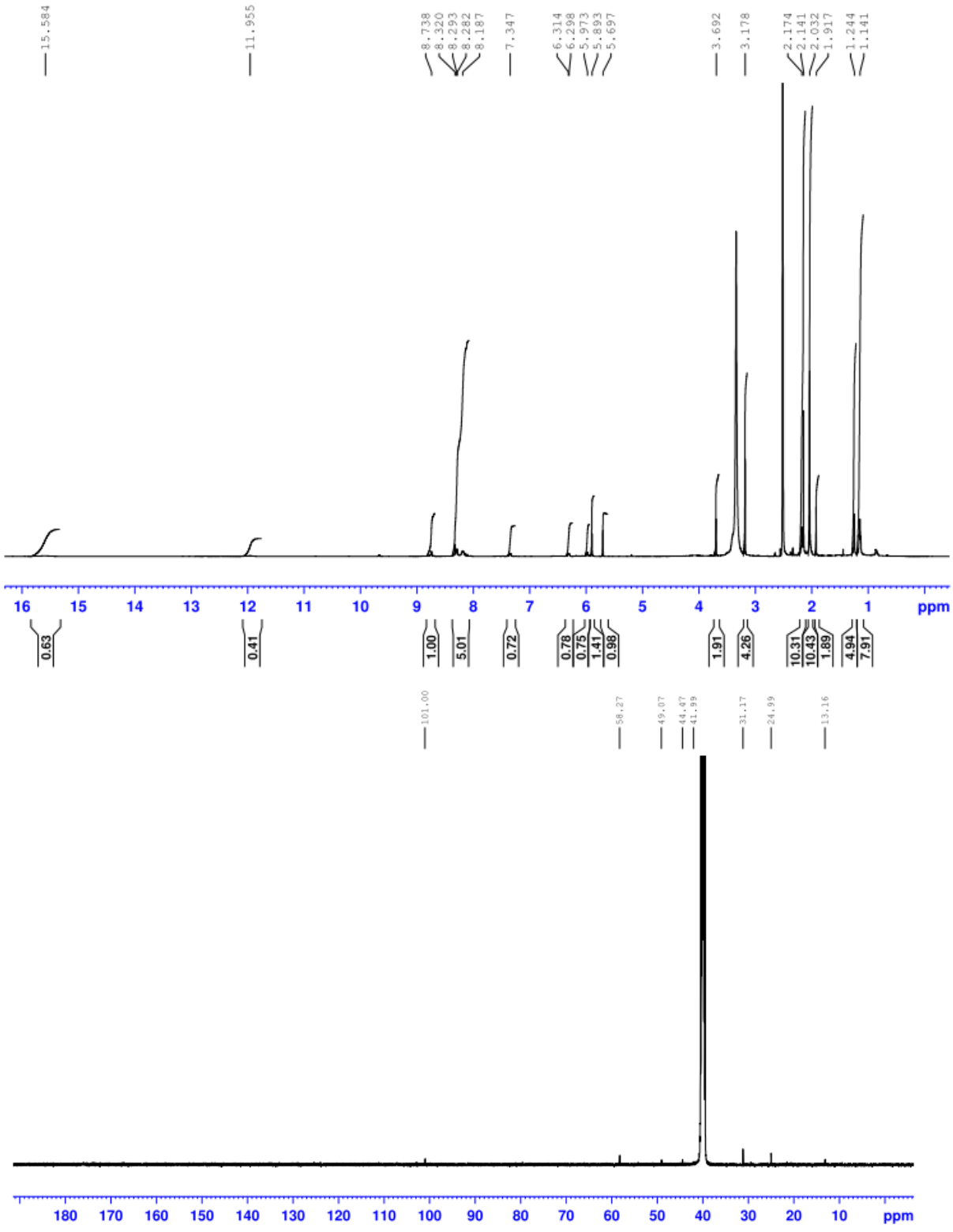

Figure 4.34: Proton and Carbon-13 NMR of Schiff base complex **1 A**

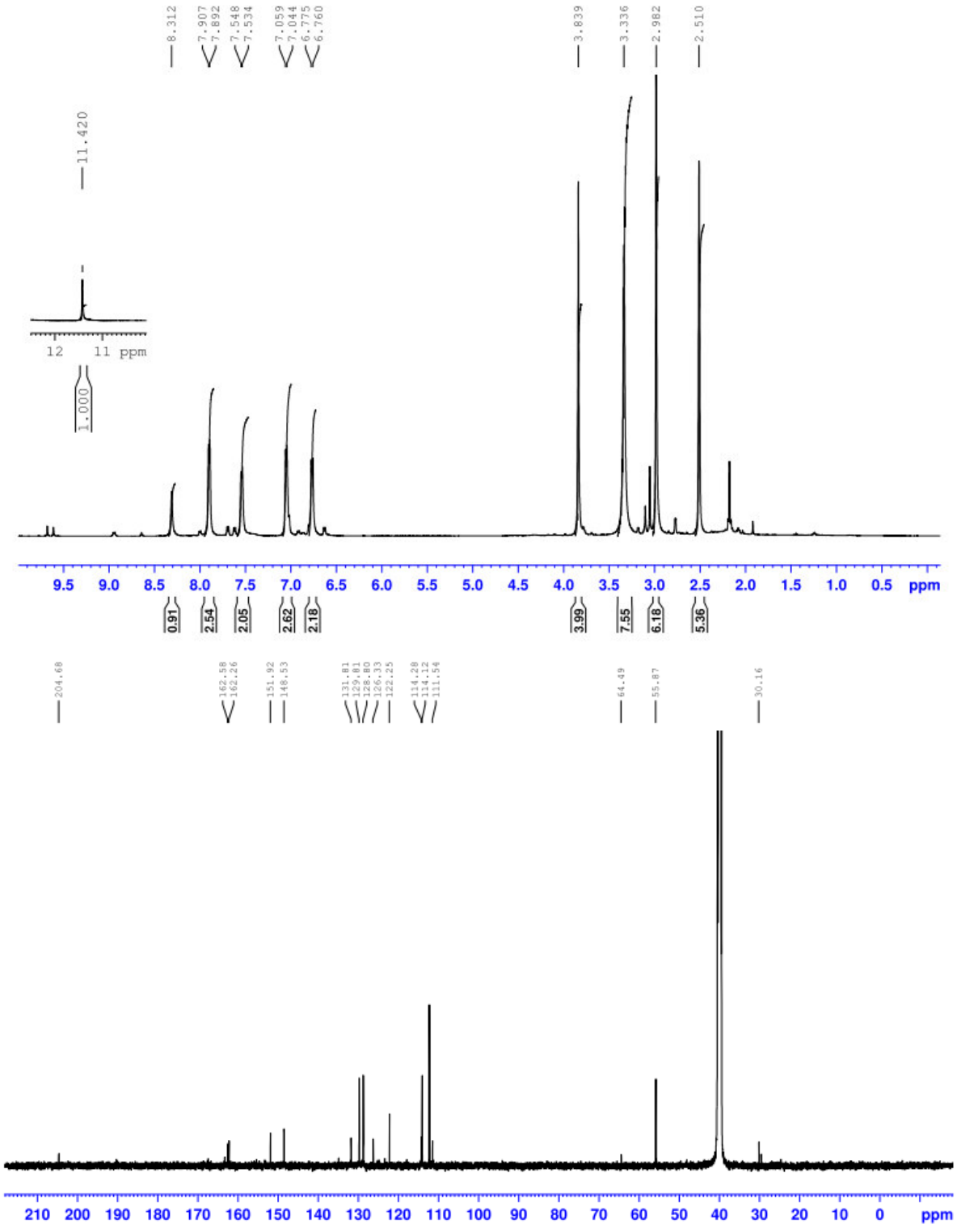

Figure 4.35: Proton and Carbon-13 NMR of Schiff base complex **1 B**

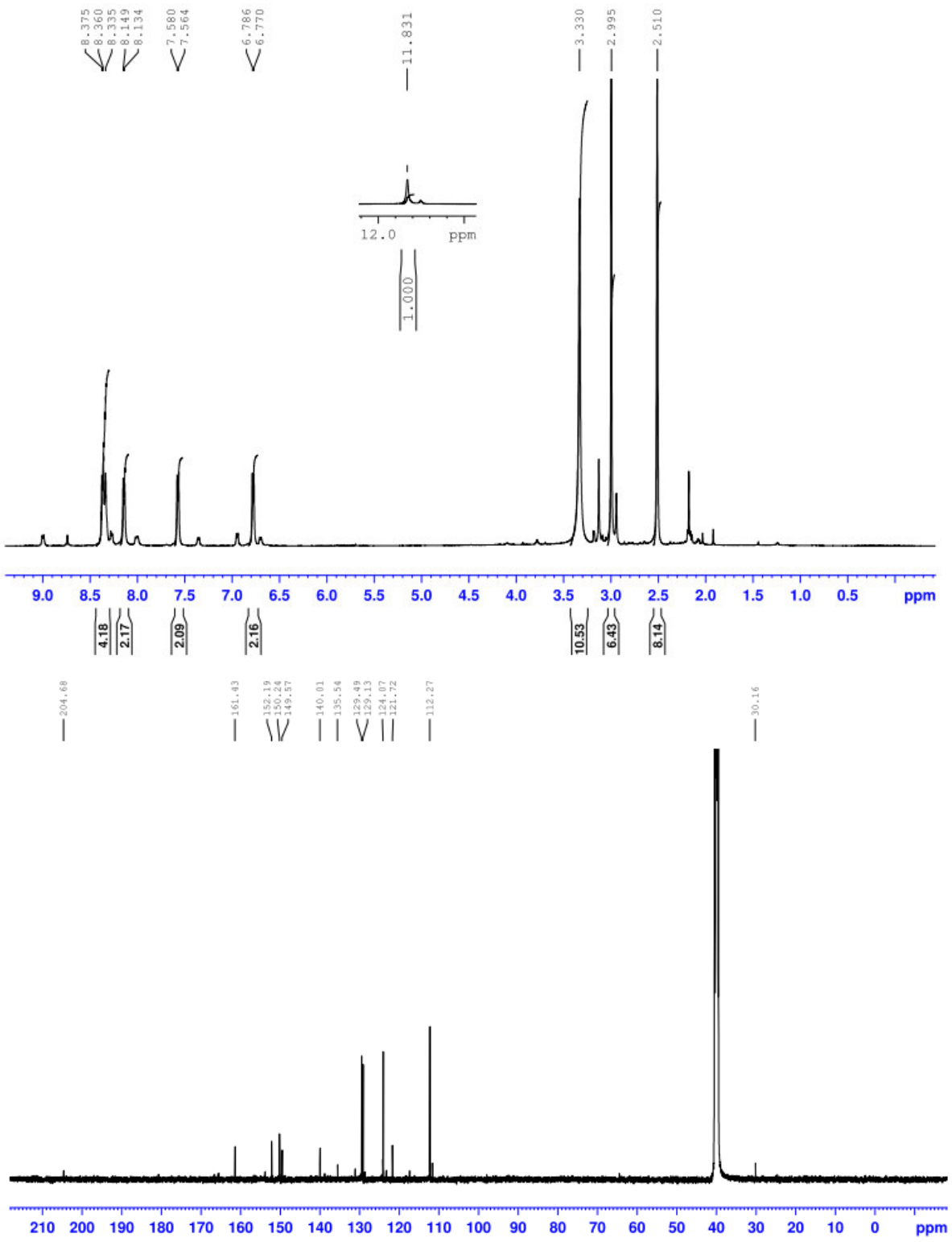

Figure 4.36: Proton and Carbon-13 NMR of Schiff base complex **1 C**

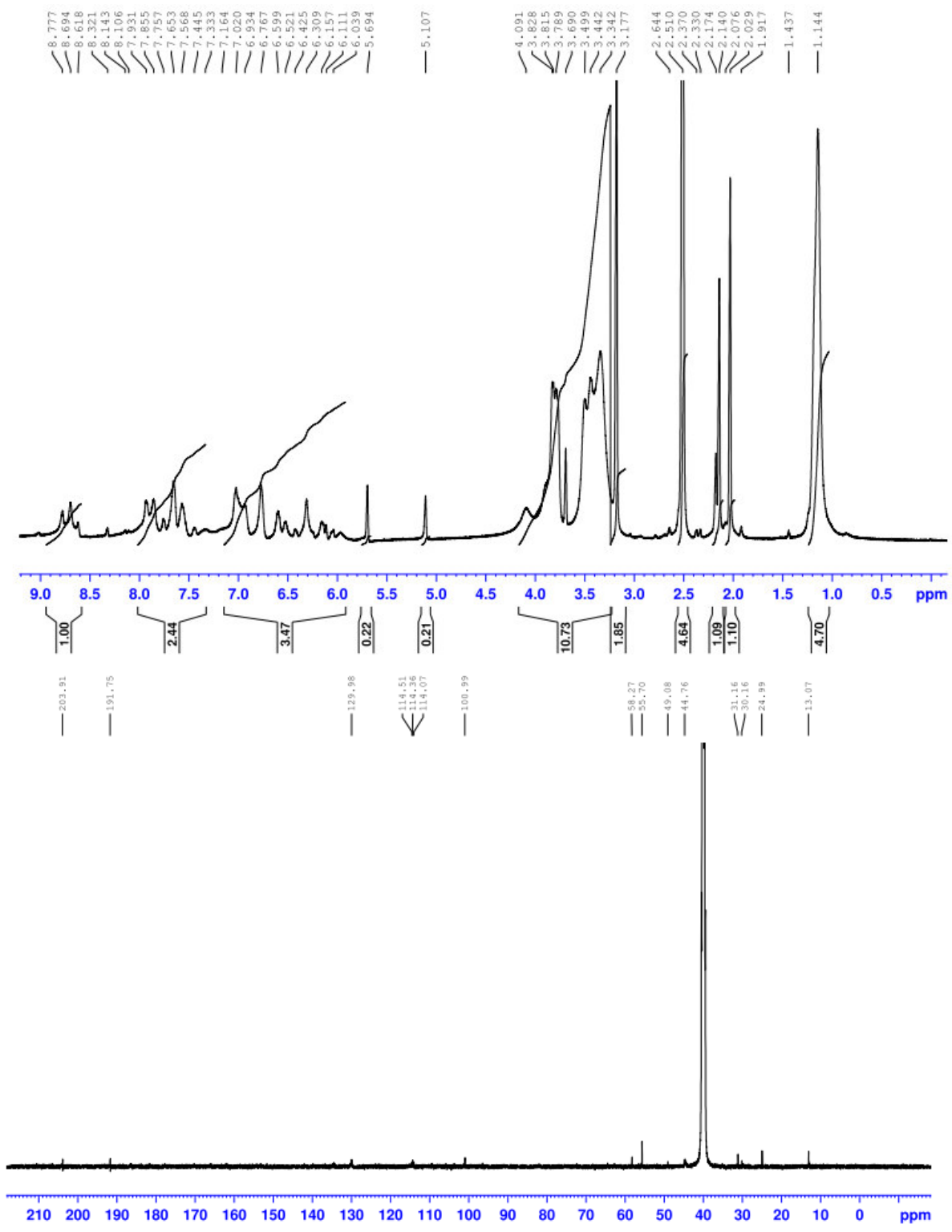

Figure 4.37: Proton and Carbon-13 NMR of Schiff base complex **1 D**

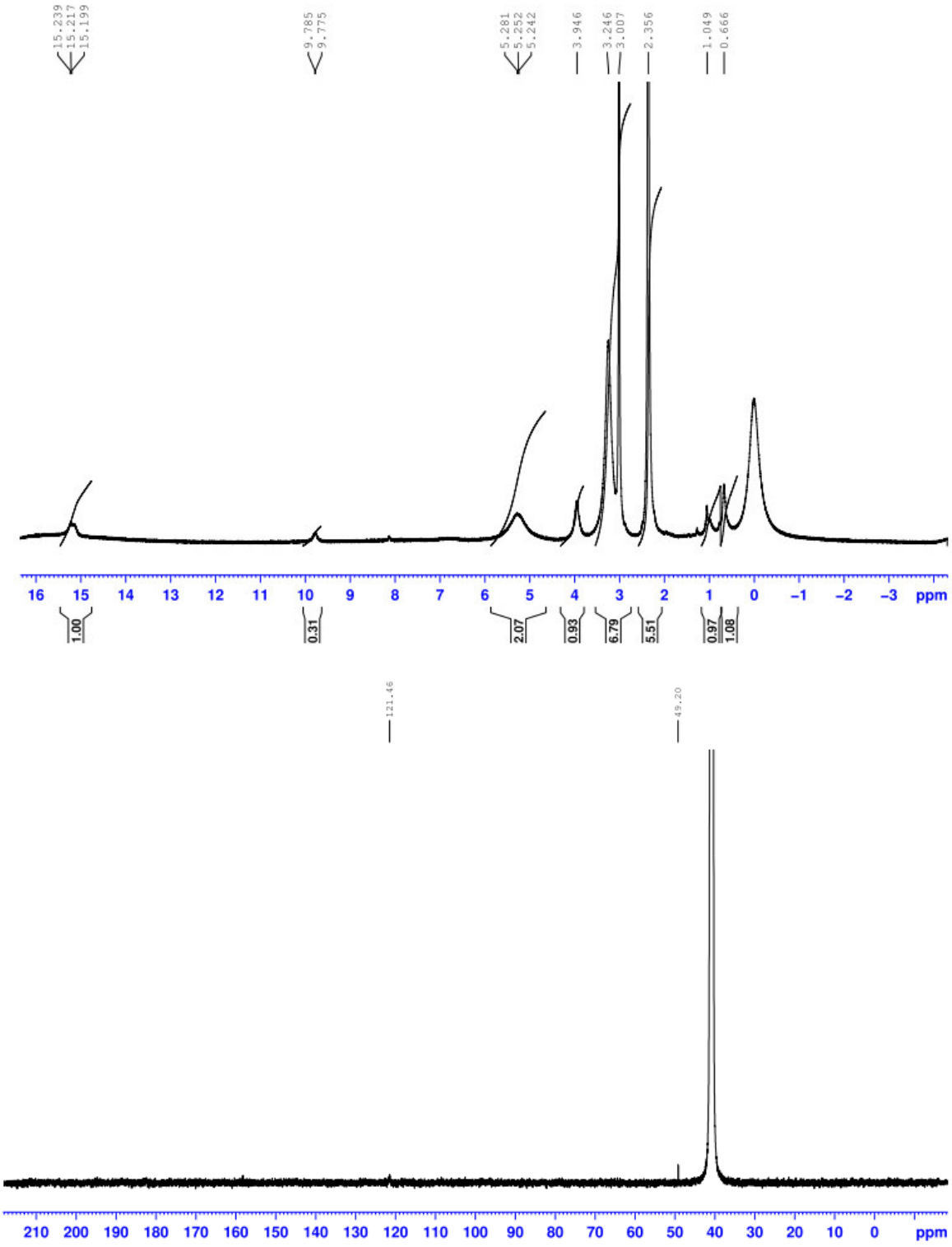

Figure 4.38: Proton and Carbon-13 NMR of Schiff base complex **2 A**

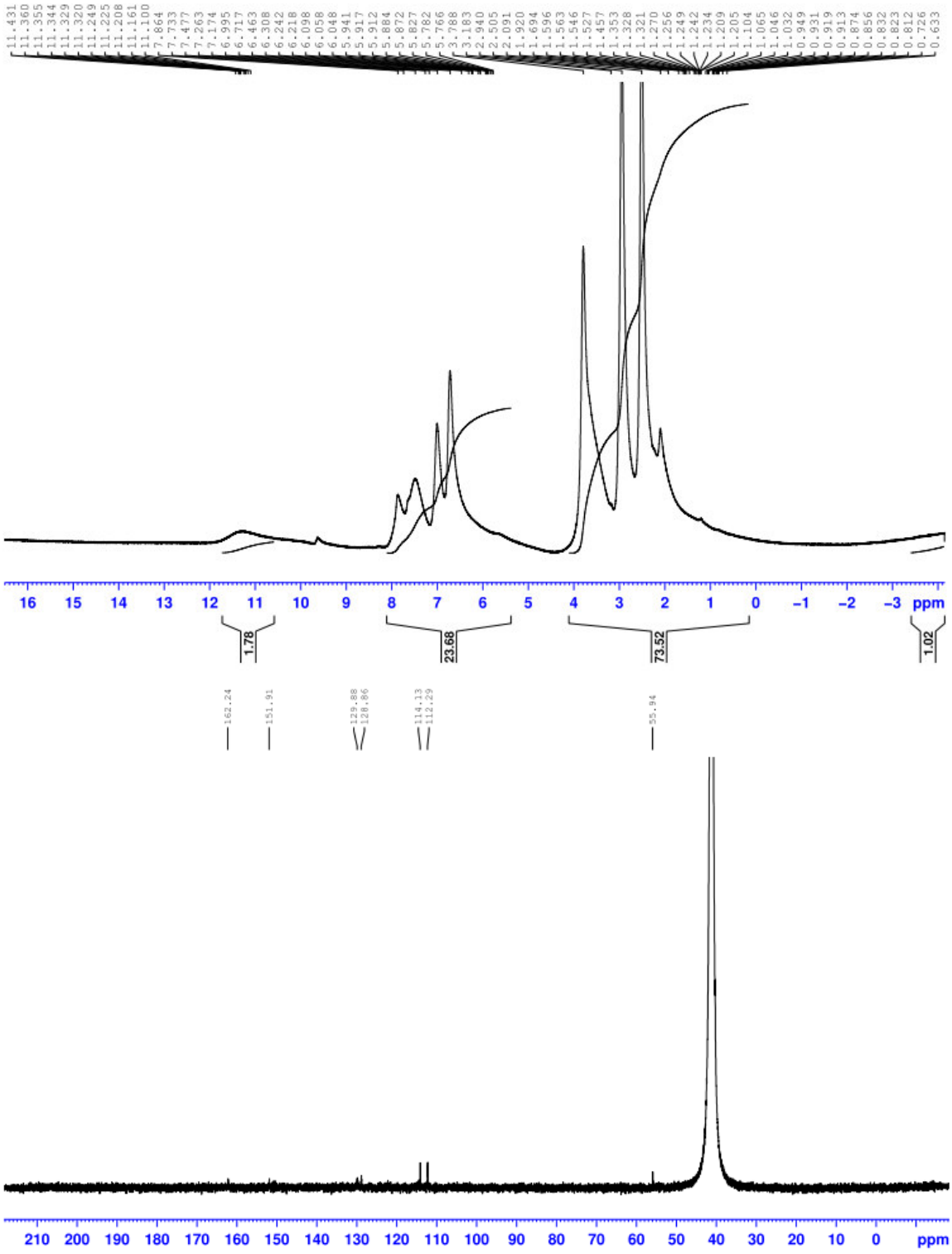

Figure 4.39: Proton and Carbon-13 NMR of Schiff base complex **2 B**

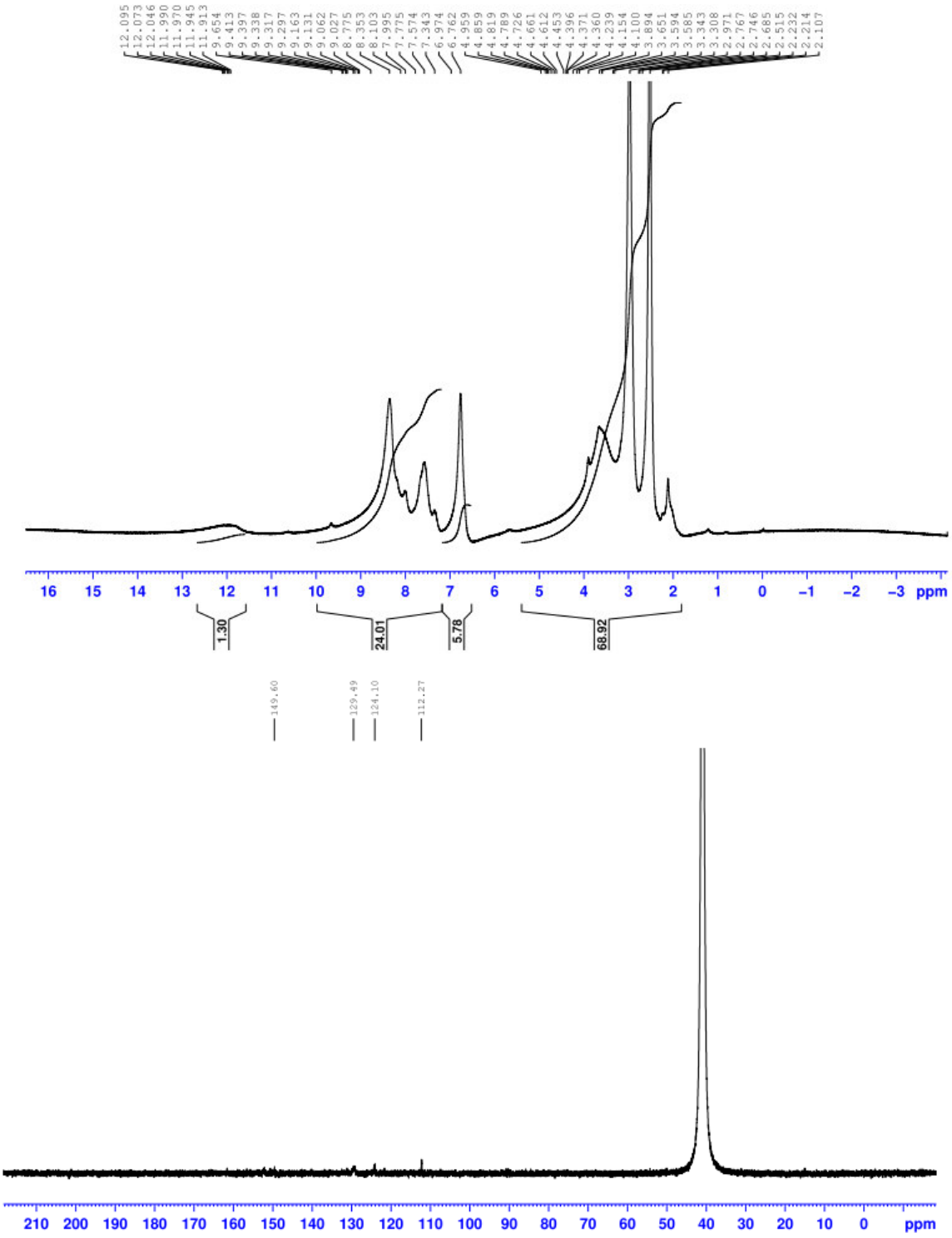

Figure 4.40: Proton and Carbon-13 NMR of Schiff base complex **2 C**

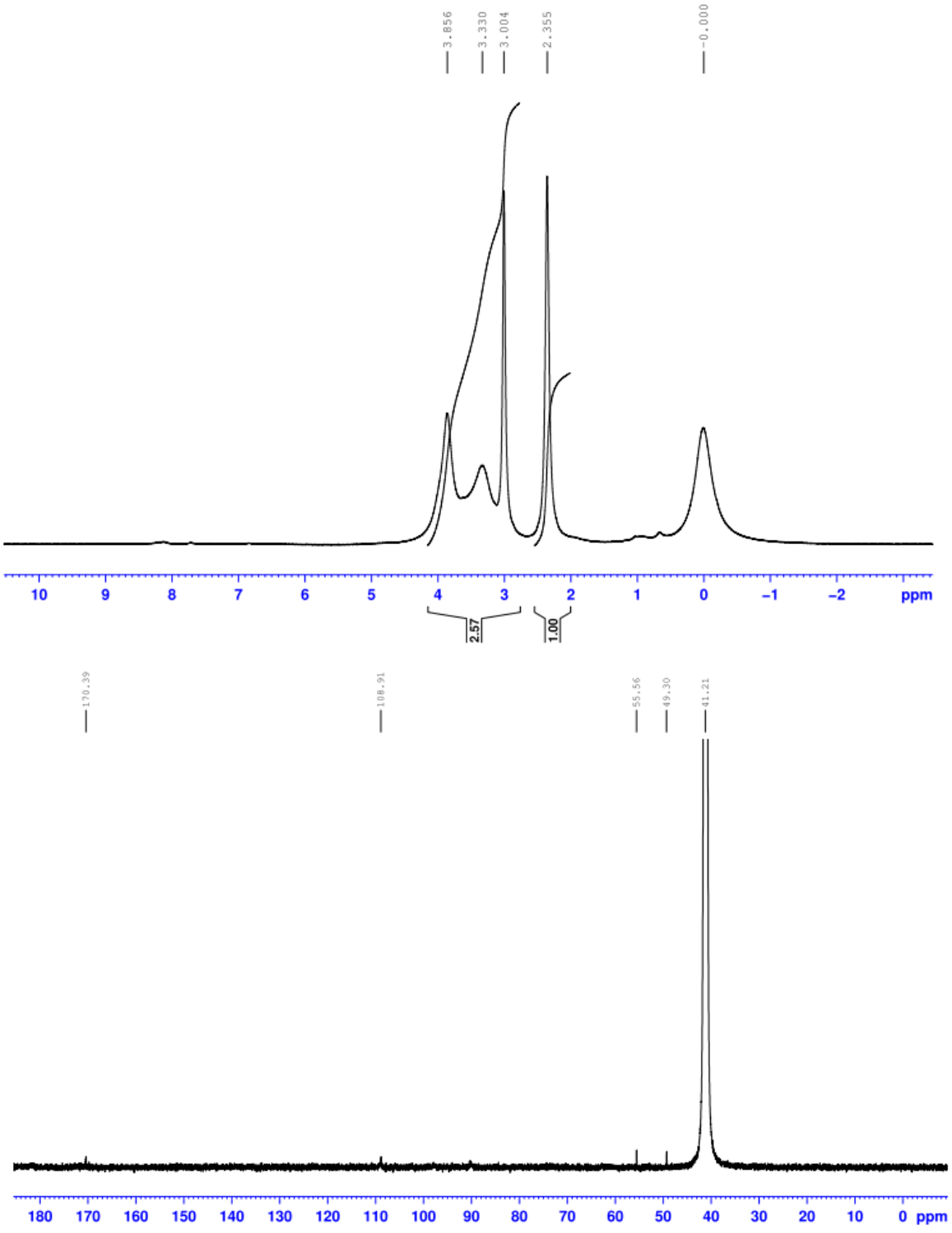

Figure 4.41: Proton and Carbon-13 NMR of Schiff base complex **2 D**

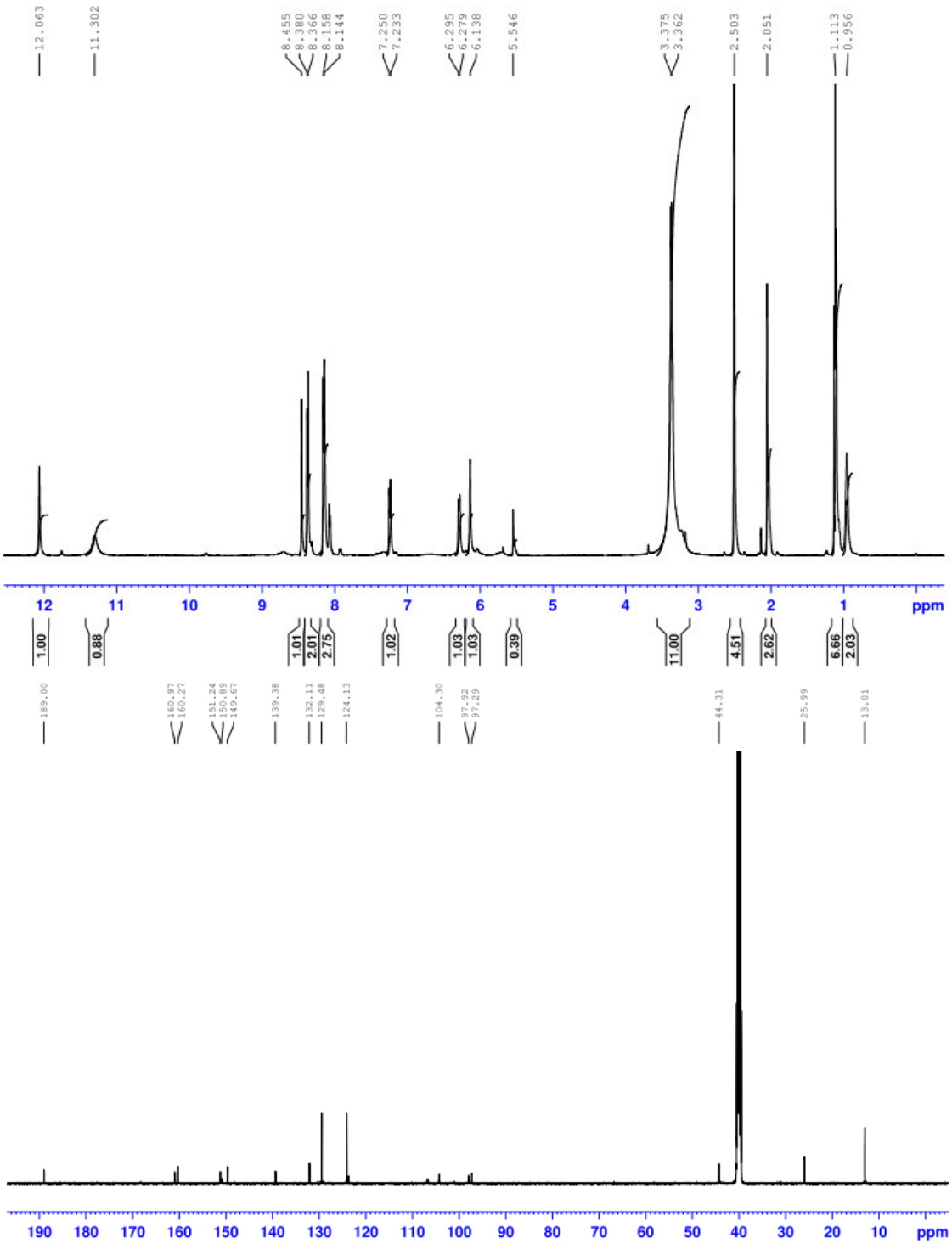

Figure 4.42: Proton and Carbon-13 NMR of Schiff base complex **3 A**

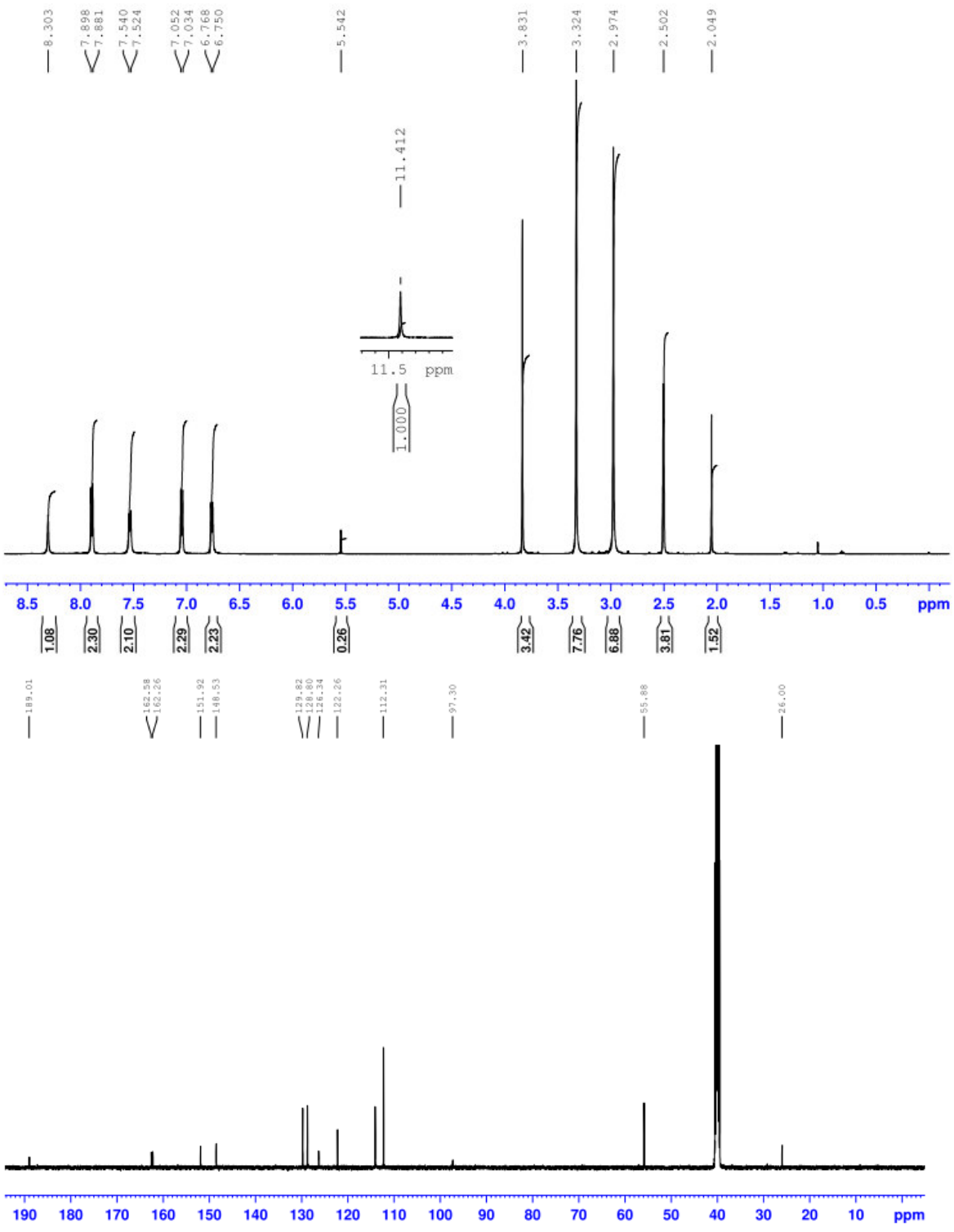

Figure 4.43: Proton and Carbon-13 NMR of Schiff base complex **3 B**

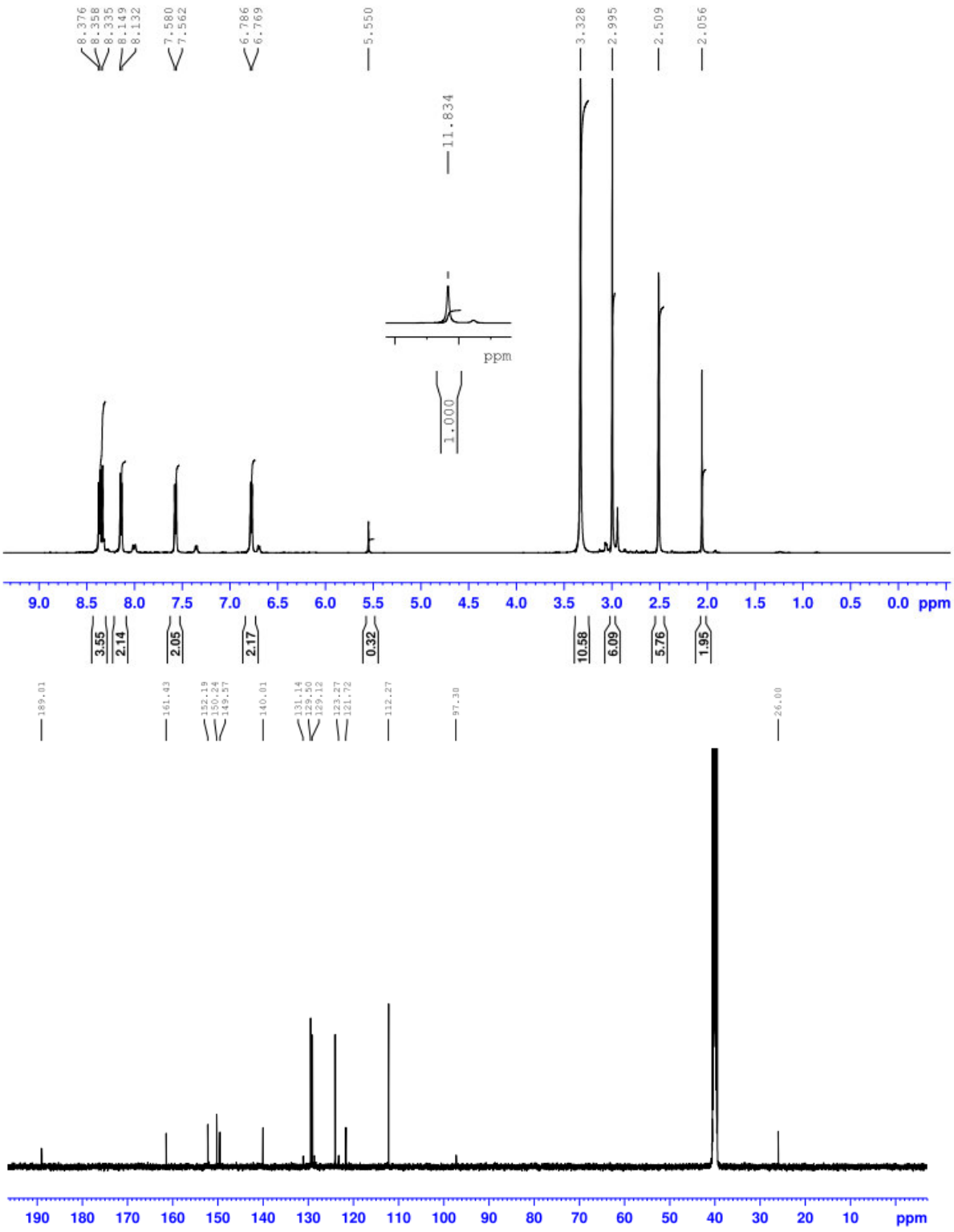

Figure 4.44: Proton and Carbon-13 NMR of Schiff base complex **3 C**

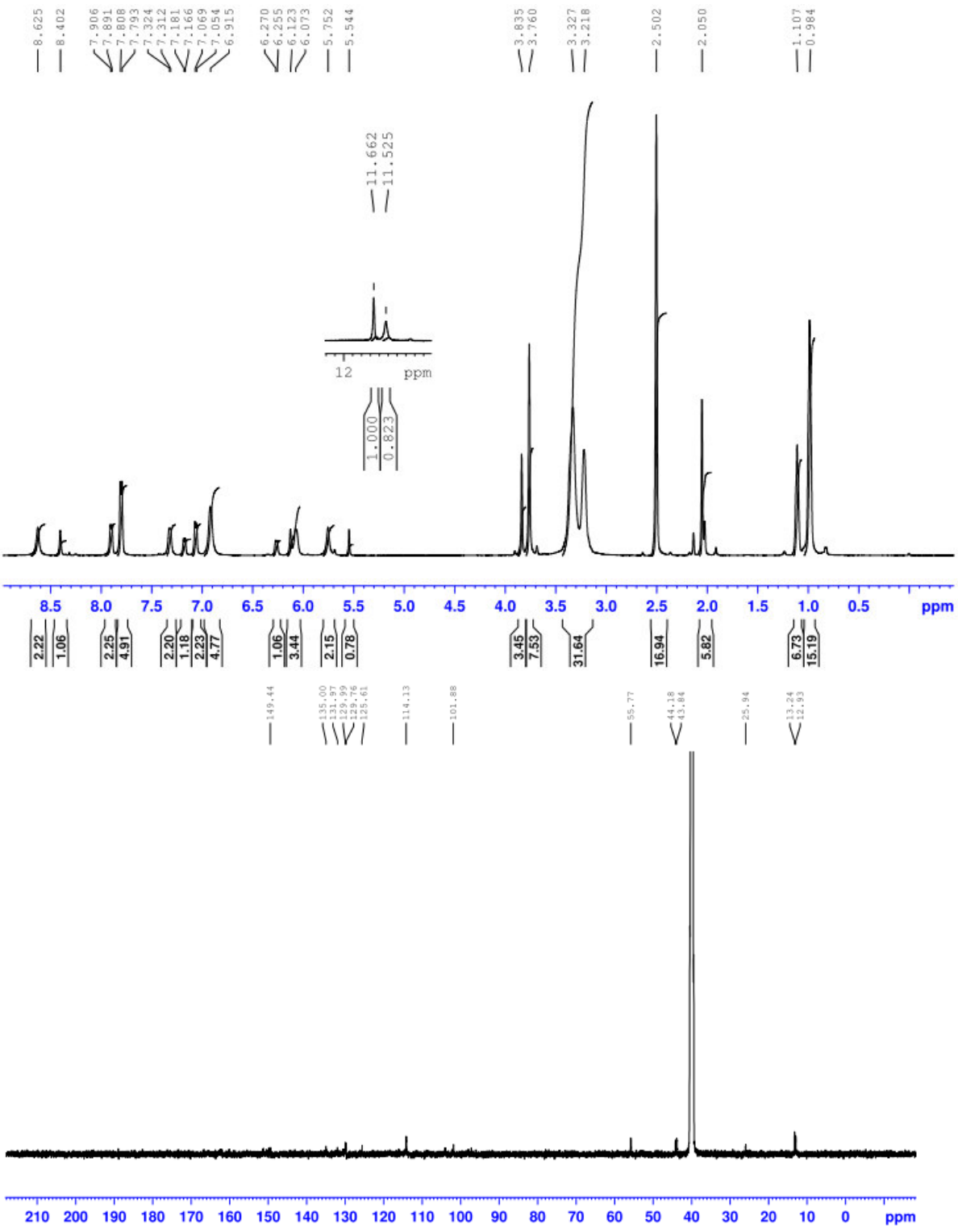

Figure 4.45: Proton and Carbon-13 NMR of Schiff base complex **3 D**

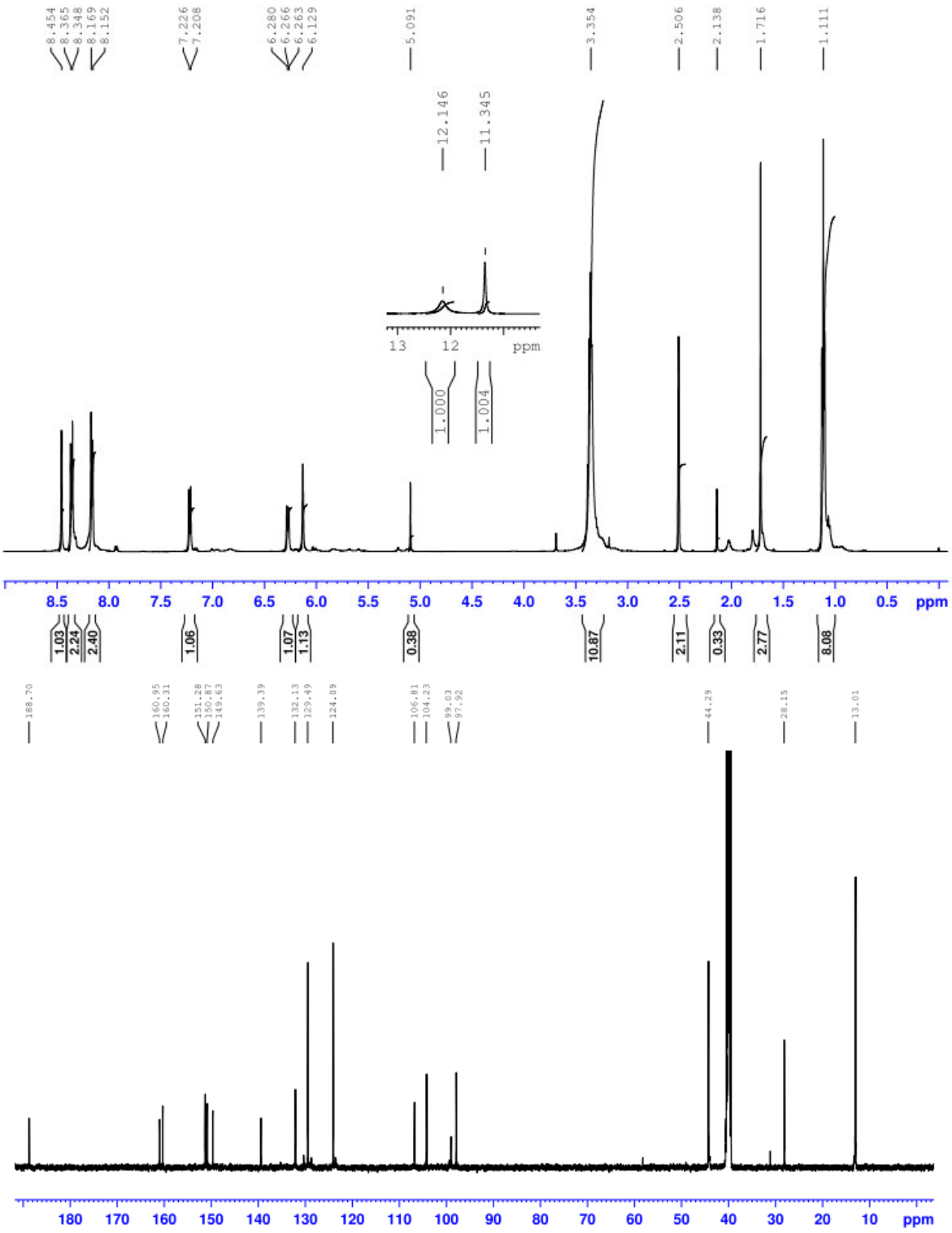

Figure 4.46: Proton and Carbon-13 NMR of Schiff base complex **4 A**

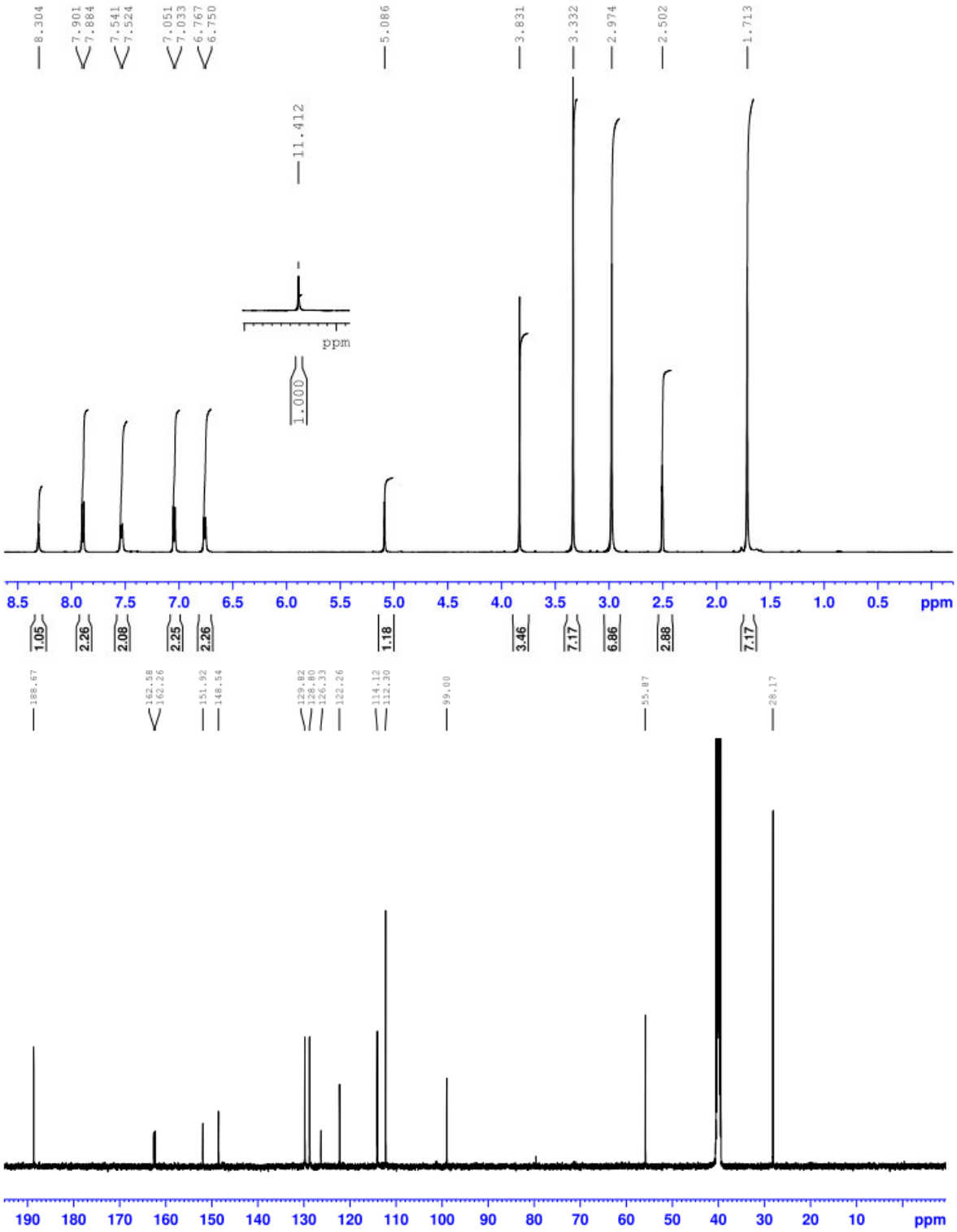

Figure 4.47: Proton and Carbon-13 NMR of Schiff base complex **4 B**

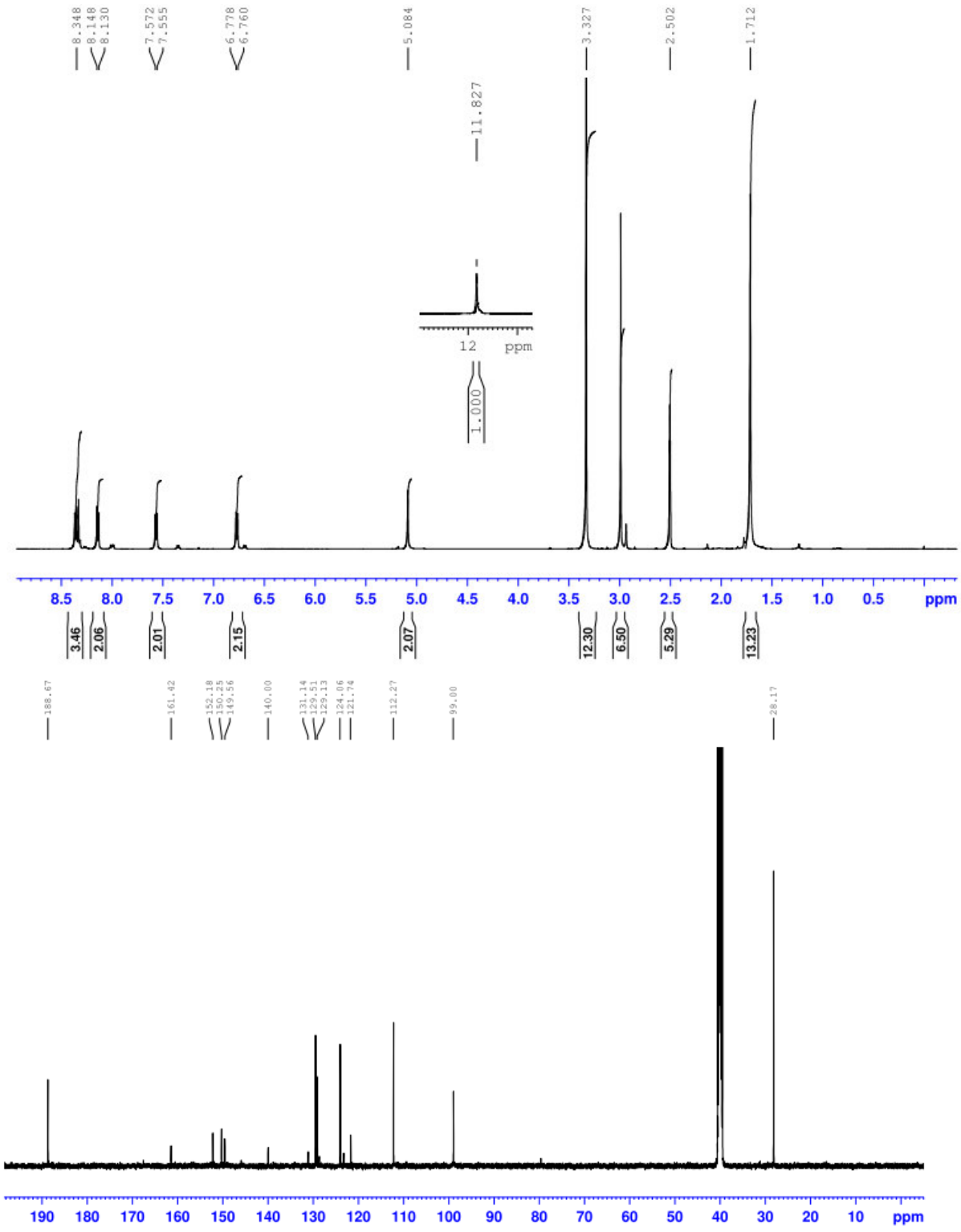

Figure 4.48: Proton and Carbon-13 NMR of Schiff base complex **4 C**

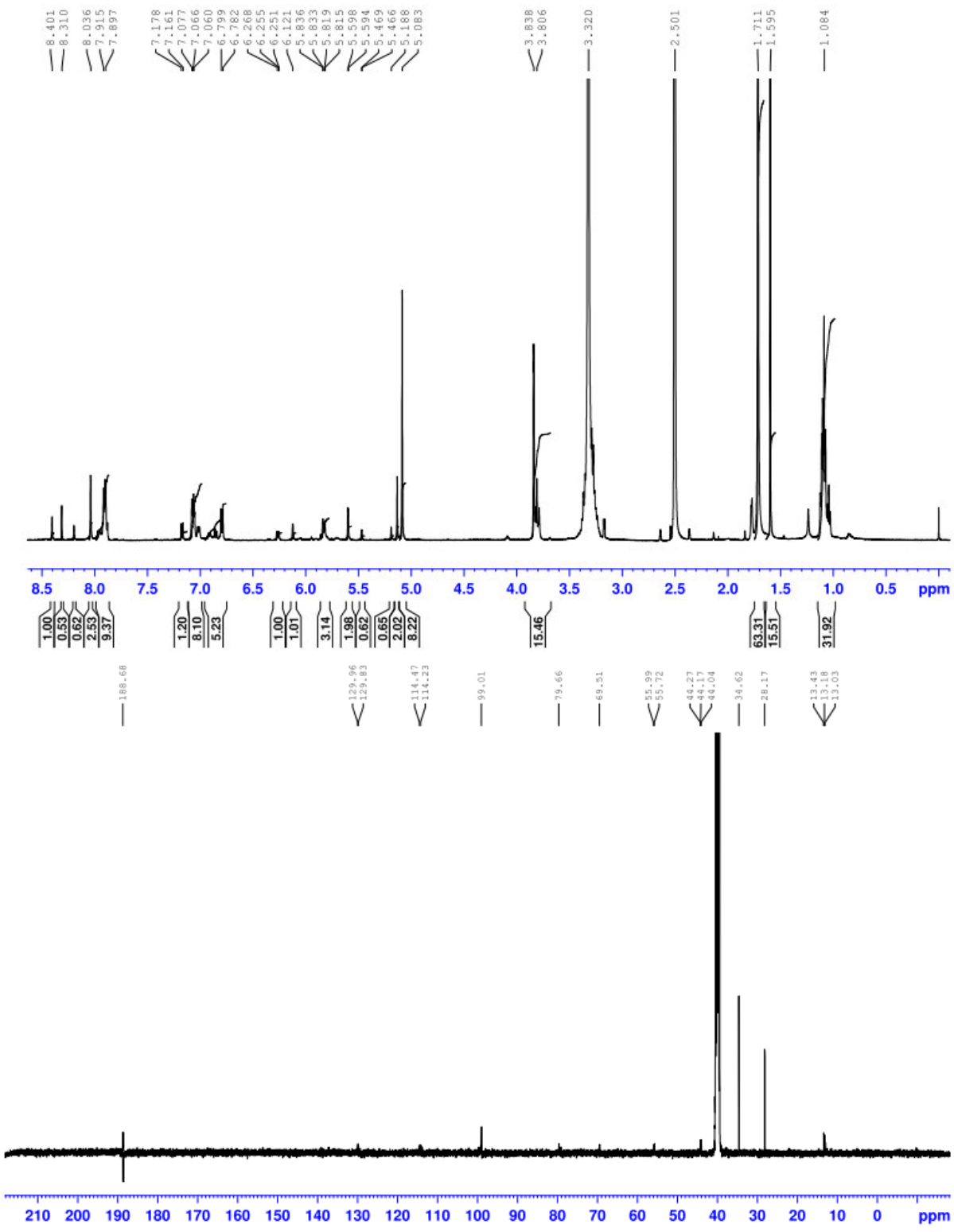

Figure 4.49: Proton and Carbon-13 NMR of Schiff base complex **4 D**

Table 4.8: Chemical Shifts of Proton NMR of Schiff Base Complexes 1A to 4D

	Chemical Shift (δ) ppm						
	Assignment						
SBC	Aliphatic hydrogen	CH_3 of Solvent	Aromatic ring hydrogen	Aromatic ring hydrogen	Azomethine hydrogen	Phenolic hydrogen	Amino hydrogen
SBC 1A	1.141 – 1.244	3.178 – 3.692	5.697 – 6.314	8.187 – 8.738	7.345	11.955	15.584
SBC 1B		3.36 – 3.839	6.760 – 7.059	7.534 – 7.907	8.312	11.420	
SBC 1C		3.330	6.770 – 6.786	8.134 – 8.375	7.564 – 7.580	11.831	
SBC 1D	1.114 – 1.437	3.177 – 4.091	5.694 – 6.599	6.767 – 8.321	9.775		
SBC 2A	1.049	3.007 – 3.949	5.244 – 5.281				15.199 – 15.239
SBC 2B			5.766 – 7.864			11.100 - 11431	
SBC 2C			6.762 – 9.654			11.931 – 12.095	
SBC 2D							
SBC 3A	0.956 – 1.113	3.362 – 3.375	6.138 – 6.295	8.144 – 8.455	7.233	11.302	12.063
SBC 3B		3.324 – 3.831	6.750 – 7.052	7.524 – 7.898	8.303	11.412	
SBC 3C		2.995 – 3.328	6.769 – 7.580	8.132 – 8.376		11.834	
SBC 3D	0.984 – 1.107	3.218 – 3.835	6.073 – 6.270	6.915 – 7.906	8.402	11.525 – 11.662	
SBC 4A	1.111 – 1.716	3.354	6.129 – 6.280	8.152 – 8.454	7.208	11.345	12.146
SBC 4B	1.713	3.332 – 3.831	6.750 – 7.051	7.524 – 7.901	8.304	11.412	
SBC 4C	1.712	3.327	6.760 – 6.778	7.555 – 8.348	8.348	11.827	
SBC 4D	1.084 – 1.711	3.320 – 3.838	5.083 – 6.268	6.782 – 8.036	8.401		

Table 4.9: Chemical Shifts of Carbon-13 NMR of Schiff Base Complexes 1A to 4D

	Chemical Shift (δ) ppm							
	Assignment							
	Methyl carbon	Methylene carbon	Methoxy carbon	Aromatic carbon	Aromatic carbon	Azomethine carbon	Phenolic carbon	Ketonic Carbon
SBC								
SBC 1A	13.01	24.99 – 31.17			126.33 – 131.81			
SBC 1B		30.16		111.54 – 114.28	129.13 – 140.01	148.53 – 151.92	162.26 – 162.58	204.68
SBC 1C				112.27 – 124.07		149.57 – 152.19	161.43	204.68
SBC 1D	13.07	24.99 – 31.16		114.07 – 114.51		129.98		203.91
SBC 2A						121.46		
SBC 2B				112.29 – 114.13	128.86 – 129.88	151.91	162.24	
SBC 2C				112.27	124.10 – 129.49	149.60		
SBC 2D							170.39	
SBC 3A	13.01	25.99 – 44.31	97.29			139.38	160.27 – 160.97	189.00
SBC 3B		26.00	97.30	112.31 – 129.82			162.26 – 162.58	189.01
SBC 3C		26.00	97.30	112.27 – 123.27	129.21 – 131.14	140.01	161.43	189.01
SBC 3D	13.24	25.94			125.61 – 135.00	149.44		188.70
SBC 4A	13.01	28.15	97.92	104.24 – 132.13		139.39	160.31 – 160.95	
SBC 4B		28.17	99.00	112.30 – 129.82		148.54	162.26 – 162.58	188.67
SBC 4C		28.17	99.00	112.27 – 131.14		140.00	161.42	188.67
SBC 4D	13.03 – 13.43	28.17	99.01	114.23 – 114.47	129.83 – 129.96			188.68

4.3.4 Thermogravimetric and Derivative thermogravimetric analysis

Thermogravimetric and derivative thermogravimetric analysis (TGA/DTA) of synthesized Schiff base complexes were measured in nitrogen atmosphere from 0ºC to 900ºC. The results obtained are presented in figures 4.50 to 4.59. [6-8]

The TGA of SBC 1A, figure 4.50, shows the sample gaining mass which may be due to oxidation of the metal before a multistage decomposition taking place and stability achieved. The DTA also showed several endothermic reactions in the process.

The TGA of SBC 1B, figure 4.51, showed multistage decomposition from 37.58ºC before stability was established at 374ºC. The DTA also show about five endothermic processes to have occurred in the sample. The TGA of SBC 1C, figure 4.52, initially gained weight due to oxidation before a multistage decomposition process started from 128ºC. The DTA shows four main endothermic reaction processes taking place. The TGA of SBC 1D, figure 4.53, shows a multistage decomposition taking place in the sample from 160.98ºC with the DTA indicating four endothermic processes taking place in the sample.

The TGA of SBC 2A, figure 4.54, shows a multistage decomposition of the sample with no stable intermediate. The DTA shows two very small endothermic processes occurring. The TGA of SBC 4.55, shows multistage decomposition of the sample with two stable intermediates at 142oC and 209oC corresponding to endothermic reactions in the DTA.

The TGA of SBC 3C, figure 4.56, show a single decomposition peak which started at 268oC. A single stage decomposition peak is an indication of the presence of a pure sample. The DTA of SBC 3C also shows a single endothermic peak. The TGA of SBC 3D, figure 4.57, started with weight gain characteristic of an atmospheric reaction with oxygen and oxidation of a metal. A multiple decomposition process with relatively stable intermediates is then observed. The DTA also shows three endothermic peaks in the reaction.

The TGA of SBC 4A, figure 4.58, shows multiple decomposition peaks with no stable intermediate which is also observed in the DTA. The TGA of SBC 4B, figure 4.59, shows multiple decomposition process with no stable intermediates.

Comparing the TGA and DTA of Schiff base ligands and Schiff base complexes synthesized, it can be observed that Schiff base ligands formed products that formed a single decomposition peak indicating the presence of a single substance. This is seen in the TGA/DTA of Schiff base ligands 1 to 4. The Schiff base complexes on the other hand, showed multistage decomposition

processes taking place in the TGA/DTA indicating the presence of several reaction products in the sample. The only Schiff base complex that showed a single decomposition process is SBC 3C.

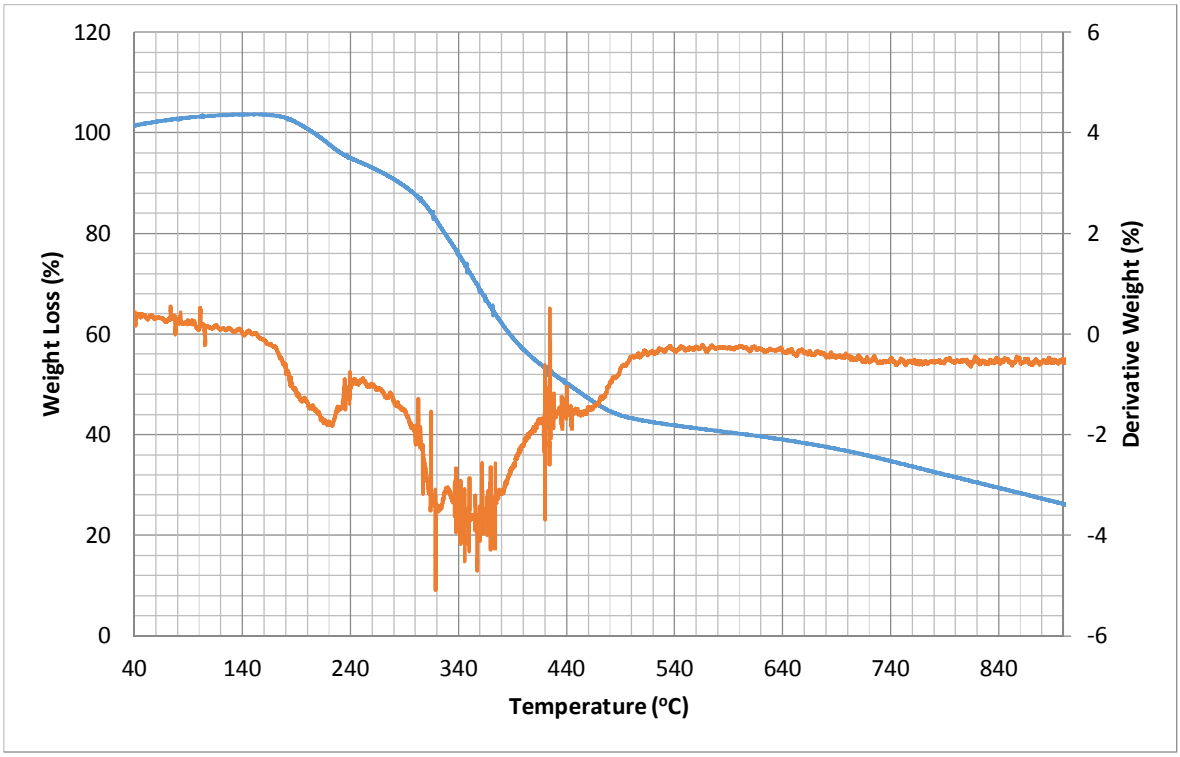

Figure 4.50: Thermogravimetric and derivative thermogravimetric analysis of Schiff base complex 1A

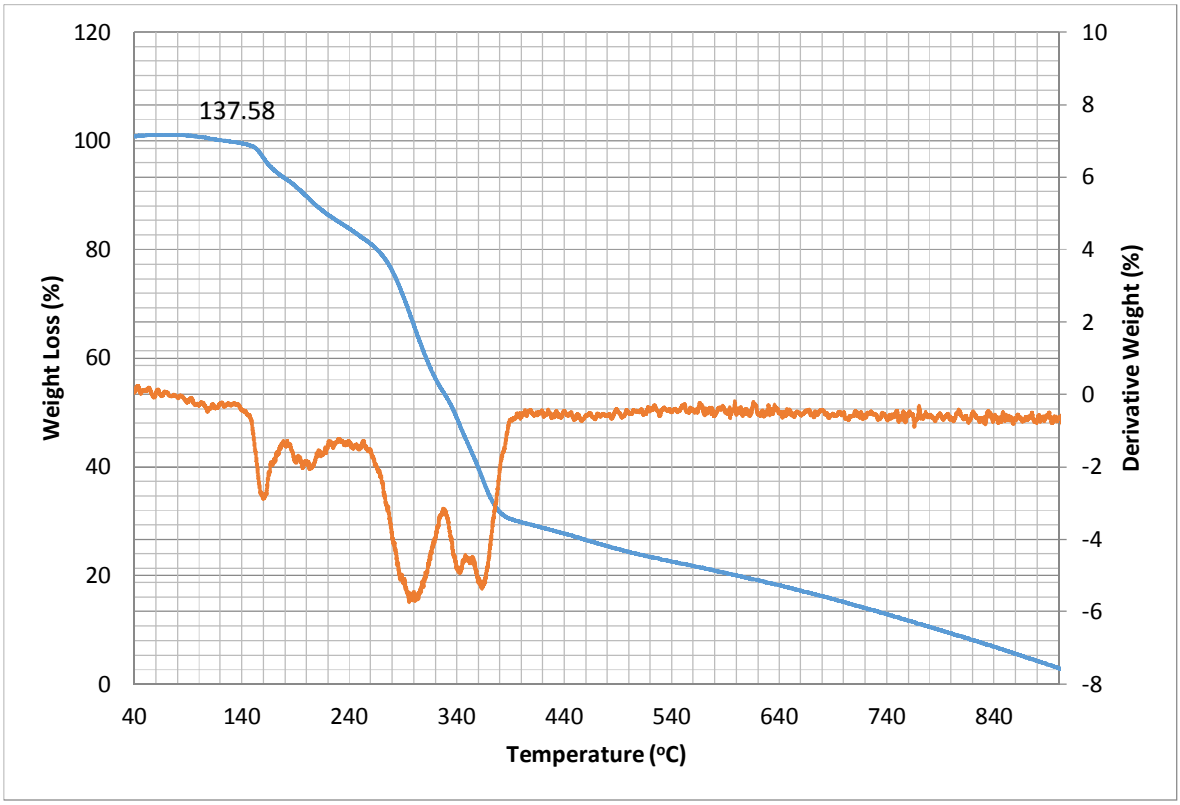

Figure 4.51: Thermogravimetric and derivative thermogravimetric analysis of Schiff base complex 1B

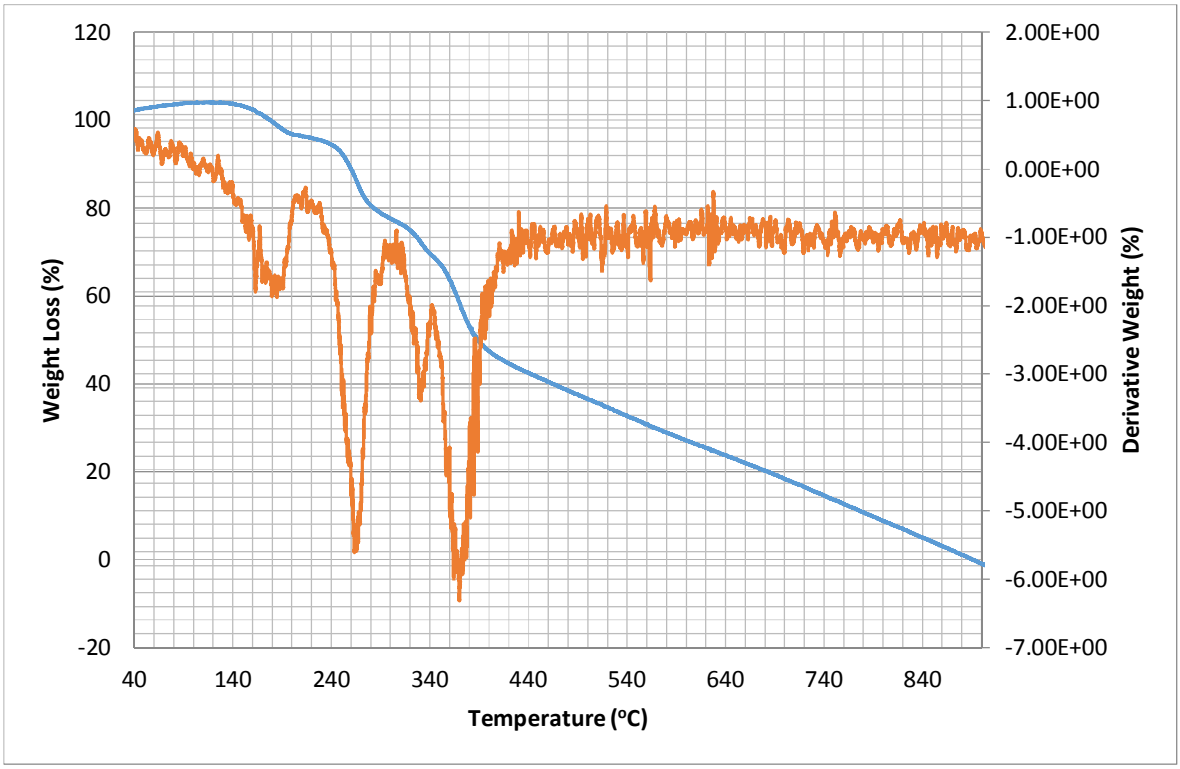

Figure 4.52: Thermogravimetric and derivative thermogravimetric analysis of Schiff base complex 1C.

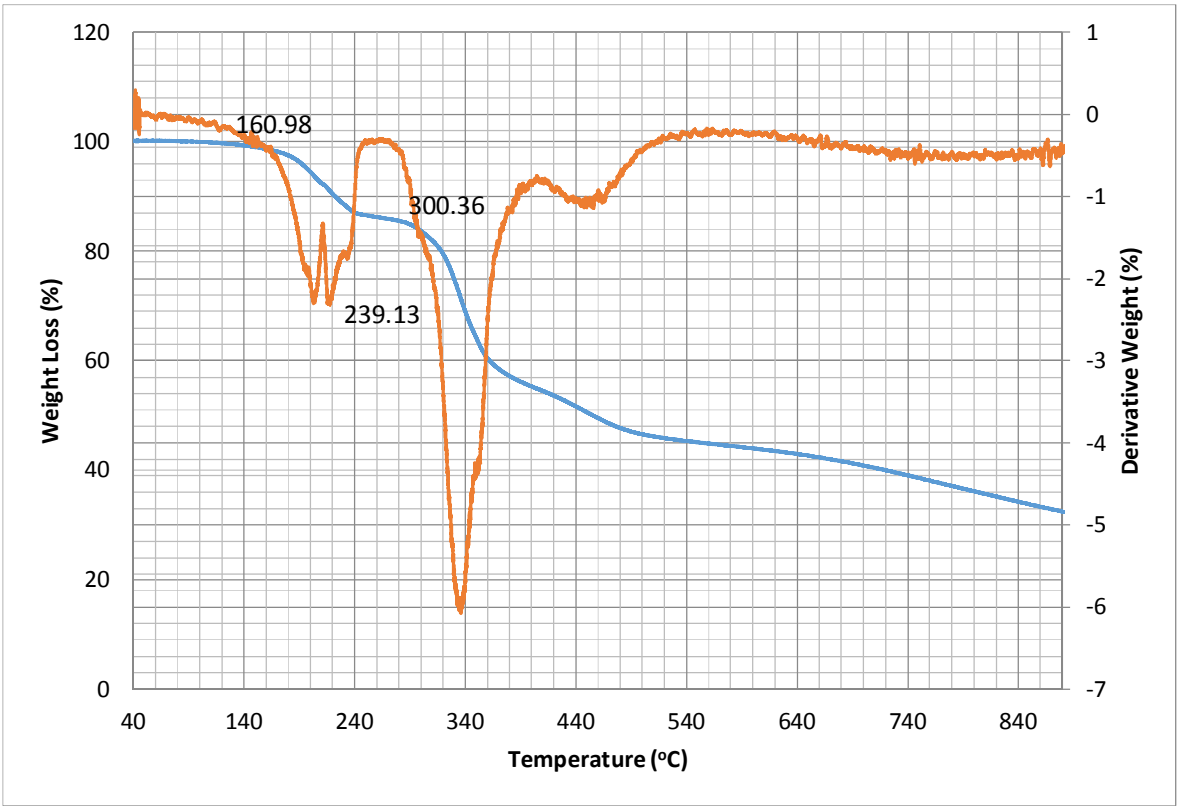

Figure 4.53: Thermogravimetric and derivative thermogravimetric analysis of Schiff base complex 1D**.**

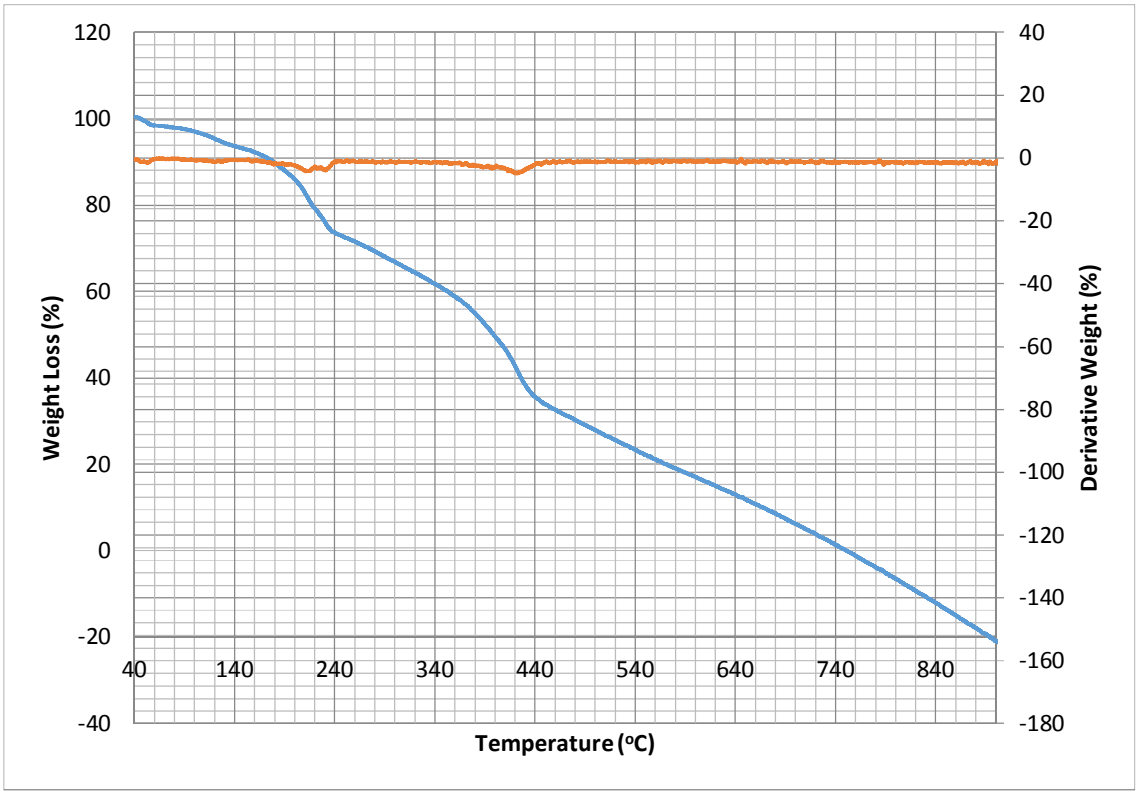

Figure 4.54: Thermogravimetric and derivative thermogravimetric analysis of Schiff base complex 2A

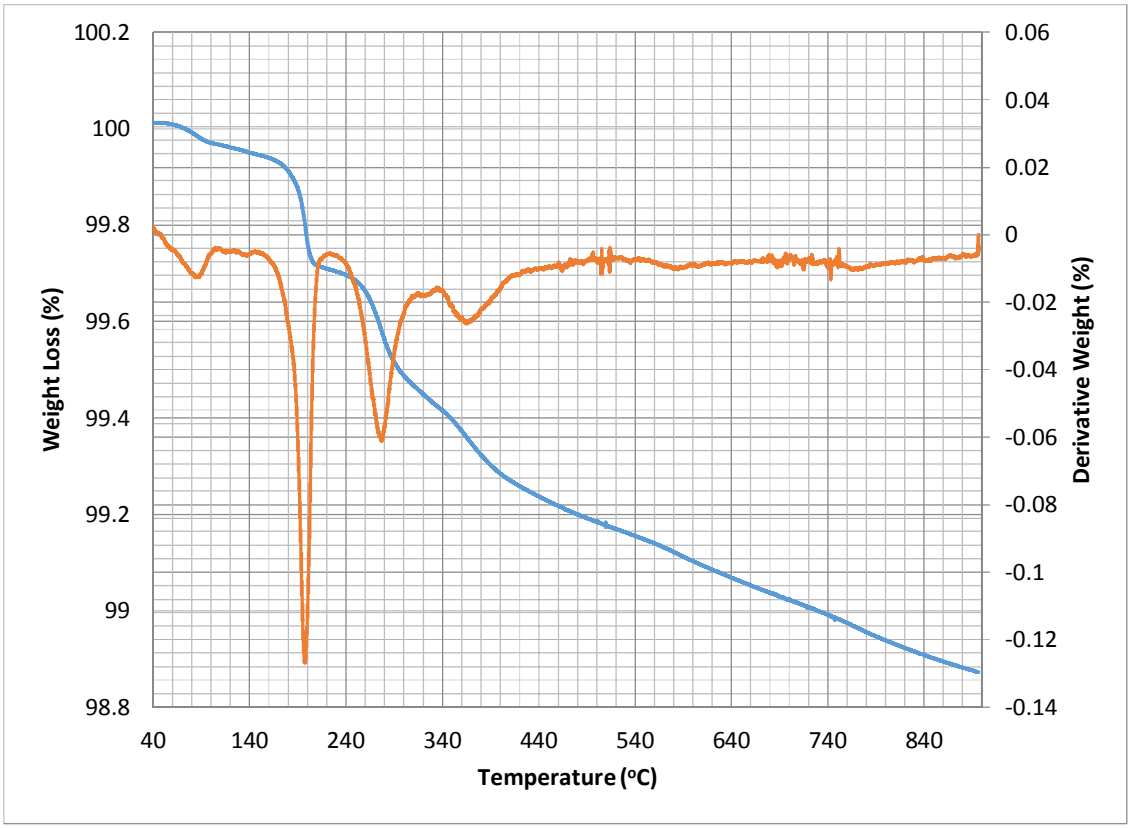

Figure 4.55: Thermogravimetric and derivative thermogravimetric analysis of Schiff base complex 3A

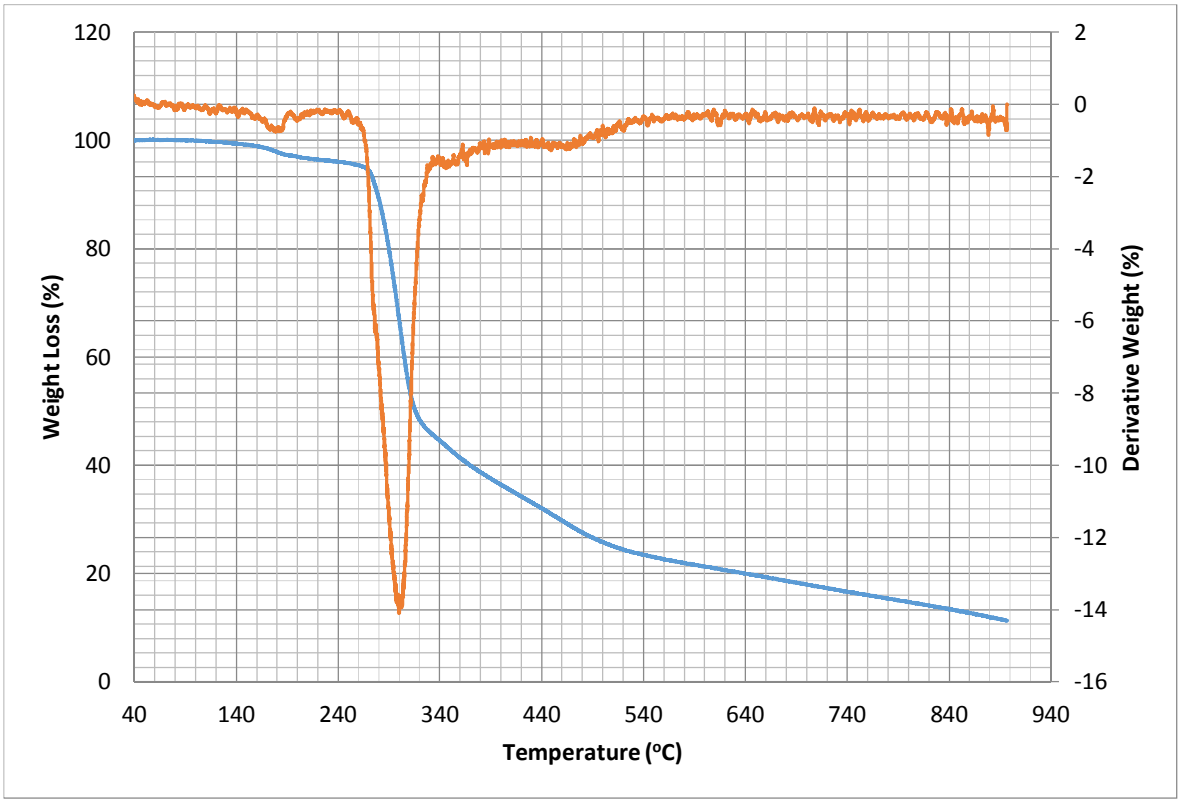

Figure 4.56: Thermogravimetric and derivative thermogravimetric analysis of Schiff base complex 3C.

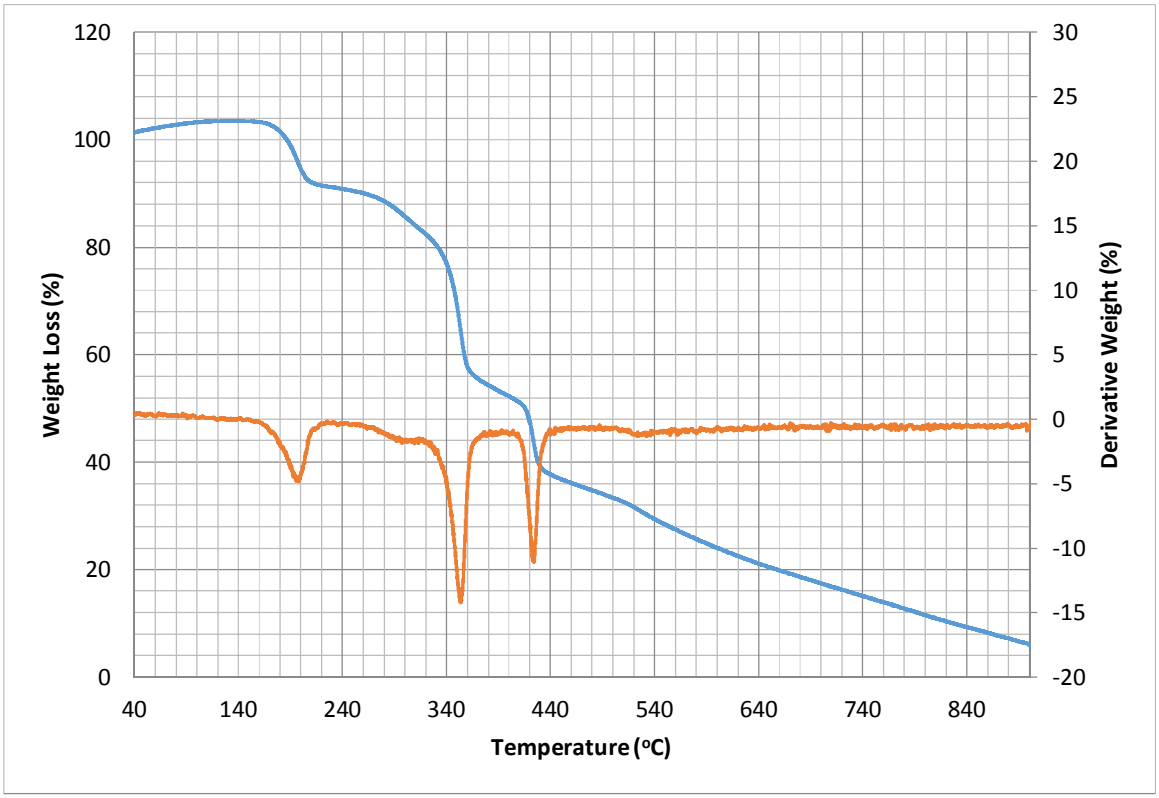

Figure 4.57: Thermogravimetric and derivative thermogravimetric analysis of Schiff base complex 3D.

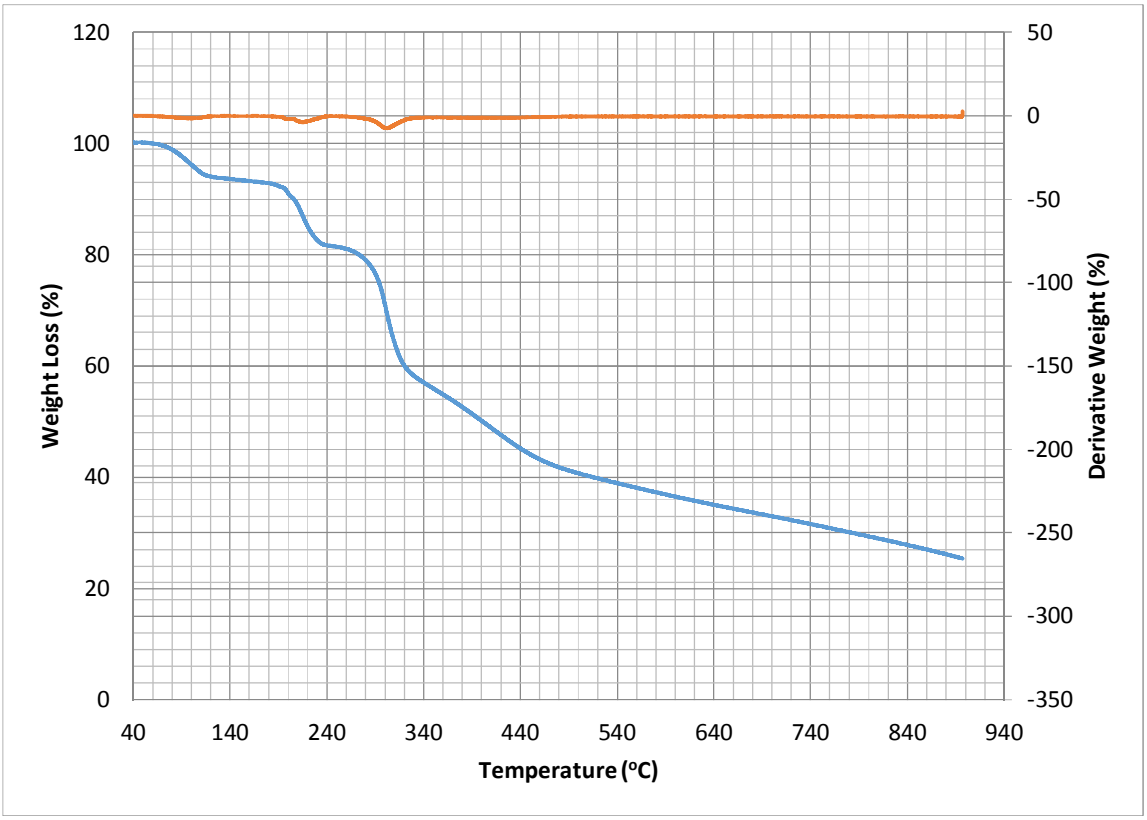

Figure 4.58: Thermogravimetric and derivative thermogravimetric analysis of Schiff base complex 4A

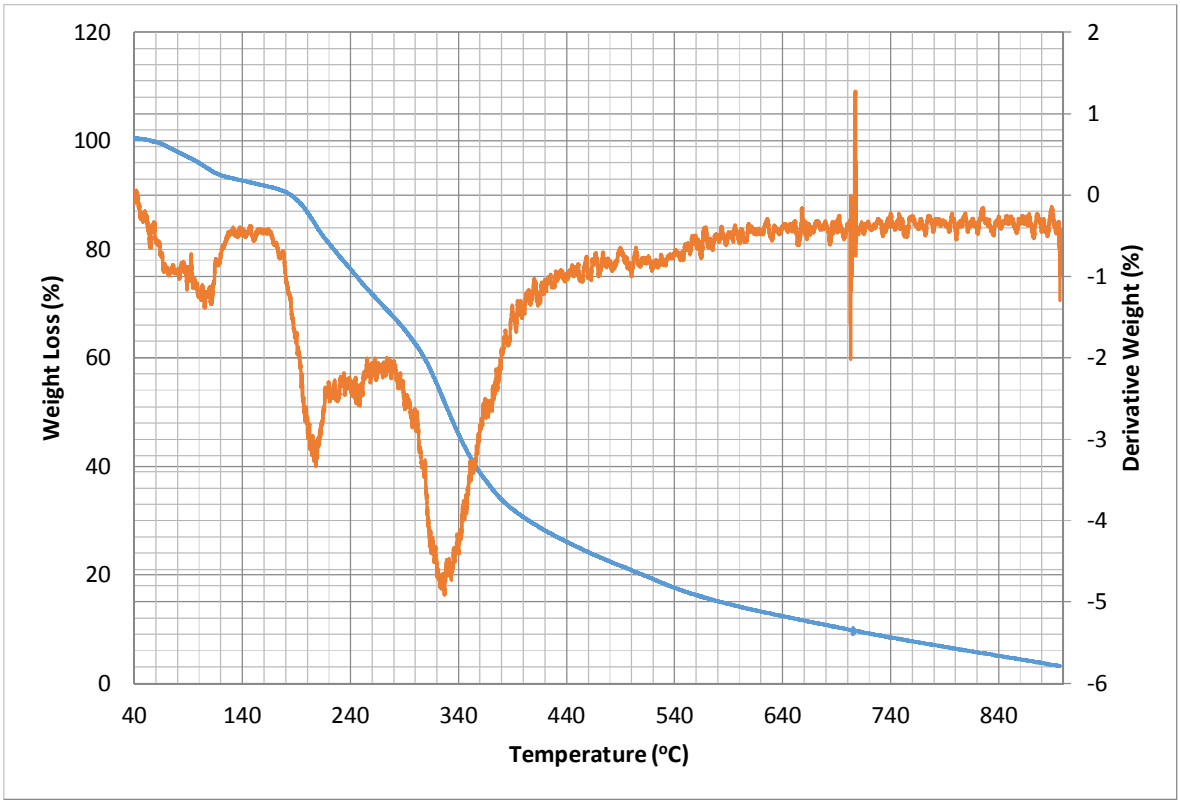

Figure 4.59: Thermogravimetric and derivative thermogravimetric analysis of Schiff base complex 4B.

4.4 Biological Evaluation

IN VITRO ANTIBACTERIAL ACTIVITY OF SYNTHESISED LIGANDS AGAINST *S. aureus* AND *E. faecalis* ISOLATES

METHODS

Reconstitution of the ligands

Different weights of the ligands were weighed and dissolved in absolute ethanol. To counteract the effect of ethanol in the dissolved solutions a disc that was placed only in ethanol was used as a control during the antimicrobial assays.

Bacterial strains

A list of the *S. aureus* and *E. faecalis* isolates used in the study are shown in Table 1. A total of 10 *S. aureus* and 5 *E. faecalis* were used in the analysis. The identities of the isolates used in the study were confirmed using preliminary [Gram staining, catalase test, haemolysis on blood agar) and confirmatory (serotyping, specific PCR analysis and the Matrix-assisted laser desorption/ionization time of flight (MALDI-TOF) Mass Spectrometry].

Table 4.10: Number of *S. aureus* isolates that were positively identified using the MALDI Biotyper technique

Isolate Number	Identity of isolates based on tests used	Isolate Number	Identity of isolates based on tests used
1RO4	*Staphylococcus aureus*	DEEL4-2	*Enterococcus faecalis*
1RO6	*Staphylococcus aureus*	STL1-3	*Enterococcus faecalis*
1RO9	*Staphylococcus aureus*	MP3-1	*Enterococcus faecalis*
2RO4	*Staphylococcus aureus*	MP3-2	*Enterococcus faecalis*
2RO5	*Staphylococcus aureus*	V2-2	*Enterococcus faecalis*
3RO6	*Staphylococcus aureus*		

3RO9	*Staphylococcus aureus*
4R4	*Staphylococcus aureus*
4R5	*Staphylococcus aureus*
15Z1	*Staphylococcus aureus*

In vitro* antimicrobial assay using *S. aureus* and *E. faecalis

All of the synthesized compounds were evaluated for *in vitro* antimicrobial activity. Antibacterial activity was tested against two Gram-positive bacteria, including *Staphylococcus aureus and Enterococcus faecalis*, using established antimicrobial agents as standards. The Ligands (Lig 1a, Lig 2a, SBC 2A, SBC 2C, SBC 1C, SBC 3C, SBC 3B, SBC 4a, SBC 1d, Lig IV, Lig 2R, SBC 1B, SBC 4B, SBC 3d, SBC 2d, SBC 2B, SBC 1a, Lig 3a, SBC 3a, SBC 4d and SBC 4C) were screened for antimicrobial activity using a modification of the Kirby-Bauer disc diffusion technique (Kirby *et al.,* 1996). Punched 6mm paper discs were autoclaved and soaked in different concentrations (0.01g, 0.03g, 0.06g and 0.1g) of the ligands. To determine the minimum inhibitory concentrations of the ligands different weights were also used. Bacterial suspensions were prepared and aliquots of 100µl were spread-plated on solidified Muller Hinton agar. Using sterile needles paper discs with different concentrations of the ligands were plated on the surface of the agar. The antibiotics that appear in Tables 2 and 3 were used as standards in order to validate methodology against *S. aureus* and *E. faecalis* respectively and also for comparison of minimum inhibition concentration (MIC) values. Inoculated plates that contained either the antibiotic or the ligands were incubated aerobically at 37ºC for 24 hours. Zones of inhibition were measured in millimetres after 24 hours of incubation at 37°C and results for the antibiotics were interpreted according to CLSI recommendations. The strains were classified as susceptible, or resistant according to supplier instructions and for the purposes of analysis, intermediate susceptibility was regarded as susceptible.

Control strains

The reference strains *E. faecalis* ATCC 6569 and *S. aureus* ATCC® 25923 were used for quality controls during analysis.

Table 4.11: Antibiotics that were used against *S aureus* in the study. The superscripts [a] to [d] indicate the generally accepted concentrations of antibiotics in the discs according to the standard method stipulated by the manufacturer, Mast Diagnostics, Merseyside, United Kingdom

Group	**Antibiotic**	**Abbrev**	**Disc conc. (µg)**	**Inhibition zone (mm)**		
				R	**I**	**S**
Penicillins	Penicillin	PG	10[b]	≤20	21-28	≥29
	Oxacillin	OX	5[a]	≤9	10-13	≥14
	Ampicillin	AMP	10[b]	≤11	12-14	≥15
Aminoglycosides	Streptomycin	S	10[b]	≤11	12-14	≥15
	Kanamycin	K	30[d]	≤13	14-17	≥18
	Gentamycin	GM	10[b]	≤12	13-14	≥15
Macrolides	Erythromycin	E	15[c]	≤13	14-22	≥23

Tetracyclines	Oxytetracycline	OT	10[b]	≤14	15-18	≥19
Glycopeptides	Vancomycin	V	30[d]	≤9	10-11	≥12
	Teicoplanin	TEC	30[d]	≤10	11-13	≥14
Sulphonamides	Sulphamethoxazole	Smx	15[c]	≤10	11-15	≥19

PG (Penicillin G), OX (Oxacillin), AMP (Ampicillin), S (Streptomycin), K (Kanamycin), GM (Gentamycin), E (erythromycin), OT (Oxytetracycline), VA (vancomycin), TEC (Teicoplanin), Smx (Sulphamethoxazole).

Table 4.12: Antibiotics that were used against *Enterococcus faecalis* in the study. The superscripts [a] to [d] indicate the generally accepted concentrations of antibiotics in the discs according to the standard method stipulated by the manufacturer, Mast Diagnostics, Merseyside, United Kingdom

Group	**Antibiotic**	**Abbrev**	**Disc conc. (µg)**	**Inhibition zone (mm)**		
				R	**I**	**S**
Penicillins	Penicillin	PG	10[b]	≤20	21-28	≥29
	Ampicillin	AP	10[b]	≤11	12-14	≥15
	Amoxicillin	A	10[d]	≤19	-	≥20

Aminoglycosides	Streptomycin	S	10[b]	≤11	12-14	≥15
	Kanamycin	K	30[d]	≤13	14-17	≥18
	Gentamycin	GM	10[d]	≤12	13-14	≥15
Macrolides	Erythromycin	E	15[c]	≤13	14-22	≥23
Tetracyclines	Tetracycline	T	10[b]	≤14	15-18	≥19
Glycopeptides	Vancomycin	VA	30[d]	≤9	10-11	≥12
	Teicoplanin	TEC	30[d]	≤10	11-13	≥14
Quinolones	Ciprofloxacin	CIP	5[d]	≤15	16-20	≥21
	Norfloxacin	Nor	10[d]	≤12	13-15	≥17
β-lactamase	Chloramphenicol	C	30[d]	≤12	13-17	≥18

Results

Antimicrobial resistance profiles of *S. aureus* isolates against the ligands

A total of 21 ligands were tested against confirmed *S. aureus* and *E. faecalis* strains and only 4 exhibited antimicrobial activities. Values for the inhibition zone diameter data are shown in Table 4. As shown on the table at weights 0.01g, 0.03g, 0.06g and 0.1g none of the ligands were effective against the *S. aureus* and *E. faecalis* isolates. However when the weights were increased to 0.3053g, 0.2472g, 0.3980g and 0.3789g for SBC 1B, SBC 2d, SBC 2B and SBC 1a respectively the growth of *S. aureus* was inhibited significantly (Tables 4 and 5). An interesting trend was the fact that these four ligands exhibited antimicrobial activities against both species tested. Therefore the values or concentrations 0.3053g, 0.2472g, 0.3980g and 0.3789g for SBC 1B, SBC 2d, SBC 2B and SBC 1a respectively were considered the minimum inhibitory concentrations (MICs) defined as the lowest concentration of an antimicrobial agent or a ligand that inhibits visible growth of a microorganism after overnight incubation. Some of the ligands had no antimicrobial effects on both the environmental and control *S. aureus* strains. This was evident with Lig IV and Lig 2 were 0.8g and 0.6047g of the compounds did not produce any zone of growth inhibition.

Table 4.13: Inhibition zone diameter data obtained against *Staphylococcus aureus* in the study.

Sample ID	SBC 1B					Sample ID	SBC 2d				
	0.01g	0.03g	0.06 g	0.1 g	0.3053g		0.01 g	0.03 g	0.06 g	0.1 g	0.2472 g
4R5-1	6	6	6	6	9	4R5-1	6	6	6	6	12
4R4-1	6	6	6	6	11	4R4-1	6	6	6	6	12
1R6-1	6	6	6	6	10	1R6-1	6	6	6	6	12
3R6-1	6	6	6	6	10	3R6-1	6	6	6	6	8
2R4-1	6	6	6	6	8	2R4-1	6	6	6	6	10
15Z1-1	6	6	6	6	12	15Z1-1	6	6	6	6	8
1R9-1	6	6	6	6	10	1R9-1	6	6	6	6	8
3R9-1	6	6	6	6	12	3R9-1	6	6	6	6	12
2R5-1	6	6	6	6	8	2R5-1	6	6	6	6	10
1R4-1	6	6	6	6	8	1R4-1	6	6	6	6	10

Sample ID	**SBC 2B**					**Sample ID**	**SBC 1a**				
	0.01g	0.03g	0.06 g	0.1 g	0.3980g		0.01 g	0.03 g	0.06 g	0.1 g	0.3789 g
4R5-1	6	6	6	6	8	4R5-1	6	6	6	6	10
4R4-1	6	6	6	6	8	4R4-1	6	6	6	6	12
1R6-1	6	6	6	6	9	1R6-1	6	6	6	6	8
3R6-1	6	6	6	6	11	3R6-1	6	6	6	6	8
2R4-1	6	6	6	6	8	2R4-1	6	6	6	6	11
15Z1-1	6	6	6	6	10	15Z1-1	6	6	6	6	12
1R9-1	6	6	6	6	8	1R9-1	6	6	6	6	9
3R9-1	6	6	6	6	8	3R9-1	6	6	6	6	8
2R5-1	6	6	6	6	12	2R5-1	6	6	6	6	12

1R4-1	6	6	6	6	10	1R4-1	6	6	6	6	11
***S. aureus* (ATCC 25923)**	6	6	6	6	13						

Table 4.14: Inhibition zone diameter data obtained against *Enterococcus faecalis*.

Sample ID	**SBC 1B**					**Sample ID**	**SBC 2d**				
	0.01 g	0.03 g	0.06 g	0.1 g	0.3053 g		0.01 g	0.03 g	0.06 g	0.1 g	0.2472 g
DEEL4-2	6	6	6	6	12	DEEL4-2	6	6	6	6	13
STL1-3	6	6	6	6	8	STL1-3	6	6	6	6	11
MP3-1	6	6	6	6	8	MP3-1	6	6	6	6	10
MP3-2	6	6	6	6	9	MP3-2	6	6	6	6	9
V2-2	6	6	6	6	7	V2-2	6	6	6	6	9

Sample ID	**SBC 2B**					**Sample ID**	**SBC 1a**				
	0.01 g	0.03 g	0.06 g	0.1 g	0.3980 g		0.01 g	0.03 g	0.06 g	0.1 g	0.3789 g
DEEL4-2	6	6	6	6	12	DEEL4-2	6	6	6	6	12
STL1-3	6	6	6	6	10	STL1-3	6	6	6	6	8
MP3-1	6	6	6	6	12	MP3-1	6	6	6	6	9
MP3-2	6	6	6	6	8	MP3-2	6	6	6	6	10
V2-2	6	6	6	6	10	V2-2	6	6	6	6	10
***E. faecalis* (ATCC 6569)**	6	6	6	6	9						

Antibiotic resistance of *S. aureus* isolates

A total 10 *S. aureus* isolates were tested to evaluate their susceptibilities against a panel of 11 antimicrobial agents. Data depicting the susceptibilities of the isolates were presented as

percentages and are shown in Table 6. Generally a large proportion (70%) of the *S. aureus* isolates tested was most often susceptible to all the antibiotics. However, a small proportion (20% to 30) of these isolates was resistant to penicillin G, ampicillin and tetracycline.

Table 4.15: Inhibition zone diameter data obtained against *S. aureus* in the study.

	PG	S	E	AMP	SXT	TEC	VA	TE	OX	CN	K
					Antibiotic inhibition zone diameter data						
4R3	6	10	6	6	22	11	10	12	10	10	14
4R4	6	19	18	6	21	11	12	18	10	17	18
1R6	35	15	20	30	20	13	12	25	18	20	20
3R6	35	15	24	34	6	13	12	21	19	21	19
2R4	40	18	30	40	35	12	12	8	22	24	25
15Z1	23	14	20	24	21	12	13	20	9	14	20
1R9	30	19	20	33	24	12	12	26	12	20	20
3R9	32	18	23	35	20	13	11	22	15	20	20
2R5	40	20	27	35	25	16	13	6	20	23	25
1R4	38	18	25	30	20	12	11	18	20	24	21

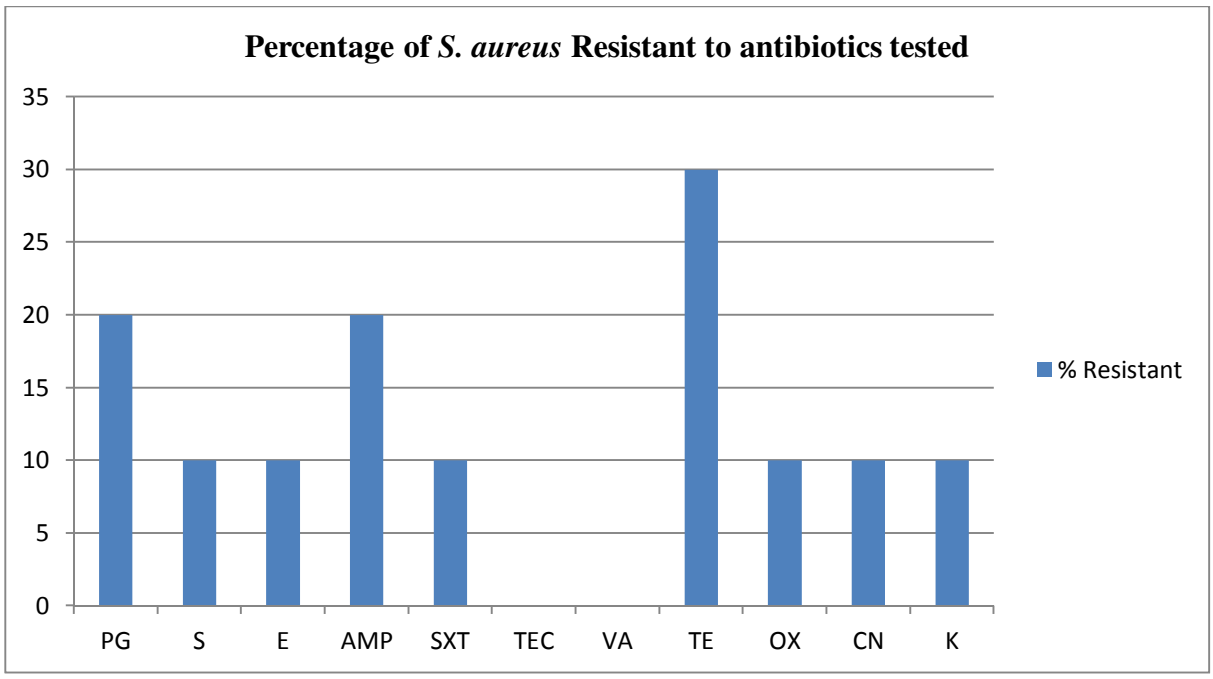

Figure 4.60: Percentage antibiotic resistance of *S. aureus* isolates.

Antibiotic resistance profiles of *E. faecalis* isolates

All the 5 *E. faecalis* isolates were subjected to antibiotic susceptibility tests using a panel of 13 antimicrobial agents. Results are shown in Tables 5. Generally, large proportions (60.0% to 100%) of isolates were resistant to kanamycin, amoxicillin, ampicillin, streptomycin and penicillin G. On the contrary, isolates showed little resistance to streptomycin, ciprofloxacin, norfloxacin, gentamycin, erythromycin and teicoplanin. Generally, susceptibility to penicillin may indicate susceptibility to both ampicillin and amoxicillin for enterococci that are not able to produce β-lactamase enzyme and vice versa (CLSI, 2007). This may account for the trend observed. Moreover, resistance to ampicillin and penicillin among enterococci resulting from the production of β-lactamase enzyme is not easily detected using conventional disc diffusion tests (CLSI, 2007).

Despite the fact that multiple antibiotic resistant *E. faecalis* isolates were obtained in the present study, the isolates were only susceptible to very high concentrations of the ligands tested. However, an interesting observation was the fact that all the isolates were susceptible to four of the ligands tested.

Table 4.16: Antibiotic inhibition zone diameter data for *E. faecalis*

	Antibiotic IZD data (mm)				
	Sample Identities				
Antibiotics	**DEEL4-2**	**STL1-3**	**MP3-1**	**MP3-2**	**V2-2**
VA(30)	8	6	10	14	16
PG(10)	6	6	10	18	6
AP(10)	6	6	16	6	6
A(10)	8	6	8	20	18
S(10)	18	6	16	6	17
K(30)	20	12	20	6	10
GM(10)	20	10	20	18	14
E(15)	8	14	9	20	14
OT(10)	21	6	18	21	18
CIP(5)	12	18	14	15	35
Nor(10)	16	22	18	12	12
C(30)	20	18	20	14	22
TEC(30)	6	14	6	18	16

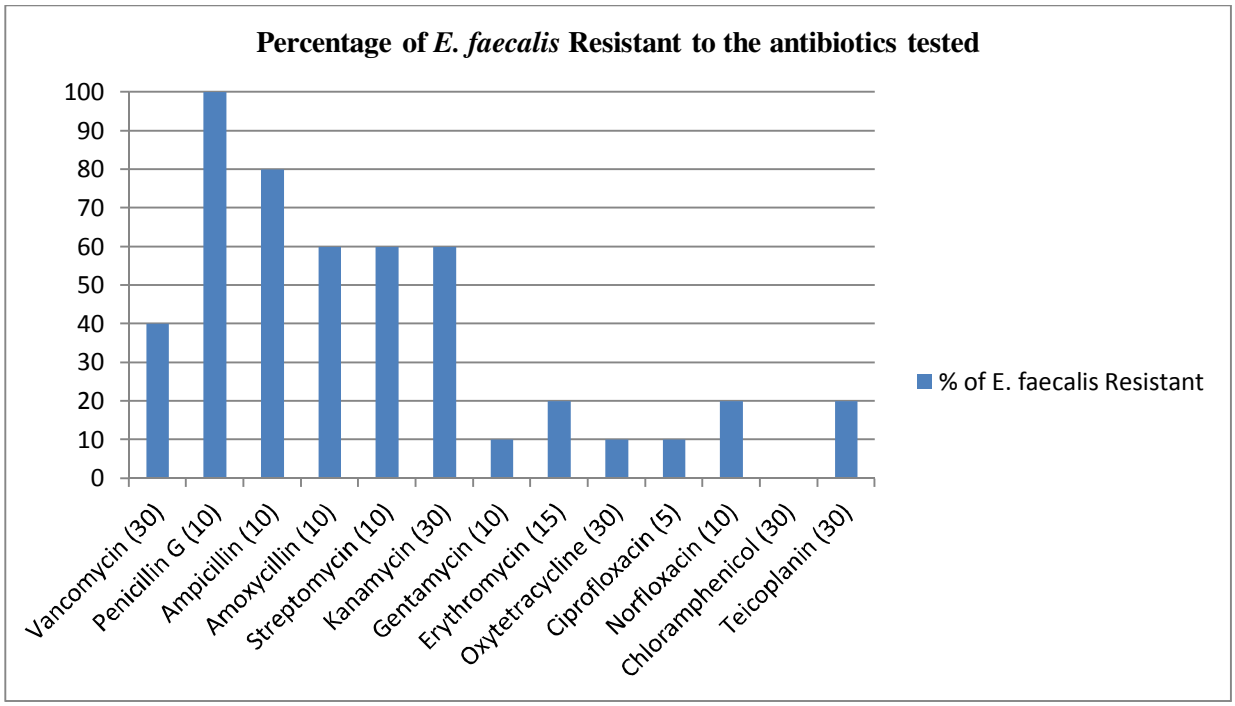

Figure 4.61: Percentage antibiotic resistance of *E. faecalis* isolates.

REFERENCES

[1] POURALIMARDAN, O., ANNE-CHRISTINE, C., JANIAK, C. & HOSSEINI-MONFARED, H. (2007). Hydrazone Schiff base-manganese(II) complexes: Synthesis, crystal structure and catalytic reactivity. *Inorg. Chim. Acta*. 360, 1599 – 1608.

[2] CANPLAT, E., SAHAL, H., KAYA, M. & GUR, S., (2014), Synthesis, characterization, antibacterial and antifungal activities studies of copper(II), cobalt(II) and zinc(II) complexes of the Schiff base ligandderived from 4,4-diaminodiphenylether. *J. Chem. Soc. Pak.* 36(1), 106 – 112.

[3] SAM, N., AFFAN, M.A., SALAM, M.A., AHMAD, F.B. & ASARUDDIN, M.R., (2012), Synthesis, spectral characterization and biological activities of organotin(IV) complexes with orth-vanillin-2-hydrazinopyridine (VHP). *O. J. Inorg. Chem.* 2, 22 – 27.

[4] SHIVHARE, S., MISHRA, R., GHARIA, A. & GAUTAM, M.D., (2012), Synthesis, characterization and antimicrobial studies of Cu(II) and Ni(II) complexes with Schiff base derived from N-aminorhodanine and salicyladehyde. *Int. J. Pharm. Sci.* 4, 394 – 397.

[5] ONAL, Z., YILDIRIM, I., KANDEMIRLI, F. & ARSLAN, T., (2010), Experimental and theoretical studies on the reactions of 1-amino-5-benzoyl-4-phenyl-1H-pyrimidine-2-one/-thione compounds with ethyl acetoacetate. *J. Struct. Chem*. 21, 809 – 816.

[6] BARTYZEL, A. (2013), Synthesis, crystal structure and characterization of manganese(III) complex containing a tetradenate Schiff base. *J. Coord Chem*. 66(24), 4292 – 4303.

[7] EL-HASHASH, M.A.A., SOLIMAN, Y. & EL-SHAMY, I.E. (2012), Synthesis and antimicrobial evaluation of some annelated phthalazine derivatives and acycloC-nucleosides from 1-chloro-4-(2,4,6-trimethylphenyl) phthalazine precursor. *Turk. J. Chem.* 36, 347 – 366.

[8] MOHAMED, G.G., OMAR, M.M. & HINDY, A.M. (2006), Metal complexes of Schiff bases: preparation, characterization and biological activity. *Turk. J. Chem*. 30, 361 – 382.

CHAPTER 5

CONCLUSIONS

In this study, we have successfully synthesized several metal acetylacetonates and hydrazide Schiff base ligands and complexes. Four hydrazide Schiff base ligands were synthesized, L1, 4-(diethylamino)-2-hydroxybenzaldehyde with 4-nitro benzohydrazide, L2, 4-(diethylamino)-2-hydroxybenzaldehyde with 4-methoxy benzohydrazide, L3, 4-(dimethylamino) benzaldehyde with 4-nitro benzohydrazide and L4, 4-(dimethylamino) benzaldehyde with 4-methoxy benzohydrazide.

The synthesized Schiff base ligands were reacted with four metal acetylacetonates (cobalt, magnesium, manganese and vanadium) to form Schiff base complexes. The metals were chosen as metals found in natural systems. Cobalt is found in blood, magnesium in chlorophyll, manganese and vanadium in some food.

The metal acetylacetonates, Schiff base ligands and complexes were characterized by FTIR, ^{1}H-NMR, ^{13}C-NMR, TGA and DTA.

Fourier Transform infrared spectroscopy (FTIR) of the acetylacetonates showed the formation of metal acetylacetonates as characterized by the absence of the carbonyl stretching ν(C=O) vibration in metal acetylacetonate spectra as compared to pure acetylacetone. Metal acetylacetonates also showed the presence of metal oxygen vibration frequency, ν(M-O-C), in the spectra obtained.

Thermogravimetric analysis (TGA) and Derivative or Differential Thermogravimetric analysis (DTA) of the Schiff base ligands showed the presence of a single decomposition product in L1, L2, L3 and L4 indicating the formation of a single reaction product.

Proton and carbon thirteen Nuclear Magnetic Resonance (^{1}H- and ^{13}C-NMR) spectroscopy of the Schiff base ligands indicated the presence of hydrogen and carbon-13 in different environments. The chemical shifts of the hydrogens and carbon-13 provided evidence that Schiff base ligands were formed. The strongest evidence is the presence of the azomethine hydrogen and carbon in

the spectra of the Schiff base ligands. The presence of aromatic hydrogens and carbon at chemical shift environments found in literature also confirmed the formation of Schiff base ligand.

Thermogravimetric analysis (TGA) and Derivative or Differential Thermogravimetric analysis (DTA) of the Schiff base complexes showed the presence of several decomposition products in a number of Schiff base complexes indicating that these Schiff base complexes were not formed in our reaction.

Proton and carbon thirteen Nuclear Magnetic Resonance (^{1}H- and ^{13}C-NMR) spectroscopy of the Schiff base complexes formed with metal acetylacetonates indicated the presence of hydrogen and carbon-13 in different environments. The chemical shifts of the hydrogens and carbon-13 provided evidence that Schiff base complexes were formed. Another strong evidence is the presence of the azomethine hydrogen and carbon in the spectra of the Schiff base complexes. The presence of aromatic hydrogens and carbon at chemical shift environments found in literature also confirmed the formation of Schiff base complex.

The Schiff base ligands and complexes were tested as antimicrobial reagents against several bacteria. A total of 21 ligands were tested against confirmed *S. aureus* and *E. faecalis* strains and only 4 exhibited antimicrobial activities. Values for the inhibition zone diameter data are shown in Table 4. As shown on the table at weights 0.01g, 0.03g, 0.06g and 0.1g none of the ligands were effective against the *S. aureus* and *E. faecalis* isolates.